DISSERTATION

submitted to the

Combined Faculties for the Natural Sciences and for Mathematics

of the Ruperto-Carola University of Heidelberg, Germany

for the degree of

Doctor of Natural Sciences

presented by

M.Sc. Carolin J. Blume

born in Heidelberg

Oral examination: …….

B-cell receptor signaling- and p53-dependent non-coding RNA expression in chronic lymphocytic leukemia

Referees: Prof. Dr. Christof von Kalle
PD Dr. Stefan Wiemann

Summary

Chronic lymphocytic leukemia (CLL) is the most common type of leukemia in adults of the Western world. It is a malignancy characterized by an accumulation of CD5 positive B-cells in blood and lymphoid organs. CLL is a very heterogeneous disease, where molecular subgroups display striking differences in treatment response and prognosis. A greater BCR signaling capacity and a loss of p53 signaling activity confer a poor prognosis. While the higher BCR signaling activity seen in CLL with unmutated *IGHV* genes supports tumor cell survival, p53 aberrations mediate resistance towards standard therapy. The aim of this work was to characterize the involvement of non-coding RNA in these two key signaling pathways of CLL cell survival and resistance.

Small RNA sequencing was applied to comprehensively assess microRNA (miRNA) and other non-coding RNA expression in peripheral blood mononuclear cells of 35 CLL patients. miRNAs were identified that display *IGHV* mutation status dependent expression, and the transcript levels of 15 miRNAs predicted *IGHV* mutation status with 82% accuracy. By abrogation of BCR signaling *in vitro* using the small-molecule inhibitor ibrutinib, the expression of miR-320c, miR-1246, miR-484, miR-17-5p, miR-155-3p and miR-27a-5p was found to be BCR signaling dependent, suggesting a role in mediating CLL cell survival. The basal expression of 10 miRNAs was associated with ibrutinib sensitivity *in vitro,* implicating an involvement of these miRNAs in the regulation of BCR signaling.

It was hypothesized that p53-dependent ncRNAs could be identified by comparison of CLL samples with or without *TP53* mutation/deletion for their ncRNA expression changes upon DNA damage-triggered p53 induction. In addition to miR-34a, a set of further miRNAs was found to be *TP53* status dependently induced (particularly miR-182-5p, miR-7-5p and miR-320d/c). Beyond miRNAs, the present data demonstrate p53-dependent expression of the long non-coding RNAs lincRNA-p21 (long intergenic non-coding RNA p21) and NEAT1 (nuclear enriched abundant transcript 1) upon DNA damage and direct p53 activation with nutlin-3. p53-dependent induction of expression was further proven in a panel of Burkitt's lymphoma (BL) cell lines including cell lines with genetically engineered knockout or knockdown of p53. p53 ChIP demonstrated direct binding of p53 to the NEAT1 promoter. This provides first evidence of p53-dependent regulation of long non-coding RNAs in CLL and BL. The discovery of p53-dependent NEAT1 induction, which is an integral part of nuclear paraspeckles, paves the way for further research on the role of paraspeckles in tumor cell apoptosis and resistence. The current work identifies additional components of the p53-dependent DNA damage response in lymphoma.

The results of these studies provide new insight into the involvement of miRNAs and lncRNAs in two key signaling pathways regulating cell survival and treatment resistance in CLL and lymphoma.

Zusammenfassung

Die chronisch lymphatische Leukämie (CLL) ist die häufigste Form der Leukämie in Erwachsenen der westlichen Hemisphäre. Charakteristisch für diese maligne Erkrankung ist die Akkumulation von CD5 positiven B-Zellen im Blut und in den Lymphorganen. CLL ist eine sehr heterogene Erkrankung, in der molekulare Subgruppen bemerkenswerte Unterschiede im Hinblick auf Therapieansprechen und Prognose zeigen. Eine erhöhte Kapazität des B-Zell-Rezeptor (BCR) Signalwegs wie auch ein Verlust der Aktivität des p53-Signalwegs bedingen eine schlechte Prognose. Während unmutierte *IGHV* Gene über eine höhere Aktivität des BCR Signalwegs zu einem verbesserten Überleben der Tumorzellen führen, vermitteln Aberrationen in dem Tumorsuppressor p53 Therapieresistenz. Ziel dieser Arbeit war es, die Beteiligung von nicht-kodierenden RNAs (ncRNAs) in diesen beiden für das Überleben und die Resistenz von CLL-Tumorzellen zentralen Signalwegen zu charakterisieren.

Um die Expression von microRNA (miRNA) und weiteren nichtkodierenden RNA (ncRNA) in mononukleären Zellen des periphären Blutes von 35 CLL Patienten umfassend zu quantifizieren, wurden kurze RNA Transkripte (small RNA) sequenziert. Es wurden *IGHV*-Mutationsstatus abhängig exprimierte miRNAs identifiziert, und anhand der Signatur von 15 miRNAs ließ sich der *IGHV* Mutationsstatus in 82% der Proben korrekt bestimmen. Eine Unterbrechung des BCR Signalwegs durch *in vitro*-Behandlung mit dem small-molecule Inhibitor Ibrutinib führte zur differenziellen Expression von miR-320c, miR-1246, miR-484, miR-17-5p, miR-155-3p und miR-27a-5p, was deren Abhängigkeit von einem aktiven BCR demonstriert und eine Beteiligung an diesem überlebensfördernden Signalweg nahelegt. Die Assoziation der basalen Expression von 10 miRNAs mit *in vitro* Ibrutinib-Sensitivität der Proben impliziert eine Mitwirkung dieser miRNAs an der Regulation der BCR Signalaktivität.

p53-abhängige ncRNAs wurden durch einen Vergleich der Expressionsänderungen zwischen *TP53* wildtyp und *TP53* mutierten/deletierten CLL-Proben nach p53 Induktion durch DNA-Schädigung identifiziert. Zusätzlich zu miR-34a war die Expression einer Gruppe weiterer miRNAs (insbesondere miR-182-5p, miR-7-5p, miR-320d/c) abhängig vom *TP53* Mutationsstatus. Über miRNAs hinaus enthüllten die Daten dieser Arbeit die p53-abhängige Expression der langen nicht-kodierenden RNAs (lncRNAs) lincRNA-p21 (long intergenic non-coding RNA p21) und NEAT1 (nuclear enriched abundant transcript 1) nach DNA-Schädigung sowie nach direkter p53-Aktivierung mittels Nutlin-3 in CLL. Deren p53-abhängige Induktion über CLL hinaus wurde anhand einer Auswahl an Burkitt's Lymphom (BL) Zelllinien, deren p53 Expression teils durch p53 knockout oder knockdown kontrolliert worden war, nachgewiesen. Durch p53 ChIP konnte die direkte

Bindung von p53 an den NEAT1 Promoter demonstriert werden. Damit wurde erstmals die p53-abhängige Regulation langer nicht-kodierender RNAs in CLL und BL gezeigt. Die Entdeckung der p53-abhängigen Regulation von NEAT1, einem zentralen Bestandteil nukleärer Paraspeckles, bahnt weiteren Arbeiten zur Rolle der Paraspeckles in Apoptose und Resistenz von Tumorzellen den Weg. Die vorliegende Arbeit identifiziert neue Komponenten der p53-abhängigen Antwort auf DNA-Schäden in malignen Lymphomen.

Die Ergebnisse dieser Arbeit bieten neue Einblicke in die Beteiligung von miRNAs und lncRNAs an zwei für die Regulation von zellulärem Überleben und Therapieresistenz zentralen Signalwegen in der CLL und malignen Lymphomen.

Index of Contents

Summary V

Zusammenfassung VII

Index of Contents IX

List of Figures XIII

List of Tables XV

List of Abbreviations XVII

1 INTRODUCTION 1

1.1 Cancer 1

1.1.1 Characteristics of cancer 1

1.1.2 Oncogenes and tumor suppressor genes 1

1.2 B-cells and B-cell malignancies 2

1.2.1 B-cells and B-cell receptor development 2

1.2.2 B-cell malignancies and mechanisms of lymphomagenesis 4

1.3 Chronic Lymphocytic Leukemia (CLL) 6

1.3.1 Molecular subgroups 7

1.3.1.1 *IGHV* mutation status 7

1.3.1.2 Genomic aberrations 7

1.3.2 Two key signaling pathways in CLL cell survival and proliferation 9

1.3.2.1 B-cell receptor signaling 9

1.3.2.2 The p53 pathway 11

1.4 microRNAs and long intergenic non-coding RNAs 12

1.4.1 Classification, biogenesis and function 12

1.4.2 Role in human cancer and CLL 15

1.4.3 miRNAs and lncRNAs displaying BCR- or p53-dependent regulation in CLL 16

1.5 Aims of this work 18

2 MATERIAL AND METHODS 19

2.1 Material 19
2.1.1 Chemicals and Biochemicals 19
2.1.2 Consumables 20
2.1.3 Antibodies 21
2.1.4 Primers for qRT-PCR 22
2.1.5 Commercial Kits 22
2.1.6 Primary human material 23
2.1.7 Cell lines 23
2.1.8 Cell culture media and additives 23
2.1.9 Self-prepared Buffers 24
2.1.10 Instruments 24
2.1.11 Software 26
2.1.12 Databases and online tools 26
2.1.13 Other 27
2.2 Cell culture methods 27
2.2.1 Isolation of mononuclear cells from whole blood 27
2.2.2 Magnetic activated cell sorting (MACS) 27
2.2.3 Freezing, thawing and culturing of primary cells and cell lines 28
2.2.4 Cell culture treatments 28
2.2.5 Fluorescence activated cell sorting (FACS) 28
2.4.6 Cell viability assessment using CellTiter-Glo® 29
2.5 Molecular Biology 29
2.5.1 RNA isolation 29
2.5.2 RNA quantification and quality control 30
2.5.3 cDNA synthesis (reverse transcription) 30
2.5.4 Primer design for qRT-PCR 31
2.5.5 Quantitative real-time PCR (qRT-PCR) 31
2.5.6 Agarose gel electrophoresis 32

2.5.7 Small RNA library preparation 33
2.5.8 Next-generation Sequencing 33
2.5.9 Protein extraction 33
2.5.10 Determination of protein concentration 33
2.5.11 Western Blot 34
2.5.12 Chromatin immunoprecipitation (ChIP)-PCR 34
2.6 Bioinformatics and Statistics 35
2.6.1 Read processing and mapping 35
2.6.2 Data analysis and statistics 35
3 RESULTS 37
3.1 Establishment and validation of the small RNA sequencing approach 37
3.2 Induction of known p53 targets after DNA damage in primary CLL cells 40
3.3 Overview of RNA expression in primary CLL cells as captured by small RNA sequencing 45
3.3.1 RNA families detected by the approach 45
3.3.2 miRNA expression profiles at baseline 46
3.4 Identification of BCR signaling-dependent miRNA in CLL 47
3.4.1 Baseline miRNA expression and *IGHV* status 47
3.4.2 The impact of BTK inhibition on miRNA expression 48
3.4.3 Baseline miRNA expression and *in vitro* ibrutinib sensitivity 50
3.4.4 Summary of BCR-dependent miRNAs in CLL 53
3.5 Identification of p53-dependent ncRNAs in primary CLL cells 54
3.5.1 *TP53* status dependent miRNA induction 54
3.5.2 Deriving insights into the regulation of long RNA transcripts from a small RNA sequencing screen 57
3.5.3 Potential targets of p53-dependently regulated miRNAs in CLL 58
3.5.4 p53 dependent long non-coding RNA induction 59
3.5.4.1 lincRNA-p21 in CLL 59

3.5.2.3 NEAT1 in CLL 61

3.5.5 Comparison of p53 pathway activity in treated and untreated *TP53* wild-type CLL 65

3.6 p53 dependency of lincRNA-p21 and NEAT1 expression in the Burkitt's Lymphoma (BL) cell line model 67

3.6.1 lincRNA-p21 and NEAT1 induction in BL cell lines 67

3.6.2 NEAT1 and lincRNA-p21 expression in BL cell line models of controlled p53 expression 68

3.6.3 Assessment of p53 binding to the NEAT1 promoter 71

3.6.4 Summary of p53-dependent ncRNAs in CLL and BL 72

4 DISCUSSION 73

4.1 miRNA expression profiles predict *IGHV* status and associate with *in vitro* ibrutinib sensitivity 74

4.2 BTK inhibition identifies a set of five BCR signaling-dependent miRNAs 76

4.3 miR-182, miR-7 and miR-320d/c are novel p53-dependent miRNAs in CLL 77

4.4 p53-dependent long non-coding RNAs identified in primary CLL and BL cell lines 80

4.4.1 p53-dependent lincRNA-p21 expression in CLL and BL 80

4.4.2 p53-dependent NEAT1 expression in CLL and BL 81

4.5 CLL high-risk patients display p53 pathway impairment independent of *TP53* and *ATM* aberrations 84

5 CONCLUSION AND PERSPECTIVE 85

References 87

Appendix 103

Publications and Conferences 109

Declaration 111

Acknowledgements 113

List of Figures

Figure 1. The hallmarks of cancer. 1

Figure 2. B-cell differentiation in the germinal center (GC). 4

Figure 3. Cellular origin and frequent genetic aberrations in non-Hodgkin lymphoma..... 5

Figure 4. CLL patient survival by *IGHV* mutation status..... 7

Figure 5. Probability of survival from diagnosis in CLL patients of five genetic subgroups. 8

Figure 6. CLL BCR signaling with focus on Bruton's tyrosine kinase. 10

Figure 7. Mechanisms of p53 activation and regulation of downstream targets, highlighting components aberrant in CLL. 11

Figure 8. The miRNA biogenesis pathway..... 13

Figure 9. Long non-coding RNAs as regulators and targets of p53..... 18

Figure 10. Establishment and validation of small RNA sequencing. 38

Figure 11. Graphical summary of the screening approach used in this study. 39

Figure 12. Effects of 5 Gy irradiation (IR) on cell apoptosis. 41

Figure 13. Examples of the impact of 5 Gy irradiation (IR) on cell viability / apoptosis... 42

Figure 14. Effects of 5 Gy irradiation (IR) on p53 target gene expression..... 43

Figure 15. DNA damage-triggered p21 and miR-34a-5p induction by patient treatment status. 44

Figure 16. Expression of RNA subgroups detected by small RNA sequencing..... 46

Figure 17. Basal miRNA expression profiles detected by small RNA sequencing..... 47

Figure 18. miRNA expression changes due to 1 µM ibrutinib treatment for 24 hours..... 49

Figure 19. Expression of six ibrutinib-regulated miRNAs in the 12 primary CLL samples in non-treated (NT) condition and after 24h with 1 µM ibrutinib (PCI). 50

Figure 20. Cell viability post *in vitro* ibrutinib treatment, stratified by *IGHV* status. 51

Figure 21. Hierarchical clustering of basal expression of miRNAs displaying robust differential expression in regard to cell viability post *in vitro* ibrutinib treatment..... 52

Figure 22. Unsupervised hierarchical clustering of IR-induced expression changes of the 300 most variably expressed miRNAs over 34 CLL patient samples. 55

Figure 23. DNA damage triggered lincRNA-p21 induction in CLL. 60

Figure 24. Correlation of DNA-damage triggered lincRNA-p21 induction with p21 induction and cell viability. 61

Figure 25. LincRNA-p21 expression 24 h post induction with 10 µM nutlin-3 or vehicle control in primary CLL samples. 61

Figure 26. NEAT1 induction upon DNA damage in primary CLL cells. 63

Figure 27. NEAT1 expression 24 hours after irradiation (IR) or no treatment (NT) of primary CLL cells. 64

Figure 28. NEAT1 expression 24 h post induction with 10 µM nutlin-3 or vehicle control in primary CLL samples. 65

Figure 29. Induction of lincRNA-p21 and NEAT1 in CLL stratified by patient treatment, *TP53* and *ATM* status. 66

Figure 30. Time course of lincRNA-p21 and NEAT1 induction in $TP53^{wt}$ and $TP53^{mut}$ Burkitt's Lymphoma cell lines. 68

Figure 31. Effect of nutlin-3 treatment on p53 expression in BL cell lines of defined p53 status. 68

Figure 32. Effect of nutlin-3 treatment on apoptosis in BL cell lines of defined p53 status. 69

Figure 33. Expression of p21, lincRNA-p21 and NEAT1 upon nutlin-3 treatment of primary CLL and BL cell lines. 70

Figure 34. ChIP-PCR for p53 binding in the promoter regions of NEAT1 and p21. 71

Figure 35. Unsupervised hierarchical clustering of p53 targets identified in primary CLL samples. 72

Figure 36. Summary of p53 targets identified in CLL. 83

Figure S1. Induction of the top four p53-dependently regulated miRNAs upon irradiation 108

List of Tables

Table 1. The most frequent genomic aberrations in CLL overall, and in refractory cases. 8

Table 2. qRT-PCR program run for the quantification of lincRNA-p21, NEAT1 and p21. 32

Table 3. Summary of clinical and genetic characteristics of the patients samples screened. 40

Table 4. miRNAs differentially expressed with respect to *IGHV* status. 48

Table 5. miRNA signature for the classification of samples according to *IGHV* status. .. 48

Table 6. miRNAs differentially regulated upon ibrutinib treatment..... 49

Table 7. miRNAs regulated with 10% increase of cell viability after 1 µM ibrutinib *in vitro.* 53

Table 8A. miRNAs regulated upon DNA damage in *TP53*^{wt} (n = 15) CLL samples. 56

Table 8B. miRNAs regulated upon DNA damage in *TP53*$^{del/mut}$ CLL (n = 10) not listed in A. 57

Table 9. Top mRNAs induced in previously untreated *TP53*^{wt} compared to *TP53*$^{del/mut}$ samples 24 h post irradiation..... 58

Table 10. mRNAs predicted to be targeted by p53-dependent miRNAs upon DNA damage. 59

Table 11. Top 10 ncRNAs induced in previously untreated *TP53*^{wt} compared to *TP53*$^{del/mut}$ samples 24 h post irradiation. 62

Table 12. p53 dependence of miRNAs with reported differential basal expression in deleted versus disomic 17p in CLL. 79

Table S1. Detailed sample genetics and grouping for comparison of ncRNA expression…….. 103

Table S2. *TP53* mutation status of the cell BL cell lines used.……104

Table S3. Comparison of the 30 highest expressed miRNAs in CLL baseline samples to previously reported CLL sequencing screens……...105

Table S4. mRNAs inversely correlating to miR-574-5p expression, and predicted to be targeted by miR-574-5p……106

Table S5. ncRNAs differentially expressed between previously untreated *TP53*^{wt} and high-risk *TP53*^{wt} samples at baseline……107

List of Abbreviations

AKT	Protein kinase B (PKB)
APC	Allophycocyanine
ASCC3	Activating signal cointegrator 1 complex subunit 3
AML	Acute myeloid leukemia
ATM	Ataxia telangiectasia mutated
A-to-I editing	Adenosine to inosine editing
ATR	Ataxia telangiectasia and Rad3-related protein
B-ALL	B-cell acute lymphocytic leukemia
Bax	BCL2-associated X protein
BBC3	B-cell lymphoma 2 binding component 3
BCL2	B-cell lymphoma 2
BCR	B-cell receptor
BL	Burkitt’s lymhoma
BRAF	V-raf murine sarcoma viral oncogene homolog B1
BTK	Bruton's tyrosine kinase
C/EBPβ	CCAAT/enhancer-ginding protein beta
Cas9	CRISPR associated protein 9
CD	Cluster of differentiation
CDKN1A	Cyclin-dependent kinase 1A (p21)
ChIP	Chromatin immunoprecipiation
CHK1/2	Checkpoint kinase 1 and 2
CLL	Chronic Lymphocytic Leukemia
Cp	Crossing point
CRISPR	Clustered Regularly Interspaced Short Palindromic Repeats
CTNNB1	Catenin (cadherin-associated protein) beta 1
DNA	Desoxyribonucleic acid
DDB2	Damage-specific DNA-binding protein-2
del	Deletion / deleted
DGCR8	DiGeorge Critical Region 8
dis	Disomic
DLBCL	Diffuse large B-cell lymphoma
DLEU	Deleted in leukemia
DMSO	Dimethyl-sulfoxide
EBV	Epstein-Barr virus
EEF1A1	Eukaryotic translation elongation factor 1 alpha 1

ERK	Extracellular signal-regulated kinase
eRNA	Enhancer RNA
FACS	Fluorescence-activated cell sorting
FBS	Fetal bovine serum
FC	Fold change
FCRL2	Fc receptor-like 2
FL	Follicular lymphoma
FOXO4	Forkhead Box O4
FUS	Fused in Sarcoma
GADD45α	Growth arrest and DNA damage-inducible protein 45 alpha
GAPDH	Glycerinaldehyde-3-phosphate dehydrogenase
GAS5	Growth arrest-specific 5
GC	Germinal center
Gy	Gray
h	Hour
HCDR3	Heavy-chain complementarity determining region 3
HOTAIR	Hox antisense intergenic RNA
HR	Homologous recombination
HRP	Horseradish peroxidase
IG	Immunoglobulin
IGHV	Immunoglobulin heavy chain variable region
IR	Irradiation
ITAM	Immunoreceptor tyrosine-based activation motif
kd	Knockdown
ko	Knockout
lincRNA	Long intergenic non-coding RNA
lincRNA-EPS	LincRNA erythroid prosurvival
lncRNA	Long non-coding RNA
MACS	Magnetic-activated cell sorting
MALAT1	Metastasis associated lung adenocarcinoma transcript1
MALT	Mucosa associated lymphoid tissue
MDM2	Double minute-2
MEG3	Maternally expressed 3
M-*IGHV*	Mutated immunoglobulin heavy chain variable region
min	Minute
miRNA, miR	MicroRNA

mRNA	Messenger RNA
mt tRNA	Mitochondrial transfer RNA
mut	Mutation /mutated
ncRNA	Non-coding RNA
NEAT1	Nuclear enriched abundant transcript 1
NF-YA	Nuclear transcription factor Y alpha
NF-κB	Nuclear factor kappa light-chain enhancer of activated B-cells
NHEJ	Non-homologous end joining
NONO	Non-POU domain-containing octamer-binding protein
NOTCH1	Notch homolog 1, translocation-associated (Drosophila)
nt	Nucleotide
NT	Non-treated
PAGE	Polyacrylamide-gelelecrophoresis
PANDA	p21 associated ncRNA DNA damage activated
PBMNC	Peripheral blood mononuclear cell
PBS	Phosphate buffered saline
PCNA	Proliferating cell nuclear antigen
PCR	Polymerase chain reaction
PE	Phycoerythrin
PI	Propidium iodide
PI3K	Phosphoinositide 3-kinase
PLCγ2	Phospholipase Cγ2
PLXNB2	Plexin B2
pri-miRNA	Primary transcripts of microRNA
PT	Previously treated (patients)
PUMA	p53 upregulated modulator of apoptosis
qRT-PCR	Quantitative real-time polymerase chain reaction
RBM14	RNA binding motif protein 14
RE	Response element
RNA	Ribonucleic acid
RPS19	Ribosomal protein 19
RPE	R-Phycoerythrin
RPMI	Roswell Park Memorial Institute medium
rRNA	Ribosomal RNA
RT	Room temperature
SEM	Standard error of the mean

SF3B1	Splicing factor 3B1
SFPQ	Splicing factor proline/glutamine-rich
shRNA	Short hairpin RNA
SMZL	Splenic marginal zone lymphoma
snoRNA	Small nucleolar RNA
snRNA	Small nuclear RNA
SYK	Spleen tyrosine kinase
TNFRSF10B	Tumor necrosis factor receptor superfamily, member 10b
TP53	Tumor protein 53
TRBP	Human immunodeficiency virus transactivating response RNA-binding protein
TRIM22	Tripartite motif containing-22
tris	Trisomy
tRNA	Transfer RNA
U.S.	United States of America
U-*IGHV*	Unmutated Immunoglobulin heavy chain variable region
UT	Untreated (patients)
VH	Variable region of the immunoglobulin heavy chain
Xist	X-inactive specific transcript
ZAP70	Zeta associated protein 70

1 Introduction

1.1 Cancer

1.1.1 Characteristics of cancer

Tumor cells arise from normal cells through an evolutionary process that eventually enables them to evade the body's control mechanisms and multiply at unphysiologic frequency[1]. The characteristics obtained by the malignant cells have been summarized as the 'hallmarks of cancer' by Hanahan and Weinberg in 2000[2], revised in 2011[3] and illustrated in Figure 1. These acquired functional capabilities including the resistance to cell death, replicative immortality or invasion and metastasis are present in virtually all cancers. However, the biological mechanisms underlying their development and their chronological sequence vary greatly in different cancer types, among tumors of the same entity, and even among the cells composing a tumor[2,3].

Cancer is a disease of genetic and epigenetic alterations affecting genes that regulate cellular integrity and tissue homeostasis[4-8]. Depending on the outcome of their activation, those genes are termed tumor suppressor genes or oncogenes.

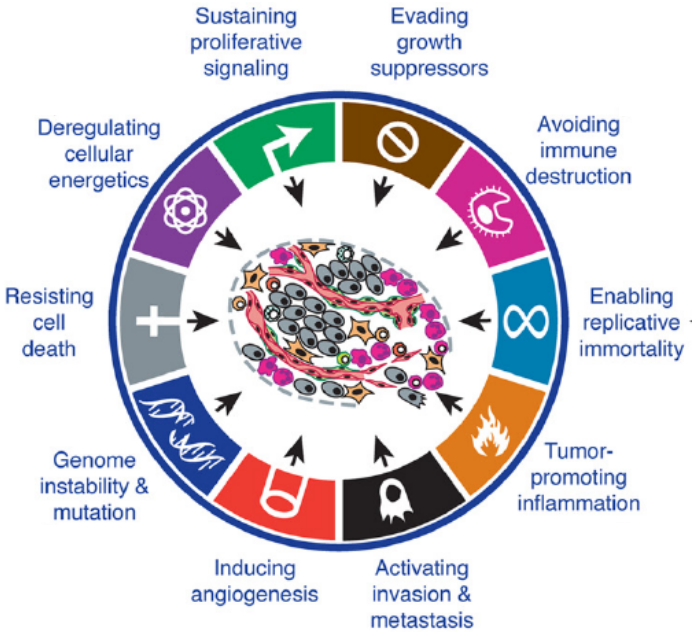

Figure 1. The hallmarks of cancer. Acquired capabilites of tumor cells as summarized by Hanahan and Weinberg, 2011[3].

1.1.2 Oncogenes and tumor suppressor genes

Oncogenes develop from normal, non-cancerous proto-oncogenes through mutation, translocation, amplification or epigenetic mechanisms ('gain of function') to promote tumorigenesis. As such, they are frequently involved in cellular proliferation and signal transduction. A single, monoallelic, alteration in a proto-oncogene can be sufficient for

transformation, illustrating the dominant effect of oncogene activation. Myc (c-Myc), for example, is a transcription factor which is frequently found overexpressed in cancer through gene amplification, leading to a higher expression of genes involved in cell cycle progression including cyclin A and E[9,10] . In ~80% of Burkitt's Lymphoma, a translocation (mostly t(8;14)(q24;q32)) puts c-Myc under the control of a strong immunoglobulin heavy chain locus promoter, resulting in overexpression of the oncogene[10]. Supported by accompanying second-hit mutations which counterbalance the pro-apoptotic pathways (e.g. p53) activated to safeguard the cell against *MYC*-induced transformation, mice transgenic for this translocation almost invariably develop aggressive lymphomas[11-13].

In contrast, tumor suppressors prevent malignant transformation. Here, a decreased activity ('loss of function') promotes, i.e. increases the likelihood of, carcinogenesis. As it typically requires the presence of only a single functional gene for its activity, tumor suppressor genes are recessive, requiring 'two-hit' inactivation of both alleles[8,14]. Inheritance of one mutant allele can increase tumor susceptibility, as only one further mutation is needed to inactivate gene function[8]. This is often observed in familial cancer syndromes. Tumor suppressor genes are involved in cellular processes such as cell cycle checkpoint responses, DNA damage detection and repair, differentiation and tumor angiogenesis. The retinoblastoma gene (RB) which is frequently found deleted in hereditary and sporadic retinoblastoma was the first tumor suppressor gene to be identified[14]. By inhibiting e.g. E2F, a major negative regulator of the cell cycle, it prevents proliferation by blockade of G1/S-phase progression[15]. p53 is a key tumor suppressor and is inactivated by deletions and/or somatic mutations in more than 50% of cancers[8]. It is an exception to the 'two-hit' rule, as mutant p53 protein can exert a dominant negative effect by preventing the activity of wild-type protein from the second allele[16]. p53 causes G1 phase arrest and apoptosis upon DNA damage, guarding the cell against genotoxic insult[17]. Multiple stresses inducing p53 and downstream outcomes have been described, emphasizing its key role in tumor suppression (delineated in section 1.3.2.2).

1.2 B-cells and B-cell malignancies

1.2.1 B-cells and B-cell receptor development

The human immune system is composed of an innate and an adaptive part. The innate immune system quickly reacts as first-line defense to microbial pathogens in a generic way. The adaptive immune system relies on antigen-specific recognition by receptors expressed on the surface of clonally expanded B- and T-cells. It triggers targeted responses against pathogens, which take several days or weeks to develop and generate long lasting immunity. B-cells play a major role within the adaptive immune

system by producing specific antibodies, presenting antigens and generating memory cells that can be activated upon repeated infection with the same pathogen[18].

B-cell development and maturation starts from stem cells within the bone marrow and occurs through numerous stages that are characterized by changes in the specific structure of the B-cell receptor (BCR). This cell-membrane bound surface immunoglobulin (sIg) consists of two identical heavy-chain (H) and two identical light-chain (L) polypeptides, which are covalently linked by disulphide bridges and display a specific antigen-binding site. The corresponding genes occur as separate fragments that are assembled into the active gene by V(D)J recombination[19,20]. During early B-cell development in the bone marrow, first the H region is remodeled through randomly joining together one of about 50 functional variable (V_H) genes, one of about 27 functional diversity (D_H) and one of 6 joining (J_H) gene segments. The L region is similarly rearranged by combination of the V_L and J_L genes, generating high receptor diversity. Only B-cells expressing a functional, non-autoreactive BCR differentiate into mature, naïve B-cells and leave the bone marrow[21]. Subsequently, they can participate in immune responses upon antigen binding to the BCR in the peripheral blood, but more frequently, antigen-activated B-cells undergo T-cell-dependent immune responses and clonal expansion in the germinal centers (GCs). GCs are specialized structures in secondary lymphoid tissues such as the lymph nodes and spleen, illustrated in Figure 2. Here, the Ig genes are further modified by somatic hypermutation occurring at the complementarity determining regions, resulting in mutated *IgHV* (immunoglobulin heavy chain variable region) genes and tremendous BCR diversity. While most mutations result in reduced antigen binding affinity of the BCR to the cognate antigen leading to apoptotic cell death, cells with mutations conferring enhanced affinity are positively selected and can undergo class-switch recombination. Here, the original constant regions (C) of the BCR, usually IgM or IgD, can be replaced to IgG, IgE or IgA by chromosomal recombination. Subsequently, B-cells can differentiate into memory B-cells or antibody producing plasma cells and leave the GC[20,22].

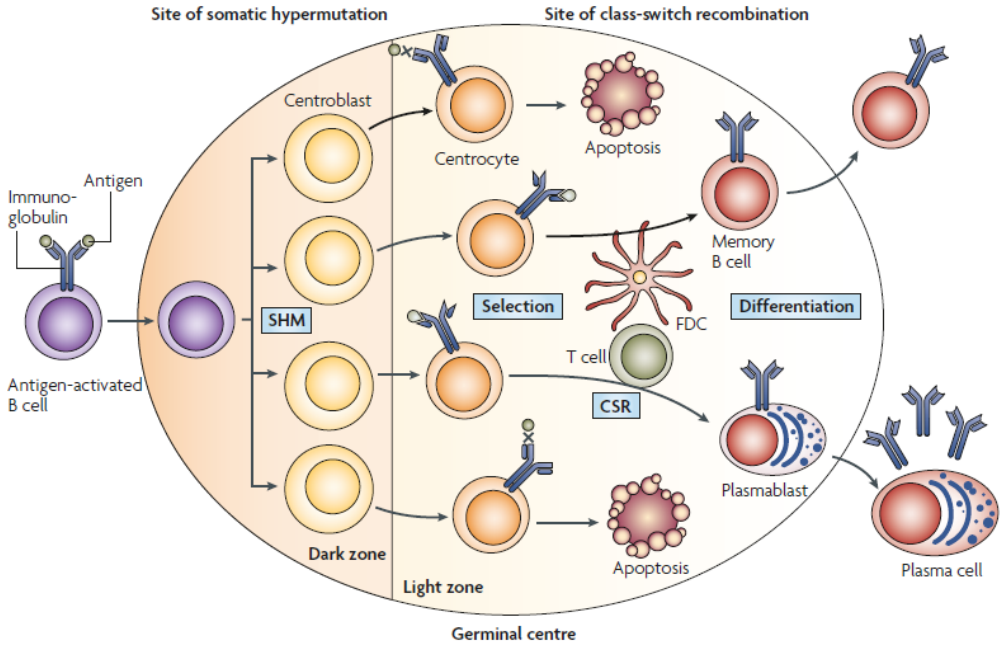

Figure 2. B-cell differentiation in the germinal center (GC). Antigen-activated B-cells differentiate into centroblasts that undergo clonal expansion and somatic hypermutation (SHM) in the dark zone, introducing base-pair changes into the IgV region of the heavy and light chain. Centroblasts differentiate into centrocytes and move to the light zone where they are selected for improved BCR antigen affinity, supported by antigen presentation by T-cells and follicular dendritic cells (FDCs). Positively selected B-cells can undergo class-switch recombination (CSR) and differentiate into memory B-cells or plasmablasts to be released from the GC. Centrocytes producing an unfavourable BCR upon SMH (low affinity, auto-reactivity) undergo apoptosis (Klein *et al.*, 2008).

1.2.2 B-cell malignancies and mechanisms of lymphomagenesis

The World Health Organization (WHO) classifies lymphomas into Hodgkin- and non-Hodgkin Lymphoma, the latter encompassing mature B-cell neoplasms, mature T-cell and NK (natural killer cell) neoplasms and posttransplantation lymphoproliferative disorders[23]. B-cells account for about 95% of lymphomas[20]. In the Western world, about 19 new cases of non-Hodgkin lymphoma are diagnosed in 100,000 individuals annually, making it the 7th most frequent cancer diagnosed and the 9th most frequent cause of cancer death in the U.S.[24,25]. B-cell lymphomas are classified according to the developmental stage of their cell of origin and thus sub-divided into about 20 different types[23]. The most common (in the U.S.) are diffuse large B-cell lymphoma (DLBCL), follicular lymophoma (FL) and chronic lymphocytic leukemia (CLL). By gene expression profiling and surface marker phenotyping, the assignment of tumor cells to a distinct cell of origin is for some types very clear (Figure 3). CLL however is a remarkably heterogeneous disease, for which various cells of origins are debated and no consensus

has been found to date[26,27]. In about half of the patients, CLL cells carry unmutated *IgHV* genes, suggesting pre-GC B-cells as normal counterpart. In the remaining half they carry somatically mutated *IgHV* genes, suggesting B-cells past the GC response as origin[28,29]. This distinction is of great biological and therapeutic relevance.

B-cell transformation is promoted by at least four mechanisms: I) Somatic mutations and/or chromosomal aberrations, II) BCR signaling, III) the microenvironment and/or VI) viral infection.

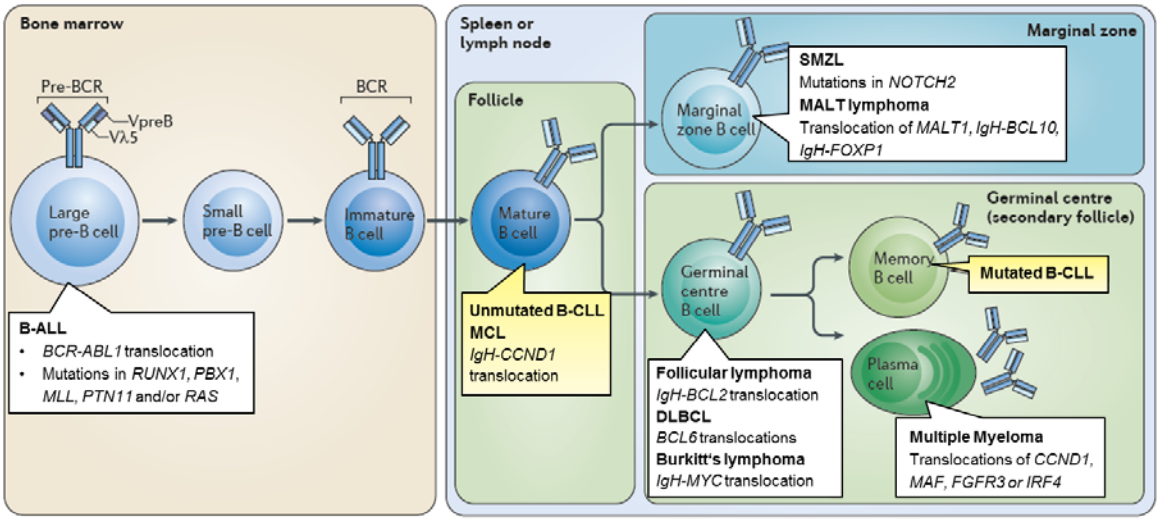

Figure 3. Cellular origin and frequent genetic aberrations in non-Hodgkin lymphoma. B-cell malignancies arise at different stages of B-cell development. Frequently, genetic aberrations contribute to pathogenesis and characterize the type of B-cell lymphoma. The germinal center is surrounded by a mantle zone (follicle) of naïve, mostly $CD5^+$ B-cells and a marginal zone in the spleen (but not in lymph nodes), a B-cell rich zone between B-cell follicles and the T-cell area. (B-ALL, B-cell acute lymphocytic leukemia; CLL, chronic lymphocytic leukemia; SMZL; splenic marginal zone lymphoma; MCL, mantle cell lymphoma; DLBCL, diffuse large B-cell lymphoma; MALT, mucosa associated lymphoid tissue (Rickert 2013, modified).

Most lymphomas are derived from GC- or post-GC B-cells. The GC constitutes a highly proliferative environment to generate large amounts of immunoglobulin for antigen elimination[30]. This background supports the occurrence and accumulation of chromosomal rearrangements and somatic mutations. Some malignancies are characterized by specific cytogenetic abnormalities. Reciprocal chromosomal translocations involving an Ig locus and a proto-oncogene constitute a hallmark of B-cell lymphoma (Figure 3). Consequently, the proto-oncogene comes under the control of the active Ig locus, causing its constitutive overexpression which drives the disease[30,31]. Others, such as CLL, are not distinguished by a common genetic defect.

Another pivotal role in supporting lymphomagenesis is taken by the BCR. Ablation of BCR expression on mature B-cells in mice leads to apoptosis, establishing BCR

signaling as a determinant of B-cell survival[32,33]. There is strong evidence that stimulation by antigen binding contributes to survival and proliferation of lymphoma cells. Whether this survival signal is supplied by autonomous or antigen-induced activation is a matter of ongoing debate[20].

An important role of the microenvironment (i.e. nurse-like cells, T-cells, mesenchymal stromal cells and matrix factors[34]) for the survival and/or proliferation of transformed B-cells is demonstrated by lack *in vitro* proliferation of many lymphoma cells without its support. FL cells, for example, require co-culture with $CD4^+$T-cells or stromal cells[35], whereas CLL cells need support by stromal cells (or their secreted factors) and CD40 ligand to keep in culture or proliferate, respectively[36-38]. In part, this interaction involves signaling through the BCR.

Lastly, B-cell transformation can be caused by viral infection, most frequently by Epstein-Barr virus (EBV), a herpes virus found in almost all endemic Burkitt's lymphoma and post-transplant lymphoma, and about 40% of classical Hodgkin's lymphoma[39-41]. EBV-encoded latent genes induce transformation by altering cellular gene transcription and constitutively activating key cell-signaling pathways[41].

1.3 Chronic Lymphocytic Leukemia (CLL)

Chronic lymphocytic leukemia (CLL) is characterized by the progressive accumulation of immunoincompetent $CD5^+$ B-lymphocytes, mostly arrested in G_0/G_1 phase of the cell cycle, in blood, bone marrow, lymph nodes and spleen[42]. It represents about 25-30% of all leukemias, making it the most common adult leukemia in Western countries[43]. CLL is diagnosed in 3.9 per 100 000 individuals in the U.S. annually at a median age of 72, and the incidence is nearly twice as high in men than in women[44]. While patients are usually asymptomatic at diagnosis, lymph node enlargement, constitutional symptoms and bone marrow failure are common symptoms at later stages. CLL is a very heterogeneous malignancy. Whereas it is indolent in most cases and can be monitored over years without treatment ('watch and wait' strategy), it is more aggressive in others who show a poor response to standard treatment and a survival of less than two years[45-47].

Various pathogenic mechanisms have been discussed, which include chromosomal aberrations[46,48], gene mutations[49-51], altered DNA methylation[52], deregulated (micro) RNA expression levels[53], antigen-triggered and autonomous BCR signaling[54,55] as well as the microenvironment[56]. The identification of molecular subgroups has greatly improved the understanding of underlying biology, the prediction of clinical course of the disease and the development of more stratified treatment approaches.

1.3.1 Molecular subgroups

1.3.1.1 *IGHV* mutation status

CLL can be separated into cases that have mutated *IGHV* genes and those with unmutated *IGHV* genes (defined as at least 98% sequence homology with the germline *IGHV* genes). The clinical and biological behaviour of the two subsets differs substantially, with patients of unmutated *IGHV* showing significantly poorer survival (Figure 4)[28,29,42,57].

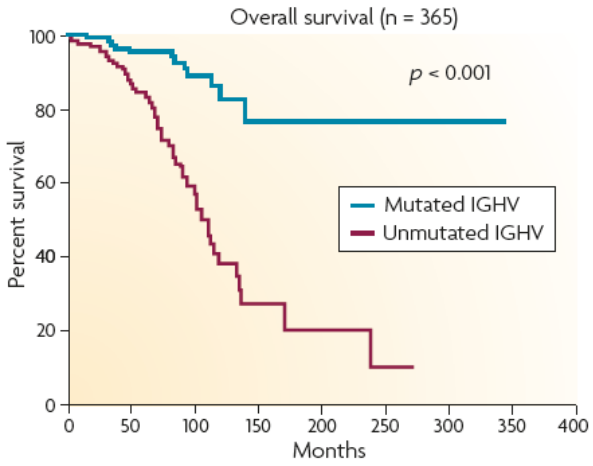

Figure 4. CLL patient survival by *IGHV* mutation status. Patients with *IGHV* unmutated genes show poorer survival than those with mutated *IGHV* (Zenz *et al.*, 2010).

While this can in part be explained by the greater likelihood of *IGHV*-unmutated CLLs to carry high-risk genetic lesions such as 11q23 and 17p13[57,58], the prime underlying reason is a differential signaling capacity through the BCR. BCR signaling is reduced in *IGHV*-mutated CLLs[59] (see also section 1.3.2.1). Unmutated CLLs additionally show higher expression levels of CD38 and tyrosine kinase zeta associated protein 70 (ZAP70), which enhance BCR signaling[60-62]. In line with this, unmutated CLLs display a greater proliferative capacity *in vivo*, which is supported by the observation of reduced telomere lengths in those tumor cells[63-65].

1.3.1.2 Genomic aberrations

Approximately 80% of CLL cases show aberrations in a few frequently affected chromosomal regions. A deletion on chromosome 13q14.3 is the most frequent one (~55%, Table 1). Still, CLL tumor cells do not show a typical, causative somatic mutation pattern.

The minimally deleted region on 13q14.3 encodes two long non-coding genes (*DLEU1* and *2*) as well as *miR-15a* and *miR-16-1,* which were the first microRNA (miRNA) genes to be found deleted in cancer[53,66]. The next most frequent aberration is a mutation and/or deletion of the *ATM* (ataxia telangiectasia mutated) gene encoding a kinase activating

p53 upon DNA damage, which in turn is central to the induction of cell cycle arrest, DNA repair and apoptosis.

Table 1. The most frequent genomic aberrations in CLL overall, and in refractory cases.

Genetic aberration	Unselected (%)	Refractory (%)
1. del13q14 (*miR-15a, miR-16-1*)	55[48]	19[67]
2. *ATM* mutation	12-14[68,69]	?
3. del11q23 (*ATM*)	12-18[48,68]	19-20[67,70]
4. trisomy 12	16-17[48,57]	7[67]
5. *NOTCH1* mutation	5-12[71-73]	13[74]
6. *TP53* mutation	7-14[73,75,76]	37[74]
7. *SF3B1* mutation	4-9[72,73]	18[74]
8. del17p13 (*TP53*)	7-9[57,75]	30-32[67,70,77]

Del13q14 (as sole aberration) confers a good prognosis (Table 1, Figure 5). In contrast, the presence of *ATM* aberrations or a deletion and/or mutation of *TP53* encoding p53 on chromosome 17p13.1 associate with a particularly poor prognosis, since conventional chemoimmunotherapy often proves ineffective[78]. Consequently, *ATM* and *TP53* aberrations are frequent among in refractory patients (Table 1) and result in poor patient survival (Figure 5, see also section 1.3.2.2). The molecular pathomechanisms underlying other recurrent aberrations such as trisomy 12 and mutations of the membrane receptor *NOTCH1* and splicing factor *SF3B1* are less well understood[79-81].

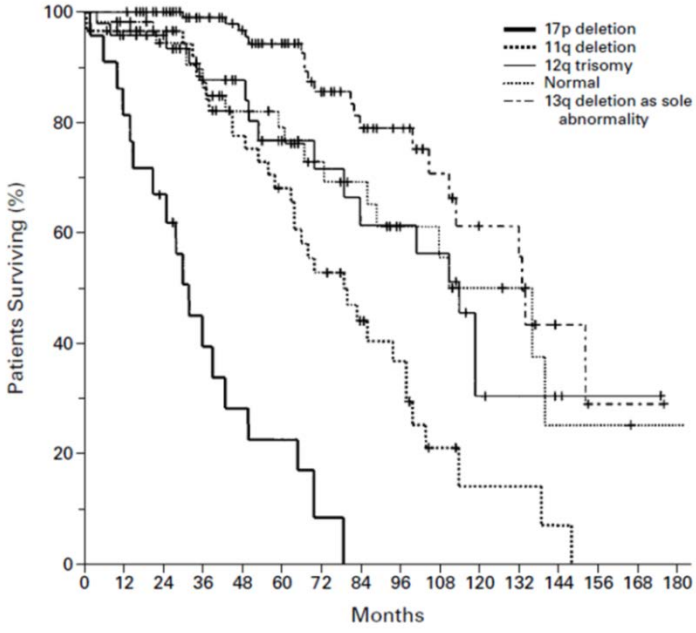

Figure 5. Probability of survival from diagnosis in CLL patients of five genetic subgroups.
(Dohner *et al.*, 2000).

1.3.2 Two key signaling pathways in CLL cell survival and proliferation

1.3.2.1 B-cell receptor signaling

Signaling through the BCR may have different consequences depending on the stage of maturation and/or (co-)activation of the B-cell. The same signals may result in apoptosis of immature or self-reactive B-cells, but in proliferation of selected, foreign antigen-specific mature cells[82]. In CLL, BCR signaling plays a vital role in the maintenance and expansion of the B-CLL clone, as indicated by a strong, constitutive activation of this signaling pathway[56,83,84]. Whether this activation is caused by specific (auto)antigens and/or cell-autonomous mechanisms is intensely debated. The concept of antigen-triggered BCR signaling is supported by a strong bias in *IGHV* gene usage. Of the ~50 functional human *IGHV* gene segments, only a selection is found highly enriched in CLL (e.g. VH1-69, VH3-21, VH3-07 and VH4-34)[85]. Moreover, in about 30% of CLL cases (both *IGHV* unmutated and mutated), the malignant cells express 'stereotyped' BCRs, i.e. the V regions of unrelated patients are nearly identical, indicating discrete antigens or structurally similar epitopes as disease drivers[54,86]. B-cells with mutated *IGHV* are thought to be selected and expanded by high-affinity binding to a restricted set of rare antigens that induce anergy[87]. In contrast, BCRs with unmutated *IGHV* sequences are considered polyreactive, enabling more frequent, low-affinity binding of the BCR and a higher BCR signaling activity[59,87,88]. This likely explains the higher tumor cell proliferation rates and poorer prognosis seen in CLL with unmutated *IGHV*.

Recently, two studies additionally suggested ligand independent ('tonic'), cell-autonomous BCR activation in CLL by binding of the heavy-chain complementarity determining region (HCDR3) on one BCR to an internal epitope of a neighboring BCR[55,89].

In any case, BCR activation has a distinct outcome: On the one hand, it triggers cytokine secretion by the CLL cells, shaping the supportive microenvironment by attracting monocytes and T-cells[38,90]. On the other hand, a powerful survival program is elicited upon downstream signaling originating from the oligomerization of BCR components (i.e. sIg and CD79A CD79B heterodimers (Ig-α/Ig-β)) and Lyn-mediated phosphorylation of the CD79A and B cytoplasmic tails[91-94] (Figure 6). The signal is further transmitted through a set of signaling pathways, particularly through spleen tyrosine kinase (SYK), Bruton's tyrosine kinase (BTK) and phosphoinositide 3-kinases (PI3Ks)[95] leading to the

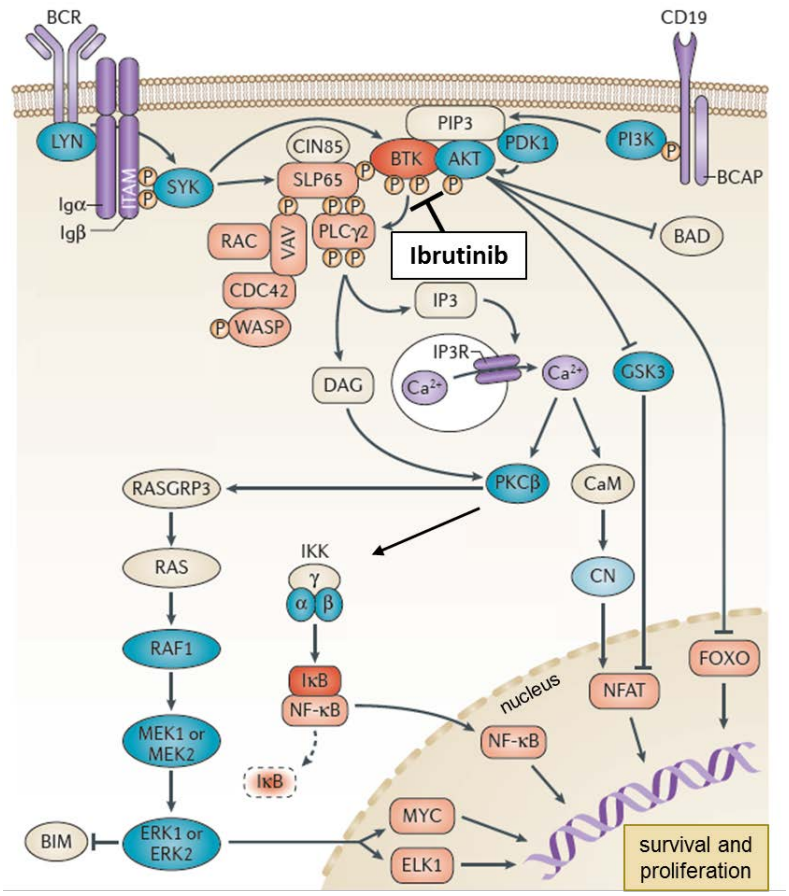

Figure 6. CLL BCR signaling with focus on Bruton's tyrosine kinase. BCR signaling results in the formation of a micro-signalosome composed of VAV, PI3K, BTK, SH2 domain-containing leukocyte protein of 65 kDa (SLP65) and phospholipase C2γ (PLCγ2), resulting in an influx of Ca^{2+}. This leads to activation of the transcription factors nuclear receptor of actiated T-cells (NFAT) and NF-κB as well as ERK. AKT is activated via PI3K, inhibiting forkhead box O (FOXO) transcription factors. BCAP, B cell adaptor for PI3K; BIM, BCL-2 interacting mediator of cell death; CaM, calmodulin; CIN85, CBL-interacting protein of 85 kDa; CN, calcineurin; DAG, diacylglycerol; GSK, glycogen synthase kinase; IκB, inhibitor of κB; IKK, inhibitor of NF-κB kinase;IP3, inositol trisphosphate; IP3R, IP3 receptor; PDK1, 3-phosphoinositide-dependent protein kinase 1; PIP3, phosphatidylinositol-3,4,5,-trisphosphate; PKC, protein kinase C (Hendriks *et al.* 2014, modified).

activation of nuclear factor kappa light-chain enhancer of activated B-cells (NF-κB)[56,96], protein kinase B/AKT[97], and extracellular signal-regulated kinase (ERK)[98] pathways.

BTK has proven to be an attractive drug target. Its inhibition with the recently developed covalent small-molecule inhibitor ibrutinib (PCI-32765) leads to decreased NF-κB and AKT-signaling and abrogation of CLL cell survival, and promises a major advance in CLL therapy[97-100]. As ibrutinib treatment resulted in a high frequency of durable remissions even in patients refractory to common chemotherapy in clinical trials up to stage III[95,101,102], it has been approved in 2014 for the treatment of refractory CLL in the U.S.. In line with a higher BCR signaling capacity in *IGHV* unmutated CLL patients, those show a better treatment response than *IGHV* mutated CLLs[95]. Likewise, the PI3Kδ inhibitor idelalisib has reached approval for the treatment of relapsed CLL in the U.S. this year[103,104], and a SYK inhibitor (fostamatinib) is in current development[105,106].

1.3.2.2 The p53 pathway

p53 is a key regulator of the cellular response to a broad range of stress signals including DNA damage and oncogene activation, as illustrated in Figure 7.

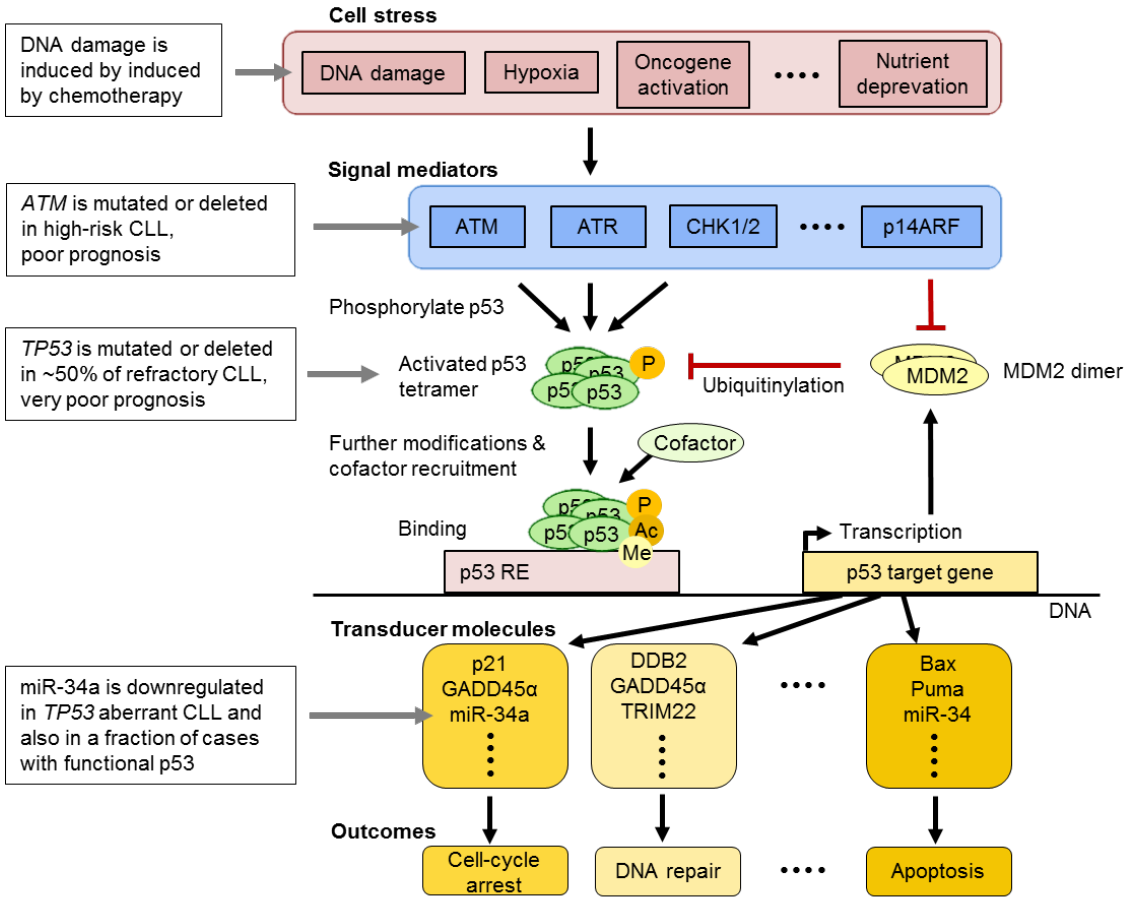

Figure 7. Mechanisms of p53 activation and regulation of downstream targets, highlighting components aberrant in CLL. Various stresses induce signal mediators increasing the half-life of p53 by phosphorylation or inhibition of its MDM2-mediated ubiquitinylation. Modifications such as acetylation (Ac) and methylation (Me) can further stabilize the protein homotetramer, which binds to a DNA p53 response element (p53 RE) and recruits cofactors to regulate the transcription of a nearby gene. Hundreds of genes can be transactivated, mediating outcomes including DNA repair, cell cycle arrest and apoptosis. ATR, ataxia telangiectasia and Rad3-related protein; CHK1/2, checkpoint kinase 1 and 2; DDB2, damage-specific DNA-binding protein-2; GADD45α, growth arrest and DNA-damage inducible α; TRIM22, tripartite motif containing-22; Bax, BCL2-associated X protein (based on Riley *et al.* 2008, Zenz *et al.* 2010, Bieging *et al.,* 2014).

In response to diverse cellular stresses that activate kinases such as ATM or inhibit the negative regulator MDM2 (double minute-2), p53 binds to p53 response elements (p53 RE) in the promoter regions of p53 target genes to activate, or - more rarely - repress

their transcription. Via transducer molecules such as GADD45α, p21 (CDKN1A) or Bax it mediates DNA repair, cell cycle arrest and apoptosis, respectively, to prevent the accumulation of genetic aberrations and maintain cellular integrity[107-110]. This key suppressor of tumorigenesis is mutated or functionally inactivated across human malignancies, enabling tumor cells to escape apoptosis, cell cycle arrest and senescence[108,109,111].

In CLL, p53 aberrations have direct implications for disease management, as they associate with progressive disease and are a main determinant of chemorefractoriness, resulting in a median survival of 3-4 years[92,93,70,112,113].

p53 deletions (del 17p13) and/or *TP53* mutations are present in about 10% of cases and up to 50% of refractory patients (Table 1). Deletions are monoallelic. In the majority of cases (>80%) the second allele is mutated[114]. *TP53* mutation in absence of 17p13 is infrequent (4-5%), but confers a similar prognosis to the patient as biallelic *TP53* inactivation[76,114], possibly due to the dominant negative effect of mutant over wild-type p53[16,115]. p53 aberrations are frequently subclonal, indicating an occurrence at later stages of tumor evolution. Beyond p53, further pathway members are often affected in CLL. Aberrations of ATM, the principal activator of p53 in the response to DNA double-strand breaks, by a deletion of 11q22-23 and/or mutation result in impaired *in vitro* DNA damage responses and reduced overall and treatment-free patient survival[68,69]. However, genetic aberrations of p53 and ATM explain only about 50-70% of poor patient outcomes, and the reason for refractoriness in the remaining cases remains largely unclear. In part it could be attributed to a low expression of p53 target miR-34a, which is associated with refractory CLL even in the absence of p53 aberrations[70,116].

1.4 microRNAs and long intergenic non-coding RNAs

1.4.1 Classification, biogenesis and function

microRNAs

microRNAs (miRNAs) represent a class of short, single-stranded non-coding RNAs of 17-25 nucleotide (nt) length which post-transcriptionally regulate the expression of the majority of protein-coding genes[117-119]. miRNAs are abundant in many human cell types. Since the initial discovery of lin-4 and let-7 in *C. elegans* in 1993[120], over 1800 human miRNAs have been annotated and listed in the miRNA reference database (miRBase v21). miRNAs are involved in the regulation of virtually all cellular processes including cell cycle, proliferation, apoptosis and differentiation[121]. Not surprisingly, their deregulation has been implicated in many diseases including cancer.

miRNA genes are transcribed by RNA polymerase II from intergenic, intronic or polycistronic loci, forming a miRNA precursor (pri-miRNA) of hairpin-shaped loop structure and several 100 nt length (see Figure 8). Processing by the Drosha-DGCR8 complex yields a ~70 nt pre-miRNA hairpin, which is exported to the cytoplasm and cleaved by the Dicer-TRBP complex, generating imperfect miRNA duplexes of mature miRNAs. These are incorporated into Argonaute (Ago2) protein complexes, forming the RNA-induced silencing complex (RISC) which retains one of the mature miRNA strands. Depending on which arm of the precursor the miRNA originates from, the mature miRNA is assigned the suffix -3p (3' arm) or –5p (5' arm, e.g. miR-155-5p). This miRNA functions as a guide, directing RISC to partially complementary sites in target mRNAs, where it binds to the 3' untranslated region. This results in silencing by translational inhibition, induced degradation and/or deadenylation of the respective mRNA[122,123].

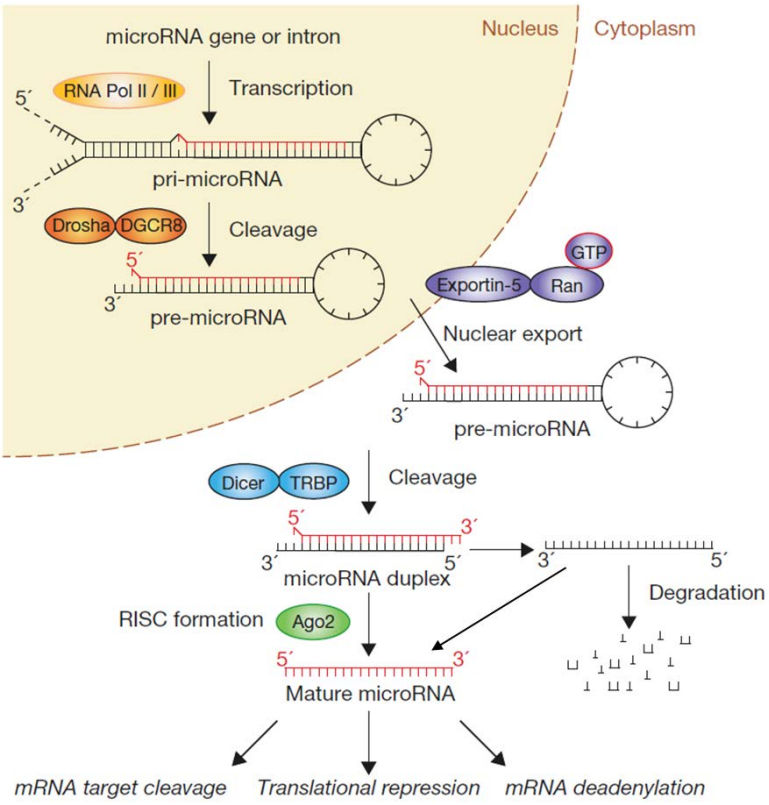

Figure 8. The miRNA biogenesis pathway. See text for explanations (Winter *et al.*, 2009, modified).

For miRNA target recognition, complementarity at miRNA positions 2-7, the 'seed region', is crucial and evolutionary conserved. Due its brevity (resulting in genomic ambiguity) and the nature of imperfect complementarity of the remaining sequence to the mRNA, one miRNA has tens to hundreds of mRNA targets[119]. Further, the functional activity of a miRNA in regulating a specific target is context-dependent and cell-type-specific, as its availability is additionally a function of abundance of alternative targets

'sponging' miRNA levels, and the affinity of the miRNA for binding to them[124-126]. One mRNA can be bound by multiple miRNAs acting in concert to regulate their target and building regulatory networks. miRNAs whose sequence only differs by one or two nucleotides (likely to have similar targets) are annotated with an additional lower case letter (e.g. miR-320a, miR-320b).

Long non-coding RNAs

Less than 2% of the human genome encodes for proteins, however, up to 80% is actively transcribed[127,128]. Substantial advances in whole-transcriptome sequencing technologies have revealed the widespread transcription of long non-coding RNA (lncRNA), which are differentiated from small non-coding RNA (such as miRNA, snoRNA (small nucleolar RNA) or piRNA (PIWI-interacting RNA)) by their length of >200 nt. It is a very heterogeneous class which is generally poorly conserved[129-131]. LncRNAs are classified according to their position relative to protein coding genes, comprising long intergenic ncRNA (lincRNA), intronic lncRNA, antisense lncRNA, transcribed pseudogenes and enhancer RNA (eRNA)[132]. The most recent release from Gencode (v19) has annotated ~14 000 human lncRNA genes[133]. In their biogenesis, lncRNA share many characteristics with mRNAs: They are transcribed mostly by RNA polymerase II and frequently show polyadenylation[134] and 5'-methylguanosine capping[135]. However, they are lowly expressed on average (about 10-fold lower than mRNA) and display a higher degree of tissue-specific expression[136,137].

Interestingly, lncRNA have been proposed as a new and potentially crucial layer of gene regulation, while the function of the majority of lncRNAs remains unknown[138]. Through their arbitrary definition by sequence length but not functional unity, a great diversity in underlying functional mechanisms to regulate gene expression in *cis* and in *trans* has been described[138,139]. One of the best-studied examples is Xist (X-inactive specific transcript), which was found to be expressed exclusively from the inactive X chromosome, and later demonstrated to mediate X chromosome silencing in female mammals through chromatin remodeling[140,141]. It was proposed to act in *cis* by remaining tethered to its site of transcription, affecting neighbouring gene regions – a model thought to be valid for a group of lncRNA that e.g. disrupt the transcription machinery by DNA binding or foster transcription by attracting transcriptional coactivators[138]. In contrast, others have been described to act in *trans* by associating with DNA-binding and regulatory proteins to guide their localization and affect target gene expression[142]. This is the case for HOTAIR, which functions as a molecular scaffold for histon modifying complexes[143]. However, the mechanisms of lncRNA function are as diverse as the group itself, further including disruption of translation, modulation of mRNA stability, masking

miRNA binding sites or acting as miRNA 'sponges'. Some lncRNA have structural functions as core components of nuclear bodies such as speckles and paraspeckles[138].

1.4.2 Role in human cancer and CLL

microRNAs

In 2002, Calin *et al.* made the seminal observation of frequent deletions and down-regulation of miR-15 and miR-16 (on 13q14) in CLL, suggesting a role of miRNA deregulation in cancer[53]. Low miR-15 and miR-16 levels have been implicated in CLL pathogenesis by increasing the expression of anti-apoptotic Bcl-2 (B-cell lymphoma 2)[66].

It has been shown that aberrant miRNA expression frequently contributes to cancer formation through deregulation of cell cycle control, proliferation, apoptosis, differentiation, migration and/or epigenetic mechanisms[144-149]. By targeting mRNA of oncogenes or tumor suppressor genes, miRNAs can function as tumor suppressors or oncogenes themselves. The oncogenic miR-17~92 cluster serves as prominent example, in which individual miRNAs target tumor suppressive members of the Bcl-2 family in acute lymphoblastic leukemia[150]. In CLL, a downregulation of miR-29 and miR-181 targeting oncogenic TCL-1 is suggested to contribute to pathogenesis[151].

Aberrant miRNA function and regulation can originate from sequence variations in miRNA genes, from aberrant transcription mediated by epigenetic mechanisms[152-154] as reported in gastric and colorectal cancer[155,156] from deregulated transcription factor activity or from impaired function of the miRNA processing machinery (e.g. Drosha, Dicer) as reported also in CLL[157-159].

Characteristic miRNA expression profiles may be exploited for early tumor detection, classification and prognosis[160-162]. This is particularly interesting in solid cancers that are difficult to access but display characteristic miRNA expression changes in the peripheral blood, as in pancreatic and lung cancer[163,164]. The remarkable stability of miRNAs in biological samples owed to relative resistance to ribonuclease degradation additionally renders them to be promising biomarkers[165]. In CLL, the expression of a set of miRNAs associates with prognosis and progression[166-168].

First miRNA-based therapeutics are in clinical development, primarily as replacement therapies to reintroduce miRNAs that are downregulated or lost in cancer cells[122]. Here, p53 downstream target miR-34a, itself a tumor suppressor downregulated in del17p/*TP53*^{mut} (and) high-risk CLL[70,116,169,170] and a broad range of other malignancies[171], was the first miRNA mimic to reach phase I clinical trials in 2013 (clinicaltrials.gov identifier NCT01829971)[171,172].

Long non-coding RNAs

There is increasing evidence for a crucial role of lncRNA deregulation in human diseases including cancer[173-176]. One of their major roles is to guide the site specificity of chromatin-modifying complexes, impacting on epigenetics. In this context, HOTAIR overexpression was shown to greatly influence gene expression to promoting invasiveness and metastasis formation in epithelial cancer cells through retargeting of chromatin structure remodeling polycomb proteins[174]. Xist has been found a potent suppressor of hematologic cancer in mice, as Xist loss resulted in X reactivation and genome-wide, cancer-promoting changes[177]. As a component of the RNA processing machinery controlling alternative pre-mRNA splicing, lncRNA MALAT1 was found overexpressed in various cancers[176] and linked to an increase in proliferation and migration in lung[178] and colorectal cancer[179]. Other lncRNAs have been described as key regulators of signaling pathways underlying carcinogesis such as the p53 pathway, as detailed in section 1.4.3.

In CLL, an altered expression profile of transcribed ultraconserved regions (T-UCR) has been reported[180] and lncRNA BIC (B-cell integration cluster) comprising oncogenic miR-155 was found overexpressed[181]. Further, the lncRNA genes *DLEU1* (deleted in leukemia) and *DLEU2* span the minimally deleted region of 13q14[182]. DLEU1 and 2 have been suggested to act on miR-15a/miR-16-1 transcription in *cis,* eventually downregulating NF-kB levels[183] and supporting tumor cell survival. A comprehensive understanding of the role of lncRNAs in CLL is lacking.

LncRNA expression is useful for refinement of diagnosis and prognostication in some cancers[184,185], whereas the exploitation of lncRNAs as therapeutic agents is still in its very beginning[186].

1.4.3 miRNAs and lncRNAs displaying BCR- or p53-dependent regulation in CLL

microRNAs

Whereas numerous studies associated miRNA expression profiles to CLL *IGHV* mutation status[169,187-189], direct BCR signaling-dependent miRNA expression has been reported only once. Upon BCR activation with anti-IgM *in vitro* and microarray-based quantification of miRNA expression changes, Pede *et al.* found the miR-132/miR-212 cluster, miR-155-3p, miR-20a-3p and miR-19b-1-5p induced[190]. However, miRNA identification was confined to the sequences on the array, and anti-IgM sets an unphysiological trigger to the pathway. Further, no direct connection to tumor cell survival or proliferation was drawn, as the targets of those miRNAs in the investigated

setting remained undetermined. Of note, in no other B-cell malignancies, a systematic screen for BCR signaling dependently expressed miRNAs has been performed.

The only established miRNA transcriptionally targeted by p53 in CLL is miR-34a-5p[70,116,169,170,191]. DNA-damaging irradiation has been shown to induce its expression[116]. miR-34 has been originally characterized as a p53 target in lung, colon and epithelial ovarian cancer cells as well as fibroblasts by several groups in parallel[192-196]. It inhibits cell-cycle progression by targeting cyclin-dependent kinases 4[163], and 6[192,197], cyclin D1[197] and transcription factor E2F3[197,198], and promotes apoptosis by targeting anti-apoptotic BCL2[196] and survivin[199]. No systematic screen for (further) p53 targets in CLL has been reported. In other tumor cells though, numerous p53-regulated miRNAs have been identified such as miR-107[200], miR-145[201] and miR-182[193]. On the other hand, miRNAs including miR-504 were described to target p53[202]. However, most miRNAs reported to target or be targeted by p53 greatly vary between entities and may be irrelevant for CLL.

Long non-coding RNAs

So far, the role of lncRNAs in BCR signaling remains unknown, and p53-dependent lncRNAs in CLL cells have not been investigated.

In contrast, several p53-dependent lncRNAs have been established in other entities (Figure 9). The lincRNAs PANDA (p21 associated ncRNA DNA damage activated) and lincRNA-p21 are located ~5 kb and ~15 kb upstream of the p21 transcription start site, respectively, but expressed independently from p21. Whereas PANDA was shown to mediate anti-apoptotic functions of p53 through sequestering transcription factor NF-YA away from pro-apoptotic target genes (e.g. Puma, Noxa)[203], lincRNA-p21 mediates repressive functions of p53 to promote apoptosis upon DNA damage[204]. In the HeLa cell line, lincRNA-p21 was shown to physically associate with *JUNB* and *CTNNB1* mRNAs, lowering their translation[205]. Recent large chromatin immunoprecipitation (ChIP)-based sequencing screens for p53 targets in cell lines provide a basis for the identification and functional characterization of novel p53-dependent lncRNAs[206-209].

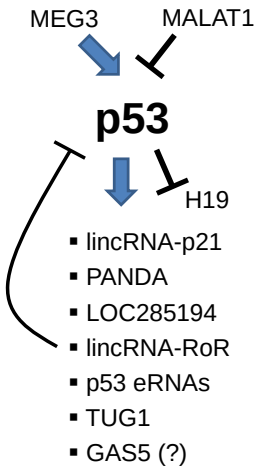

Figure 9. Long non-coding RNAs as regulators and targets of p53.
A set of lncRNAs has been functionally characterized as p53 targets. See text for details. The direct regulation of GAS5 by p53 is being discussed. MEG3, maternally expressed 3; TUG1, taurine upregulated gene 1; GAS5, growth arrest-specific 5, eRNAs, enhancer RNAs[142,210,211].

1.5 Aims of this work

The role of non-coding RNAs in promoting CLL cell survival and resistance to apoptosis remains poorly understood. Active B-cell receptor (BCR) signaling strongly supports B-cell survival and is upregulated in CLL. The tumor suppressive p53 pathway is a key mediator of apoptosis and frequently hit by genomic aberrations, which confer a particularly poor prognosis to CLL patients.

This work set out to identify 1) BCR and 2) p53 signaling-dependent microRNAs and further non-coding RNAs in primary CLL by a comprehensive next-generation small RNA sequencing-based screen. Pharmacologic inhibitors and the impaired transcriptional activity of mutant p53 in primary CLL cells were used to define novel ncRNA targets of both pathways.

The results of this work provide insight into the involvement of miRNAs in promoting primary CLL cell survival upon BCR signaling. Moreover, an overview of p53-regulated miRNA expression and the identification of novel p53-dependent long ncRNAs shall provide a better understanding of (the effects of) impaired p53 activity in CLL and potentially across cancer. In a translational sense, this work can pave the way to targets for novel, ncRNA-based therapeutic approaches.

2 Material and Methods

2.1 Material

2.1.1 Chemicals and Biochemicals

Reagent	Supplier
2-Propanol	Sigma-Aldrich, St. Louis, USA
Agarose, ultra-pure (Invitrogen)	Thermo Fisher Scientific, Waltham, USA
Annexin V 10x binding buffer	Becton Dickinson, Franklin Lakes, USA
Annexin V- APC	Becton Dickinson, Franklin Lakes, USA
Benzonase	VWR, Radnor, USA
CellTiter-Glo®	Promega, Madison, WI, USA
Chloroform	Carl Roth, Karlsruhe, Germany
DMSO	Sigma-Aldrich, St. Louis, USA
DNA ladder 50bp, 100 bp (Invitrogen)	Thermo Fisher Scientific, Waltham, USA
DNase I	Roche, Mannheim
Ethanol	Sigma-Aldrich, St. Louis, USA
Ethidium Bromide	Applichem, Darmstadt, Germany
Glycogen	Thermo Fisher Scientific, Waltham, USA
Ficoll-Paque Premium	VWR, Radnor, USA
Ibrutinib (PCI-32765)	Selleckchem, Munich, Germany
Laemmli buffer, 2x concentrate	VWR, Radnor, USA
Loading Dye, 5x	Thermo Fisher Scientific, Waltham, USA
LS columns	Miltenyi, Bergisch Gladbach, Germany
MACS BSA Stock Solution	Miltenyi, Bergisch Gladbach, Germany
MACS Rinsing Solution	Miltenyi, Bergisch Gladbach, Germany
Methanol	Sigma-Aldrich, St. Louis, USA
Milk powder	Carl Roth, Karlsruhe, Germany
Mouse serum	Agilent Technologies, Santa Clara, USA
Nutlin-3	Absource Diagnostics, Munich, Germany
PageRuler Prestained Protein Ladder (Fermentas)	Thermo Fisher Scientific, Waltham, USA
Phosphate buffered saline (PBS) (Invitrogen)	Thermo Fisher Scientific, Waltham, USA
PhosSTOP	Roche, Basel, Switzerland
Power SYBR Green PCR Master Mix	Thermo Fisher Scientific, Waltham, USA
Propidium Iodide	Sigma-Aldrich, St. Louis, USA

RNase away	Thermo Fisher Scientific, Waltham, USA
RNase-free water (Ambion)	Thermo Fisher Scientific, Waltham, USA
Sodium Acetate, 3 M, pH 5.2	Sigma-Aldrich, St. Louis, USA
SYBR® Gold Nucleic Acid Gel Stain	Thermo Fisher Scientific, Waltham, USA
TAE running buffer 1.2 M, 40x	Serva Electrophoresis, Heidelberg, Germany
TaqMan Universal PCR Master Mix II, no UNG	Thermo Fisher Scientific, Waltham, USA
Trizol (Invitrogen)	Thermo Fisher Scientific, Waltham, USA
Western Lightning® Plus-ECL, Enhanced Chemiluminescence Substrate	PerkinElmer, Waltham, USA

2.1.2 Consumables

Consumable	Supplier
Sealing film for PCR plates	Steinbrenner, Wiesenbach, Germany
Sealing film for qPCR plates	Roche, Basel, Switzerland
Cell culture flasks, T25, T75 EasyFlask	Thermo Fisher Scientific, Waltham, USA
Cell culture plates, 6-well, 12-well	Greiner BioOne, Kremsmünster, Austria
Conical tubes 15 ml, Falcon®	VWR, Radnor, USA
Conical tubes 50 ml, Falcon®	VWR, Radnor, USA
Cryo vials, system 100, PP, 2ml	VWR, Radnor, USA
Cryo-Babies®	Diversified Biotech, Dedham, USA
Eptips LoRetention, PCR-clean	Neolab, Heidelberg, Germany
FACS Tubes, BD™ Falcon™ Round-Bottom Tube (5ml)	Becton, Dickinson and Company, Franklin Lakes, USA
FasRead102 Disposable counting chambers	Immune systems, Paignton, UK
Filtertips 10µl, 20µl, 200µl, 1000µl	Starlab, Hamburg, Germany
Gel breaker tubes 3388-100	IST Engineering, Milpitas, USA
Leucosep falcons, sterile	Th. Geyer, Renningen, Germany
Mini-PROTEAN-TGX gels 4-15%, 10-well	Bio-Rad, Hercules, USA
Novex® Hi-Density TBE Sample Buffer, 5x (Invitrogen)	Thermo Fisher Scientific, Waltham, USA
Novex® TBE PAGE gel, 1.0 mm, 6% (Invitrogen)	Thermo Fisher Scientific, Waltham, USA
Novex® TBE running buffer, 5x (Invitrogen)	Thermo Fisher Scientific, Waltham, USA
Pasteur pipettes, disposable	Carl Roth, Karlsruhe, Germany

PCR tube strips 0,5 ml	Biozym, Hessisch Oldendorf, Germany
PCR tubes 0,5 ml	Biozym, Hessisch Oldendorf, Germany
Pipettes 2ml, 5ml, 10ml, 25ml, 50ml	Corning, New York, USA
Pipetting reservoir	Corning, New York, USA
Cryotube-print labels	Steinbrenner, Wiesenbach, Germany
Qubit assay tubes	Thermo Fisher Scientific, Waltham, USA
Reaction plates for PCR, 96-well	Greiner BioOne, Kremsmünster, Austria
Reaction plates for qPCR, 384-well	Roche, Basel, Switzerland
Reaction plates for qPCR, 96-well	Greiner BioOne, Kremsmünster, Austria
Reaction tubes 0,5 ml, 1,5 ml, 2 ml	Eppendorf, Hamburg, Germany
Ribbon cartrige	Steinbrenner, Wiesenbach, Germany
Scalpel, disposable	Feather, Osaka, Japan
Scepter sensors - 40 µl	Merck Millipore, Billerica, USA
Spin-X® Centrifuge Tube Filters	Sigma-Aldrich, St. Louis, USA
Trans-Blot® Turbo™ mini-size transfer stacks	Bio-Rad, Hercules, USA
PVDF membrane	Bio-Rad, Hercules, USA
Scepter sensors 40µm	Merck Millipore, Billerica, USA

2.1.3 Antibodies

Antibody	Supplier
Anti-mouse IgG (HRP)	Abcam, Cambridge, UK
Anti-rabbit IgG (HRP)	Abcam, Cambridge, UK
CD19-beads	Miltenyi, Bergisch Gladbach, Germany
CD19-PE	Becton, Dickinson and Company, Franklin Lakes, USA
GAM-RPE	Agilent Technologies, Santa Clara, USA
Mouse anti-human p53, DO-1	Becton, Dickinson and Company, Franklin Lakes, USA
Rabbit anti-human GAPDH	Abcam, Cambridge, UK

2.1.4 Primers for qRT-PCR

All oligonucleotides were ordered from Eurofins MWG Operon, Ebersberg.

Gene	5' → 3'	Reference
p21 forward (fwd)	TGTCCGTCAGAACCCATGC	own design
p21 reverse (rev)	AAAGTCGAAGTTCCATCGCTC	
Lamin B1 fwd	TCGCAAAAGC ATGTATGAAGA	Sun *et al.*[212]
Lamin B1 rev	CTCTACCAAGCGCGTTTCA	
lincRNA-p21 fwd	GGGTGGCTCACTCTTCTGGC	Huarte *et al.*[204]
lincRNA-p21 rev	TGGCCTTGCCCGGGCTTGTC	
NEAT1 fwd	CTTCCTCCCTTTAACTTATCCATTCAC	Zhang *et al.*[213]
NEAT1 rev	CTCTTCCTCCACCATTACCAACAATAC	
NEAT1 promoter fwd	GGAGATACAGTCAGGAAGAGA	own design
NEAT1 promoter rev	CACAGAAGGTGGTGATGTG	
p21 promoter fwd	CTGGACTGGGCACTCTTGTC	Mattia *et al*.[214]
p21 promoter rev	CTCCTACCATCCCCTTCCTC	

Reagent	Supplier
TaqMan® small RNA assays (Applied Biosystems)	Thermo Fisher Scientific, Waltham, USA

2.1.5 Commercial Kits

Kit	Supplier
DNA 1000 Kit	Agilent, Santa Clara, USA
High Sensitivity DNA Kit	Agilent, Santa Clara, USA
NEBNext® Multiplex Oligos for Illumina	New England Biolabs, Ipswich, USA
NEBNext® Small RNA Library Prep Set for Illumina	New England Biolabs, Ipswich, USA
Pierce BCA Protein Assay Kit	Thermo Scientific, Waltham, USA
QIAquick® PCR Purification Kit	Qiagen, Venlo, Netherlands
Quant-iT™ RNA Assay Kit (Invitrogen)	Thermo Scientific, Waltham, USA
RNA 6000 Nano Kit	Agilent, Santa Clara, USA
SuperScript® III Reverse Transcriptase Super Mix	Thermo Scientific, Waltham, USA
TURBO DNA-free™ Kit (Ambion)	Thermo Scientific, Waltham, USA

2.1.6 Primary human material

Peripheral blood from 72 patients selected for having high lymphocyte fractions (more than 76%) and fulfilling standard diagnostic criteria for CLL were obtained. The majority of patients was enrolled at the University Hospital of Heidelberg. RNA derived from peripheral blood mononuclear cells of 13 CLL patients used as part of the validation cohort for p53-dependent lincRNA-p21 induction (section 3.5.4.1) was kindly supplied by the European Research Initiative on CLL (ERIC). All patients provided written informed consent in accordance with the Declaration of Helsinki and approval obtained from the local Institutional Review Board (S-206/2011 and Te Raa *et al.*[215]). The patient cohort was selected to represent meaningful numbers of patients from high-risk groups. Clinical and genetic patient characteristics are summarized in Table 3 and S1. Buffy coats from two healthy individuals were obtained from the Heidelberg Blood Bank.

2.1.7 Cell lines

Cell line	Supplier
BL-2	DSMZ, Braunschweig, Germany
BL-7	Dr. G. M. Lenoir, IARC, Lyon, France
BL-60	Dr. G. M. Lenoir, IARC, Lyon, France
BJAB	DSMZ, Braunschweig, Germany
CA-46	DSMZ, Braunschweig, Germany
Cheptanges	A. Rickinson, Birmingham, UK
HeLa	DSMZ, Braunschweig, Germany
Ly-47	Dr. G. M. Lenoir, IARC, Lyon, France
Namalwa	DSMZ, Braunschweig, Germany
Ramos	DSMZ, Braunschweig, Germany
Salina	A. Rickinson, Birmingham, UK
Seraphine	A. Rickinson, Birmingham, UK

Cell lines were authenticated using Multiplex Cell Authentication by Multiplexion (Heidelberg, Germany) as described[216]. The single nucleotide polymosphism profiles matched known profiles or were unique.

2.1.8 Cell culture media and additives

Material	Supplier
Fetal Bovine Serum (for washing)	PAN-Biotech, Aidenbach, Germany

Fetal Bovine Serum (for cell culture)	Life Technologies, Carlsbad, USA
Human Serum	Sigma-Aldrich, St. Louis, USA
RPMI Medium 1640 (Gibco)	Thermo Scientific, Waltham, USA

2.1.9 Self-prepared Buffers

Buffer	Composition (final concentration)	Supplier
10x PBST buffer (phosphate buffered saline with Tween 20)	27 mM KCl	Carl Roth, Karlsruhe, Germany
	1.37 M NaCl	VWR, Radnor, USA
	0.5 % Tween 20	Sigma-Aldrich, St. Louis, USA
	100 mM Na2HPO4	Carl Roth, Karlsruhe, Germany
	20mM KH2PO4	Carl Roth, Karlsruhe, Germany
	in H_2O	
RIPA buffer	150 mM NaCl	VWR, Radnor, USA
	0.5 % Na-Desoxycholate	Applichem, Darmstadt, Germany
	1 % Nonidet P-40	Applichem, Darmstadt, Germany
	0.1 % SDS	Bio-Rad, Hercules, USA
	50 mM Tris pH 7.5	Applichem, Darmstadt, Germany
	in H_2O	

2.1.10 Instruments

Instrument	Supplier
-20°C Freezer	Liebherr, Biberach an der Riß, Germany
-80°C Freezer	Sanyo (Panasonic), Osaka, Japan
Analytical Balance TE 124S	Sartorius, Göttingen, Germany
Bioanalyzer 2100	Agilent, Santa Clara, USA
Camera Lumix DMC-FZ50	Panasonic, Osaka, Japan
Cell culture hood HeraSafe	Thermo Scientific, Waltham, USA
Cell culture incubator HeraCell 150	Thermo Scientific, Waltham, USA
Centrifuge 5424	Eppendorf, Hamburg, Germany
Centrifuge 5430	Eppendorf, Hamburg, Germany
Centrifuge Heraeus Fresco 17	Thermo Scientific, Waltham, USA
Centrifuge Heraeus Megafuge 16	Thermo Scientific, Waltham, USA
ChemiDoc™ XRS+ Imaging System	Bio-Rad, Hercules, USA

Chip Priming Station	Agilent, Santa Clara, USA
Cluster Station	Illumina, San Diego, USA
Cobas z 480	Roche, Basel, Switzerland
Cryogenic Freezer MVE 1500 series	MVE BioMedical, Ball Ground, USA
Electrophoreses Power Supply 200/2000	Elchrom Scientific, Cham, Switzerland
Eppi Rotator SB3	Bibby Scientific (Stuart), Stone, UK
Flow Cytometer LSR II	Becton, Dickinson and Company, Franklin Lakes, USA
Fridge Medline	Liebherr, Biberach an der Riß, Germany
Heating block TS-100	Peqlab, VWR, Radnor, USA
HiSeq2000	Illumina, San Diego, USA
Infinite M200 Pro®	TECAN, Männedorf, Switzerland
LabChip® XT	Perkin Elmer, Waltham, USA
Label printer BMP71	Brady, Milwaukee, USA
LightCycler 480 384-well	Roche, Basel, Switzerland
Microscope Axiovert 40C	Zeiss, Oberkochen, Germany
Microwave	Bartscher, Salzkotten, Germany
Minishaker MS1	IKA, Staufen, Germany
NanoDrop® Spectrophotometer ND-1000	Peqlab, VWR, Radnor, USA
Nitrogen System	German-Cryo, Jüchen, Germany
PAGE chambers	Bio-Rad, Hercules, USA
Pipetboy	Peqlab, VWR, Radnor, USA
Pipetboy acu	Integra Biosciences, Fernwald, Germany
Pipettes Research® (10µl; 20µl; 200µl; 1000µl)	Eppendorf, Hamburg, Germany
QuadroMACS separator	Miltenyi, Bergisch Gladbach, Germany
Qubit® 2.0 Fluorometer	Thermo Fisher Scientific, Waltham, USA
Scepter Handheld automated cell counter	Merck Millipore, Billerica, USA
SDS-PAGE chambers	Peqlab, VWR, Radnor, USA
SpeedVac	Thermo Fisher Scientific, Waltham, USA
Spin-down Galaxy Mini	VWR, Radnor, USA
TC10™ Automated Cell Counter	Bio-Rad, Hercules, USA
Thermocycler	Biometra, Göttingen, Germany
Transilluminator	Biotec-Fischer, Reiskirchen, Germany
Trans-Blot Turbo Transfer System	Bio-Rad, Hercules, USA
Water bath Lauda®AL5	VWR, Radnor, USA

XRAD 320	Precision X-ray, North Branford, USA

2.1.11 Software

Software	Supplier
Agilent 2100 Bioanalyzer	Agilent, Santa Clara, USA
Axiovision Rel. 4.8	Zeiss, Oberkochen, Germany
Endnote	Thomson Reuters, New York, USA
FACS Diva	Becton, Dickinson and Company, Franklin Lakes, USA
GraphPad Prism 5	GraphPad Software Inc., La Jolla, USA
Image Lab 3.0	Bio-Rad, Hercules, USA
Ingenuity®	Qiagen, Redwood City, USA
Lasergene 8	DNAStar, Madison, USA
Light Cycler 480 SW 1.5	Roche, Basel, Switzerland
Microsoft Office 2007	Microsoft, Redmond, USA
NanoDrop® ND-1000 V3.2.1	Coleman Technologies, Langley, Canada
Photoshop CS5.1	Adobe, San Jose, USA
R 3.0.1	open source
STG Picture Merge	Starglider Systems
Tecan i-control 1.6	TECAN, Männedorf, Switzerland

2.1.12 Databases and online tools

Name	Address
BLAST (NCBI)	http://blast.ncbi.nlm.nih.gov/Blast.cgi
Ensembl	http://www.ensembl.org/index.html
GtRNAdb	http://gtrnadb.ucsc.edu/
IDT PrimerQuest	http://eu.idtdna.com/Primerquest/Home/Index
miRBase	http://mirbase.org/
miRanda	http://www.microrna.org/microrna/home.do
miRwalk	http://www.umm.uni-heidelberg.de/apps/zmf/mirwalk/
PicTar5	http://pictar.mdc-berlin.de/
piRNA cluster - database	http://www.uni-mainz.de/FB/Biologie/Anthropologie/492_DEU_HTML.php
NCBI Build 37 piRNA	http://www.uni-mainz.de/FB/Biologie/Anthropologie/492_DEU_HTML.php

Primer3Plus	http://www.bioinformatics.nl/cgi-bin/primer3plus/primer3plus.cgi/
Rfam	http://rfam.xfam.org/
SNP-BLAST	www.ncbi.nlm.nih.gov/projects/SNP/SNPBlast.html
TarBase	http://diana.imis.athena-innovation.gr/DianaTools/index.php?r=tarbase/index
UCSC Genome Browser	https://genome.ucsc.edu/

2.1.13 Other

Material	Supplier
Freezing Boxes	Nalgene, Rochester, USA
Western incubation box (medium)	Li-cor, Lincoln, USA

2.2 Cell culture methods

2.2.1 Isolation of mononuclear cells from whole blood

Peripheral blood (PB) samples from CLL patients were collected in heparin-coated tubes. Mononuclear cells (MNCs) were isolated by density gradient centrifugation of 30 ml whole blood over 15 ml Ficoll-Paque Premium at 800x g, room temperature (RT) for 20 min in 50 ml Falcon tubes. The resulting PBMNC layer was harvested and washed twice with PBS supplemented with 2% FBS. PMNCs were resuspended in RPMI containing 10% FBS for further processing.

2.2.2 Magnetic activated cell sorting (MACS)

For enrichment of B-lymphocytes from peripheral blood mononuclear cells (PBMNCs) of healthy individuals, activated cell sorting with CD19 magnetic beads was performed according to the manufacturer´s protocol. To this end, after cell counting and centrifugation, cells were resuspended in 80 µl MACS buffer per $1x10^7$ PBMCs. 20 µl magnetic beads were added, followed by a 15 min incubation at 4°C in the dark. After a subsequent washing step, cells were purified on MACS LS columns during exposure to a strong magnetic field. To increase purity, B-cells were purified sequentially over 2 columns.

CD19 positive-selected B-cells were stained with a secondary goat anti-mouse antibody for subsequent FACS analyses (see 2.2.5). The cells had purities of at least 99% after MACS enrichment.

2.2.3 Freezing, thawing and culturing of primary cells and cell lines

Isolated PBMNCs were split into aliquots of $1x10^7$-$5x10^8$ cells and cryopreserved in RPMI supplemented with 10% FBS, 1% Penicilline/Streptomycine and 7,5% DMSO.

Cell lines were cryopreserved at $5x10^6$-$1x10^7$ cells per aliquot in RPMI supplemented with 10% FBS and 10% DMSO.

For culturing, cells were thawed in a waterbath pre-warmed to 37°C, transferred to PBS with 2% FBS for washing and resuspended in the desired cell culture medium.

CLL primary samples were cultured in RPMI 1640 supplemented with 10% heat inactivated human serum (HS) at 37°C and 5% CO_2. Only for the pilot small RNA sequencing screen, cells were cultured in 10% FBS instead of HS. With the exception of BL-7, all Burkitt's lymphoma (BL) cell lines as well as HeLa were kept in RPMI 1640 with 10% FBS at 37°C and 5% CO_2. BL-7 was cultured with 20% FBS. A list of the cell lines used as well as their *TP53* status is provided in table S2.

2.2.4 Cell culture treatments

For experiments with CLL primary cells, the cryopreserved samples were thawed, adjusted to 10^7 cells/ml and allowed to equilibrate for 30 min at 37°C and 5% CO_2.

For induction of DNA damage and p53, CLL samples were subjected to 5 Gy irradiation (IR) or treated with 1 µM, 5 µM or 10 µM nutlin-3 (10 mM stock in DMSO) and harvested after 24h. Untreated controls or, for nutlin-3 experiments, cells incubated with the corresponding DMSO concentration (0.01-0.1%) incubated for the same time period were included. At harvest, aliquots of every sample were prepared for viability analysis in FACS. The remainder was pelleted and lyzed in Trizol®.

For inhibition of BCR signaling at the level of BTK, CLL cells were induced with 1 µM ibrutinib (1 mM stock in DMSO) or left untreated for 24h and harvested thereafter as above.

Cell lines were seeded at 10^6 cells/ml, IR with 5 Gy, harvested 6h, 12h, and 24h thereafter, pelleted and flash-frozen in liquid nitrogen or treated with 0, 2.5 or 10 µM nutlin-3 and harvested likewise after 24h. Untreated or solvent-treated controls were included.

2.2.5 Fluorescence activated cell sorting (FACS)

Viability staining of CLL samples

To quantify apoptotic cells, double-staining with Annexin V-allophycocyanin (APC) and propidium iodide (PI) was performed. To this end, $1x10^5$ cells were washed in 200 µl PBS with 2% FBS and resuspended in 100 µl cold 1x Annexin V binding buffer. For each

sample, one aliquot was left unstained as control. To another aliquot, 2 µl Annexin V-APC and 2 µl PI (1:50 diluted in PBS) were added for a 15 min incubation at 4°C in the dark. Subsequently, 400 µl cold 1x Annexin V binding buffer were added and the samples were analysed on a BD LSR II FACS using the FACS Diva software. 10 000 events were recorded.

Staining of B-cells after MACS

To check the B-cell purity of samples after MACS, $1x10^5$ cells of the resulting B-cell fraction were washed in 200 µl PBS with 2%FBS and resuspended in 100 µl PBS with 2% FBS. For staining of CD19, 1 µl R-phycoerythrin (RPE)-coupled goat anti-mouse (GAM) antibody was added. Unstained samples were included as control. After 20 min incubation at RT in the dark, PBS with 2% FBS was added to the GAM-stained samples for washing. The pellet was resuspended with 10 µl mouse serum and incubated for 10 min at RT. It was then again washed with PBS and 2% FBS and resuspended in 300 µl PBS with 2% FBS for analysis on a BD LSR II FACS using the FACS Diva software, recording 10 000 events.

2.4.6 Cell viability assessment using CellTiter-Glo®

For screening sensitivity to ibrutinib treatment *in vitro*, cryopreserved PBMNC samples were thawed, seeded in 384 well plates at a density of 10 000 cells in 50 µl RPMI 1640 supplemented with 10% heat inactivated human serum per well. Cells were incubated with ibrutinib at 1 µM for 48 hours. Cell viability was assessed using CellTiter-Glo® assay according to the manufacturer's protocol. Data were kindly generated by Leopold Sellner.

2.5 Molecular Biology

2.5.1 RNA isolation

Total RNA was isolated using Trizol®. In brief, up to 10^7 cells were lyzed in 1 ml Trizol® and frozen at -80°C. For isolation, the lysate was allowed to adjust to room temperature for 5 min and extracted with 200 µl chloroform. For all further procedures, the RNA containing solution was kept on ice or at 4°C. After spinning at 12 000g and 4°C for 15 min, the resulting aqueous supernatant was precipitated with an equal volume of isopropanol and 10 µg glycogen at -20°C for 30 min. The precipitate was pelleted, washed with ice-cold 75% ethanol and allowed to air-dry. It was then dissolved in the desired volume of RNase-free water.

For purification of RNA from DNA contaminants, DNA digestion was performed with the TURBO DNA-free™ Kit following the manufacturer's instructions for routine DNase treatment. Up to 10 µg RNA were processed in one 50 µl reaction. After DNA digestion, RNA was purified from the kit's buffer by precipitation with an equal volume of isopropanol and 10 µg glycogen as described above. The RNA pellet was washed, dried and dissolved in RNase-free water. The RNA concentration and purity was determined on the NanoDrop® ND-100 spectrophotometer. The RNA solution was then aliquoted to avoid repeated freeze-thaw cycles, and stored at -80°C.
At the start of this project, a large batch of HeLa cells was cultured, harvested and RNA was extracted, pooled, aliquoted and stored at -80°C to serve as reference throughout all qRT-PCR experiments.

2.5.2 RNA quantification and quality control

Quantification and a first quality control of isolated RNA was performed on a NanoDrop®. The RNA concentration was determined from the absorption of 1 µl sample at 260 nm, the absorption maximum of nucleic acids. Additionally, the absorption at 230 nm and 280 nm was used to estimate the extent of contamination with phenol and protein (at 280 nm) or phenol and carbohydrates (at 230 nm).
As ubiquitous RNases quickly and easily degrade RNA, using RNA of high integrity is vital to obtain meaningful experimental results. RNA integrity of all samples prepared for small RNA sequencing was determined on a 2100 Bioanalyzer using the RNA 6000 Nano Kit according to the manufacturer's instructions. Here, stained RNA is electrophoretically separated based on size and the RNA integrity number (RIN) is calculated considering primarily the intensity and ratio of signals corresponding to 18S and 28S ribosomal RNA.
With two exceptions, only samples with a RIN of ≥ 7 were used for small RNA library preparation.

2.5.3 cDNA synthesis (reverse transcription)

cDNA synthesis for miRNA quantification

To determine the relative amount of miRNA expression, TaqMan Small RNA Assays containing target specific primer and probe sets for cDNA synthesis and quantitative real-time PCR (qRT-PCR) were used according to the manufacturer's instructions. The expression of RNU6B was used for normalization. Assay volumes were down-scaled by 50% for quantification of all miRNAs and RNU6B except for quantification of miR-34a-5p. Therefore, cDNA was synthesized from 5 or 10 ng RNA per sample in target specific 7,5 or 15 µl reactions.

cDNA synthesis for mRNA/lncRNA quantification

For long RNAs, cDNA was prepared from 120-500 ng RNA per sample using the SuperScript III First-Strand Synthesis SuperMix with random hexamer primers according to the manufacturer's instructions. The resulting cDNA was diluted to 5 ng/µl for further analyses.

2.5.4 Primer design for qRT-PCR

qRT-PCR primers for were manually designed following the subsequent criteria: A primer length of between 18 and 23 base pairs, a melting temperature preferentially between 58-65°C with less than 3°C difference between forward and reverse primer and a G/C-content of about 50-60%. Primers on the target sequence were picked using Primer3Plus and IDT PrimerQuest. Generation of hairpin structures and primer dimers was minimized using binding prediction tools of DNAStar Lasergene 8. To ensure gene specificity, primer sequences were run in BLAT and BLAST. To additionally ensure the absence of single-nucleotide polymorphisms (SNPs) within the primer sequence, SNP-BLAST was run. Primers were ordered from Eurofins.

2.5.5 Quantitative real-time PCR (qRT-PCR)

Quantification of miRNA

Target specific cDNA obtained in 2.5.3 was quantified using TaqMan Small RNA Assays following the manufacturer's protocol. The assays were run in 10 µl or 20 µl reactions in triplicates or duplicates, respectively, on 384-well-plates. A HeLa RNA sample was run on every plate as additional reference.

Quantification of long RNA transcripts (mRNA, lncRNA, promoter sequences)

For quantification of p21, NEAT1 and Lamin B1 transcripts, 2 µl of the 5 ng/µl random hexamer primed cDNA obtained in 2.5.3 were used per qRT-PCR reaction. They were added to a master mix composed of 10 µl SYBR Green, 6 µl H_2O, 1µl forward primer (5 µM) and 1 µl reverse primer (5 µM), resulting in a reaction volume of 20 µl. For lincRNA-p21 quantification, 6 µl cDNA were used and the water content of the master mix was adapted accordingly. The expression of Lamin B1 was chosen for normalization, as it was observed to be unaffected by the treatments. A HeLa RNA sample was run on every plate as additional reference. qRT-PCR was performed on a LightCycler 480 in 384-well-plates. The program was run as detailed in Table 2. A melting curve analysis was

performed to ensure assay specificity, and only wells displaying target-specific amplification were chosen for further analysis.

For NEAT1, lincRNA-p21 and Lamin B1, the primer annealing temperature was 59°C. For p21 and Lamin B1 quantification it was 58°C.

Table 2. qRT-PCR program run for the quantification of lincRNA-p21, NEAT1 and p21.

Detection Format	**Block Type**	**Reaction Volume**
SYBR Green I	384	20µl

Programs

Name	**Cycles**	**Analysis Mode**
Pre-Incubation	1	None
Amplification	40	Quantification
Melting Curve	1	Melting Curve
Cooling	1	None

Programs in detail

Target (°C)	**Acquisition Mode**	**Hold (hh:mm:ss)**	**Ramp Rate (°C/s)**	**Acquisi-tions (per°C)**	**Sec Target (°C)**	**Step Size (°C)**	**Step Delay (cycles)**
Pre-Incubation							
95	None	00:10:00	4,4		0	0	0
Amplification							
95	none	00:00:15	4,4		0	0	0
variable	None	00:01:00	2,2		0	0	0
72	single	00:00:05	4,4		37	0	0
Melting Curve							
95	None	00:00:05	4,4				
65	None	00:01:00	2,2				
97	continuous		0,06	10			
Cooling							
40	None	00:00:10	1,5		0,0	0	0

2.5.6 Agarose gel electrophoresis

To additionally ensure target specificity of qRT-PCR assays with SYBR Green, the product of the qRT-PCR reactions was run on an agarose gel and checked for the correct amplicon size. As amplicons were of 67 – 116 nt length, 3% agarose gels were prepared. Agarose was melted in 1x TAE buffer and 1-2 drops ethidium bromide were added for nucleic acid visualization. DNA samples were mixed 1:5 with 5x loading dye and loaded onto the gel; a 50 or 100 bp DNA ladder was included in every run. The gel was run at 120 V for 75 min and subsequently analyzed on a transilluminator.

2.5.7 Small RNA library preparation

For next-generation sequencing, 1 µg total RNA/sample was converted into a barcoded cDNA library using the NEBNext® Small RNA Library Prep Set for Illumina according to manufacturer's instructions with the following specifications/adaptations:

- After ligation of the 5' SR Adaptor, 18 µl H_2O were added to the 30 µl total volume, and half of the reaction volume was stored at -20°C as backup. The other half was further processed for sequencing.
- During size selection of the amplified cDNA library on a polyacrylamide gel, bands corresponding to nucleic acids of approximately 15 - 35 nt length were selected. This was performed manually for the pilot screen, whereas the LabChip® was implemented for the main screen.
- To recover nucleic acids from the gel, the crushed gel slices were eluted for at least 16 h instead of 2 h to increase the yield.

Library preparation was performed at, and supported by, the DKFZ Genomics and Proteomics Core Facility.

2.5.8 Next-generation Sequencing

Libraries were amplified on an Illumina cBot and sequenced on llumina's Hiseq 2000 platform, running 7-9 libraries per lane with 50 bp single read sequencing. Amplification and sequencing were performed by the DKFZ Genomics and Proteomics Core Facility.

2.5.9 Protein extraction

Cell aliquots intended for protein extraction were harvested at 10^6 cells per aliquot and washed once with PBS. Upon removal of all PBS, the cell pellets were snap-frozen in liquid nitrogen to disrupt the cell structure and stored at -80°C. For extraction of protein, 10^6 cells were resuspended in 20 µl RIPA buffer containing 125 U/ml Benzonase and 1x protease/phosphatase inhibitors. The sample was vortexed and kept on ice for 30 min, vortexing every 10 min.

2.5.10 Determination of protein concentration

Protein concentrations were measured using the BCA™ Protein Assay Kit according to the manufacturer's instructions. Sample protein solutions were diluted 1:10 for measurement, and concentrations were determined in a 96-well format. Chemiluminescence was detected on a microplate reader. Protein concentration was

adjusted to 2 µg/µl in all samples. Isolated protein was immediately used or stored at -20°C.

2.5.11 Western Blot

For Western Blot, protein was first separated according to size by poly-acrylamide gel electrophoresis. To this end, pre-cast Mini-PROTEAN-TGX gels 4-15% were placed into a Bio-Rad gel chamber, which was subsequently filled with 1x Bio-Rad Tris/Glycerine/SDS running buffer. Samples were mixed 1:2 with 2x Laemmli buffer and a volume equaling 10 µg protein was inserted into every lane, reserving one lane for the marker. Gels were run at 120 V for 70 min. After electrophoresis, the gels were removed from the chamber, the stacking gel was separated from the resolution gel, and the latter was used for transfer of the proteins onto a PVDF membrane.

For Western blotting, a Trans-Blot Turbo PVDF-LF membrane cut was activated in methanol for 1 min and equilibrated in transfer buffer. Per gel, two stacks of filter paper were soaked in transfer buffer. One stack was placed on the lower side of the blotting chamber, the membrane was added, then the gel and another soaked filter paper stack. Blotting was run at 25 V for 10 min.

The membrane was then briefly washed in methanol and incubated in blocking buffer (5 % milk in PBST) for 1 h at room temperature (RT). The membrane was then incubated with primary antibody diluted 1:1000 (anti-GAPDH) or 1:5000 (anti-p53) in blocking buffer at 4°C over night, or alternatively at RT for 2 h. It was then washed 3x 5 min with PBST on a shaker, then secondary horseradish peroxidase-coupled antibody in blocking buffer was added according to host species at a dilution of 1:10 000. The membrane was incubated for 1 h at RT and washed 3x 5 min with PBST. 1 ml Western Lightning *Plus*-ECL Enhanced Luminol Reagent Plus and 1 ml Western Lightning *Plus*-ECL Oxidizing Reagent Plus were mixed, added dropwise onto the membrane and incubated for 5 min at RT. Chemiluminescence was detected directly on a ChemiDoc station, capturing 10-300 s exposure. An additional white light picture of the membrane was taken to record the marker bands and later on merged with the chemiluminescence picture.

2.5.12 Chromatin immunoprecipitation (ChIP)-PCR

10^7 cells were harvested from the Séraphine $p53^{wt}$ and the isogenic $p53^{ko}$ cell line in 10 ml cell culture medium. 1% paraformaldehyde was added and incubated for 10 min at 37°C to crosslink proteins and chromatin. This was terminated by addition of 125 mM glycine and incubation for 5 min at RT. Cells were washed with cold PBS containing protease inhibitors and aliquoted, as 10^6 cells were used for each ChIP experiment. 10^6

cells were resuspended in 500 µl lysis buffer from Millipore's ChIP Assay Kit, and further steps were performed according to the manufacturer's protocol using the following specifications and adaptations: Chromatin was sheared to 200 - 400 bp using a Covaris S220 sonicator for 5 x 10 min set to duty cycle 20%, intensity 5, 200 cycles per burst, 60s. Subsequently, shearing was checked on a 1.5% agarose gel. Aliquots were saved as input control. No antibody or 2 µg DO-1 p53 antibody (from Santa Cruz Biotechnology or BD Biosciences) were added for incubation at 4°C over night. Elution and de-crosslinking were performed simultaneously, and AMPure SPRI beads were used for DNA purification post de-crosslinking according to the manufacturer's instructions. NEAT1 and p21 promoter sequences were detected by qRT-PCR running the program detailed in section 2.5.5, using 56°C and 59°C as annealing temperature, respectively, and 10 s for elongation at 72°C. Half of the PCR product was subsequently run on a 3% agarose gel.

2.6 Bioinformatics and Statistics

2.6.1 Read processing and mapping

The sequencing reads obtained were quality filtered, adaptor trimmed, size selected for reads of 17-25nt length and bowtie-aligned to the human mature miRNA sequences of miRBase v19 requesting perfect sequence identity. Likewise, reads of ≥ 15nt not mapping to mature miRNA sequences were bowtie-aligned to human mRNA and ncRNA sequences derived from a set of databases (Ensembl 71, GtRNAdb[217], Rfam 11.0, piRNA cluster database[218]). For these purposes, pipelines implemented in the HUSAR system at DKFZ were used[219] with the support of Agnes Hotz-Wagenblatt. Analyses for this study did not exclude multiple mapping reads. This was done to include miRNAs with high numbers of genomic loci (e.g. miR-1246: on chromosome 2, 3, 5, 6, 13, 14 and 17; miR-941: 7 loci on chromosome 20) and to avoid losing a large fraction of sequencing reads.

2.6.2 Data analysis and statistics

Mapped raw sequencing read count data were normalized using DESeq2 in R[220]. Only RNAs with an average of ≥ 5 counts across samples or a count of ≥ 10 in at least one of the samples were considered for further analysis. Dispersion of each RNA was estimated using the Cox-Reid adjusted profile likelihood approach[221]. The Wald test based on the negative-binomial regression model was used to detect differentially expressed RNAs, accounting for batch effect and sample pairing in the model. P-values

were adjusted for multiplicity using Benjamini-Hochberg correction. Hierarchical clustering of log_2-transformed fold changes was done using euclidean distance and Ward's linkage. The L1 penalized regression model was implemented for the identification of a miRNA signature predicting *IGHV* status.

For miRNA target identification, normalized read counts were transformed using regularized log-transformation as implemented in the rlogTransformation function in DESeq2. The batch effect was removed from the transformed count data using the removeBatchEffect function from limma[222]. Pearson's correlation coefficient including 95% confidence interval between transformed miRNA and mRNA expression levels was computed and tested using the cor.test function. miRanda[118], miRWalk[223] and TargetScan[224] were used to predict miRNA targets.

All analyses were conducted with R/Bioconductor 3.0.1 and Bioconductor package DESeq2 1.0.19[221] and greatly supported by Thomas Hielscher. Student's t-test was applied on qRT-PCR data in GraphPad Prism. All tests were two-sided. P-values below 0.05 were considered statistically significant.

3 Results

The activity of BCR signaling and the p53 signaling pathway is of central importance to CLL tumor cell survival, hence influences disease progression and patient's response to treatment. To improve our understanding of the involvement of non-coding RNAs in these contexts, this work set out to comprehensively identify novel non-coding RNAs implicated in BCR signaling or the p53 signaling pathway by applying small RNA sequencing.

3.1 Establishment and validation of the small RNA sequencing approach

To establish the sequencing and data analysis pipeline for small RNA quantification, first a pilot screen was performed on libraries generated from samples of two previously untreated *TP53*^{wt} and three *TP53*$^{del/mut}$ CLL patients (indicated by green numbers in Figure 11). Cells were treated with 5 Gy for p53 induction or left untreated, and harvested after 24 hours for RNA isolation. The dataset obtained from small RNA sequencing was checked for sufficient read coverage, read length distribution, comparability of miRNA expression levels to published datasets, and reproducibility, as discussed in the following paragraphs. For all analyses from section 3.2 forward, the datasets of pilot and main screen were combined.

In the pilot screen, an average coverage of 39.8 Mio raw reads/sample (min. 24.3 – max. 58.6 Mio/sample) were obtained, of which on average 22% perfectly mapped to mature miRNA sequences (miRBase v19). Known p53 target miR-34a-5p, serving as positive control, was represented by an average of 328 reads per sample at baseline, i.e. after 24 hours of cell culture without treatment. A dynamic range with a minimum of 15 and a maximum of 1169 reads per sample reflected expected inter-patient differences and induction after DNA damage as assessed by qRT-PCR for miR-34a-5p. The total and miRNA-34a-5p read coverages were higher compared to similar small RNA sequencing studies[225-227]. In conclusion, this sequencing depth should allow sensitive, high-resolution profiling of miRNA expression.

The length of adaptor-trimmed reads ranged from 5 to 45 nucleotides (nt) as exemplified in Figure 10A, peaking at 22 nt as expected for mature miRNA sequences. Since the length of 99.1% of human miRNAs falls within the range of 17-25 nt (miRBase v19) and short, random RNA degradation products were to be excluded, miRNA expression

analyses were confined to reads of this length range. Within this selection, on average 36% of reads mapped to mature miRNA sequences.

A comparison of the 30 most abundantly expressed miRNAs at baseline to those reported by Landgraf *et al.*[227] and Jima *et al.*[225] yielded a good overlap of 22 and 18 miRNAs, respectively (table S3).

Sequencing data reproducibility was verified by two approaches: Firstly, by independently preparing two small RNA libraries of one sample, which produced nearly identical sequencing results (R^2 = 0.99, Figure 10B) and secondly, by validating the expression of miR-34a-5p and miR-151-5p by qRT-PCR. Figure 10C, D display the correlation of expression levels as determined by the two quantification methods across all sequenced screen samples, comprising the 5x2 samples of the pilot screen. Strong correlations of qRT-PCR and sequencing data were observed (R^2 = 0.70 and R^2 = 0.76, respectively).

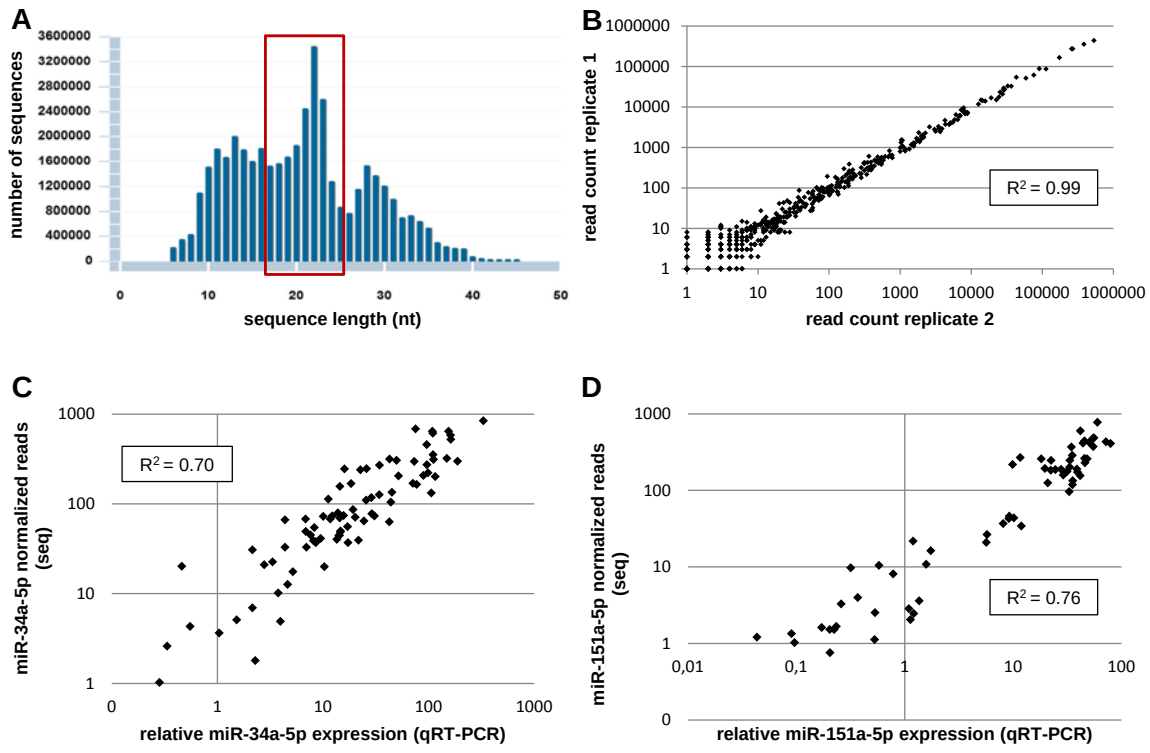

Figure 10 Establishment and validation of small RNA sequencing. (A) Read length distribution for a representative sample, indicating the 17-25 nt selection used for miRNA quantification. **(B)** Correlation of miRNA quantity in two independently prepared libraries of the same sample (technical replicates). Every dot represents one miRNA; non-normalized read counts are plotted. **(C, D)** Correlation of miR-34a-5p (n = 83) and miR-151a-5p (n = 73) expression, respectively, as quantified by small RNA sequencing (seq) and qRT-PCR.

In conclusion, the described miRNA quantification and sequencing data analysis pipeline allowed reliable, high-resolution quantification of miRNA, and qualified for application to this project's research question. It was applied to the whole screening approach used to identify p53-dependent and BCR signaling dependent ncRNA as delineated in Figure 11.

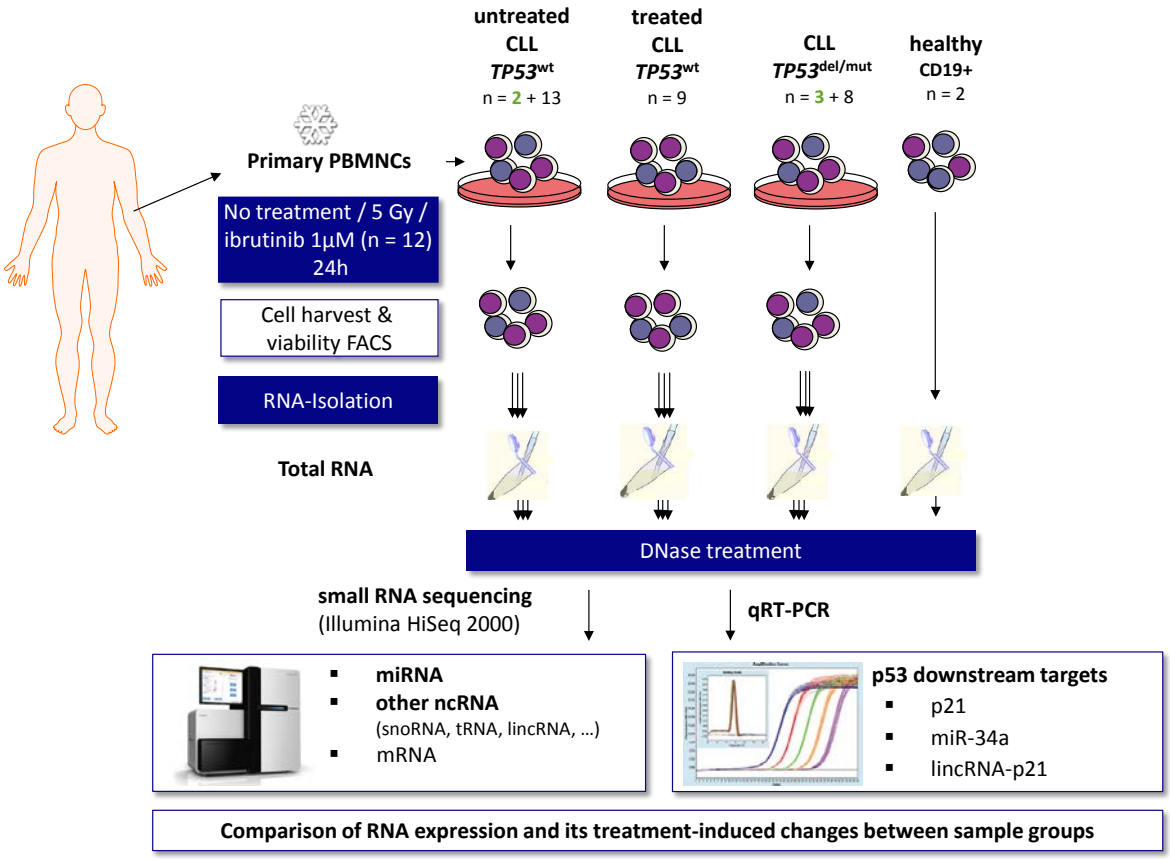

Figure 11. Graphical summary of the screening approach used in this study. The screen included peripheral blood mononuclear cells (PBMNCs) of 35 CLL patients and two healthy B-cell controls. Samples of the pilot screen (n = 5) are indicated in green. Refer to text for details.

This sample set was generated from cryopreserved peripheral blood mononuclear cells (PBMNCs) of 35 CLL patients selected for high tumor load and stratified by p53 status and prior therapy for CLL (see Table 3 for clinical and molecular characteristics) as well as two pooled CD19 positive selected healthy B-cell controls. It encompassed three different treatments in total. p53 induction by 5 Gy irradiation was used for the identification of p53-dependent ncRNA transcripts and applied on 34 samples, whereas BTK-inhibition by ibrutinib to identify BCR signaling dependent miRNAs was performed on 12 samples only; no treatment controls were prepared for all samples. Healthy B-cell controls were not taken into culture, but RNA was directly extracted from isolated cells. The irradiation dose was chosen according to Zenz *et al.*[116], who at this dose observed a strong induction of p53 target miR-34a-5p at 24 h upon treatment of primary CLL cells. A

dose of 1 µM ibrutinib had previously been demonstrated to strongly inhibit BCR signaling *in vitro*[99,100]. At 24 hours post induction, cell viability was monitored by Annexin V / propidium iodide staining and flow cytometric analysis (FACS). Total RNA was isolated, DNase treated and analyzed by qRT-PCR for the expression of selected targets of interest. RNA aliquots of the identical samples were subjected to small RNA library preparation and next-generation sequencing on an Illumina HiSeq 2000.
All further analyses were performed on the combined data of pilot and main screen.

Table 3. Summary of clinical and genetic characteristics of the patient samples screened.
11 of the 12 patients used for *in vitro* ibrutinib treatment were part of the irradiation treated sample set.

	Parameter	Irradiated	Ibrutinib treated
Clinical	Number of patients (n)	34	12
	Median age, years (range)	68 (48 - 90)	66 (49 - 77)
	Female gender (%)	44	50
	Median PB leukocytes / nl (range)	89 (27 - 262)	154 (100 - 262)
	Median PB lymphocyte fraction (% of leukocytes) (range)	95 (76 - 100)	99 (90 – 100)
	Pretreated, n (%)	17 (50)	6 (50)
FISH	13q14 deletion, n (%)	20 (59)	10 (83)
	17p13 deletion, n (%)	10 (29)	5 (42)
	11q23 deletion, n (%)	5 (15)	2 (17)
	Trisomy 12, n (%)	4 (12)	2 (17)
	8q24 amplification, n (%)	3 (9)	1 (8)
Mutations	*IGHV* unmutated (%)	17 (53)*	8 (67)
	TP53 mutation, n (%)	10 (29)	5 (33)
	ATM mutation, n (%)	2 (6)	1 (8)
	SF3B1 mutation, n (%)	7 (21)	1 (8)
	BRAF mutation, n (%)	3 (9)	2 (17)
	NOTCH1 mutation, n (%)	2 (6)	1 (8)

*= 17 of 32, as *IGHV* status was unknown for 2 patients. One sample displaying 6% *TP53* mutation (no 17p deletion) was counted as *TP53*^{wt}, as this low fraction of mutated cells is not expected to alter the p53 response.

3.2 Induction of known p53 targets after DNA damage in primary CLL cells

Prior to sequencing the main screen samples, apoptosis induction and p53 key target expression levels were monitored in PBMNCs of the cohort by qRT-PCR to examine whether *TP53* status dependent expression would be detected. Of the 34 samples that

were treated with 5 Gy irradiation (or left untreated) and harvested 24 hours thereafter, 19 were p53 wild-type, carrying no genetic abnormalities in the p53 pathway as determined by routine FISH (i.e. no *TP53* or *ATM* deletion). Five displayed monoallelic deletions of the p53 activating kinase *ATM* encoded on chromosome 11q22.3 (del11q). In 10 samples, monoallelic deletions of chromosome 17p13 (*TP53*) and / or mutations in *TP53* had been detected by FISH or 454 sequencing, respectively (for details on sample genetics, see also table S1).

Induction of apoptosis indicative of p53 activation was quantified by staining with Annexin V (marking apoptotic cells) and propidium iodide (marking cells with damaged/porous plasma membrane, i.e. late apoptotic and necrotic cells) in FACS. The expression of p21 and miR-34a-5p, two key p53 transcriptional targets was assessed by qRT-PCR.

After IR-triggered DNA damage induction, only the group of *TP53*^{wt} samples displayed a significant increase in apoptotic cells (total Annexin V positive: NT 32% vs. IR 47% (median), $p < 0.001$), whereas samples displaying genetic aberrations of *TP53* or *ATM* were largely resistant to this treatment (del11q: 31% vs. 33%, $p = 0.15$; *TP53*$^{del/mut}$ 32% vs. 36%, $p = 0.91$ (median values) (Figure 12 and Figure 13)).

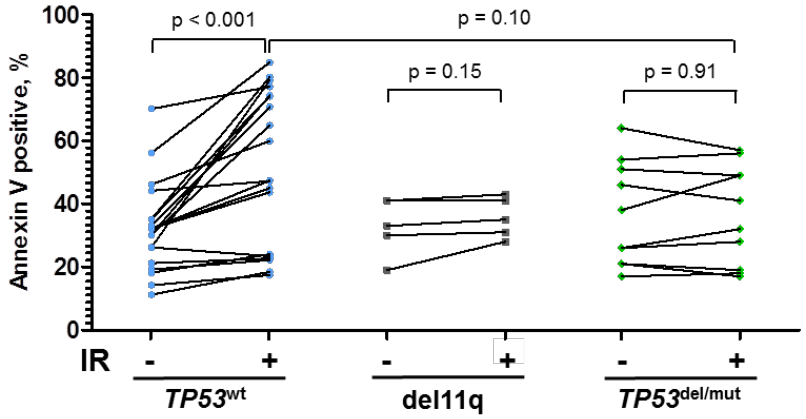

Figure 12. Effects of 5 Gy irradiation (IR) on CLL cell apoptosis. *TP53*^{wt} (n = 19), del11q (n = 5) and *TP53*$^{del/mut}$ (n = 10) samples were analyzed by Annexin V / propidium iodide (PI) staining in FACS to quantify apoptosis induction (APC-Annexin positivity).

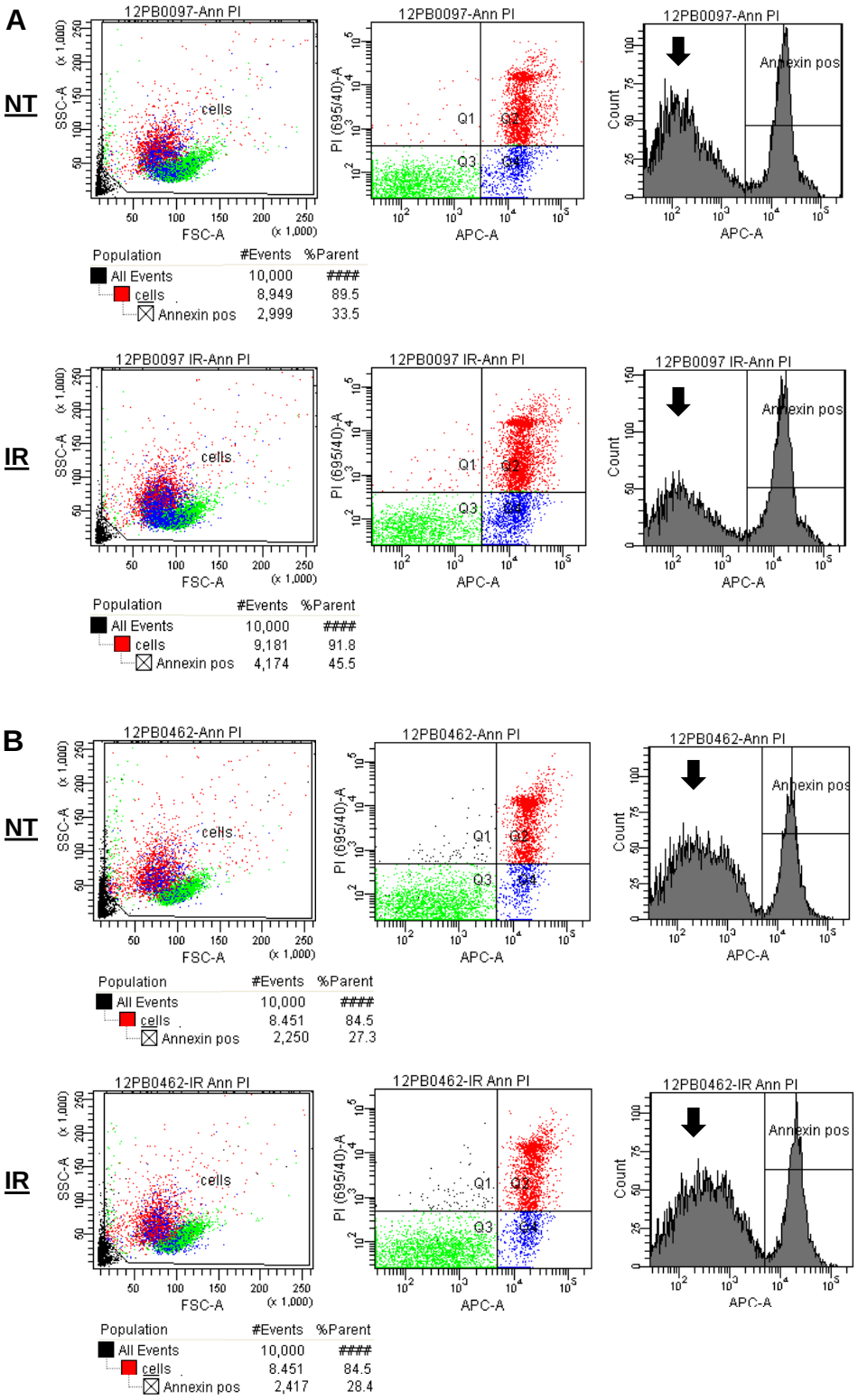

Figure 13. Examples of the impact of 5 Gy irradiation (IR) on cell viability / apoptosis. **(A)** provides a representative example of the impact of IR on cell viability of a *TP53*^{wt} sample (upper panels: NT 34%, lower panels: IR 46% Annexin positive). The increase in the apoptotic cell fraction after IR is best appreciated by the drop in viable, double-negative cells. **(B)** is a representative example of effects of IR on cell viability of a *TP53*$^{del/mut}$ sample (upper panels: NT 27%, lower panels: IR 28% Annexin positive cells). SSC, side scatter; FSC, forward scatter.

Analysis of p53 downstream target expression demonstrated a strong and significant induction of p21 expression in *TP53*^{wt} samples due to IR-triggered DNA damage (relative expression median untreated: 1.1 vs. IR: 24.8, $p < 0.001$), whereas this effect was less pronounced in del11q patients (1.3 vs. 7.9, $p = 0.17$) (Figure 14A). As expected, induction was lowest in *TP53*$^{del/mut}$ samples (1.3 vs. 3.6, $p = 0.02$). The *TP53* genetic subgroups could be clearly distinguished by their p21 expression level post IR, which was significantly higher in *TP53*^{wt} than *TP53*$^{del/mut}$ samples ($p < 0.001$). This was also true for miR-34a-5p expression. Here, markedly higher expression levels in *TP53*^{wt} than *TP53*$^{del/mut}$ samples were already detected at baseline (15.7 vs. 5.7, $p = 0.02$) (Figure 14B). Induction of miR-34a-5p and p21 was still seen in *TP53*$^{del/mut}$ samples at a low level, which is owed to the subclonality of p53 aberrations (26 - 92%) resulting in residual p53 activity.

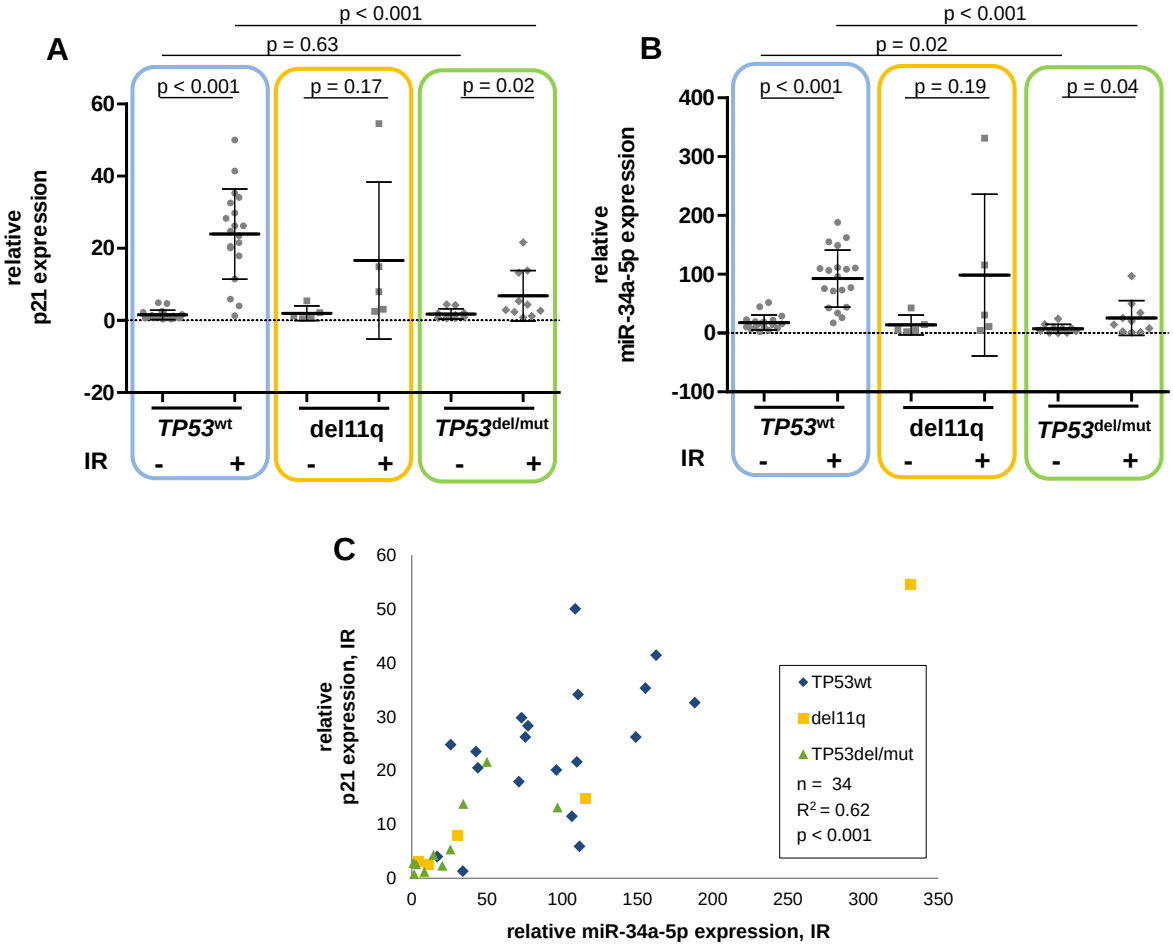

Figure 14. Effects of 5 Gy irradiation (IR) on p53 target gene expression. p21 **(A,C)** and miR-34a-5p **(B,C)** expression in the screen samples 24h post +/- 5 Gy IR quantified by qRT-PCR, by genetic status of *TP53* and *ATM* (11q). Means and standard deviations are indicated. Target gene expression was normalized to RNU6B and referenced to a HeLa sample.

While miR-34a-5p and p21 expression levels were not found to correlate in untreated samples (R^2 = 0.07, data not shown), a strong correlation was observed after IR (R^2 = 0.62, p < 0.001, Figure 14C).

The results confirmed previous data[116,191], and cohort and experimental setup appeared suitable for the identification of transcriptional p53 targets.

Patient treatment status influenced DNA damage-triggered induction levels of p21. Samples of patients previously treated for CLL displayed reduced p21 induction independent of *TP53* status (median fold increase in *TP53*^{wt}, 11q disomic, untreated CLLs (n = 15): 26.4, in *TP53*^{wt} treated CLLs (n = 9): 6.8, p = 0.001, Figure 15A). This was largely independent from ATM status of samples of treated patients, as samples with del11q or *ATM* mutation (n = 6) displayed a 10.0 fold induction, and ATM wild-type, disomic ones (n = 3) a 3.8 fold induction (p = 0.28, data not shown). This suggests impaired p53 pathway activation in tumor cells of treated CLL patients, which is independent of *TP53* and *ATM* status.

For miR-34a-5p induction, no influence of previous patient treatment was observed (4.7 fold in samples of *TP53*^{wt} previously untreated patients vs. 5.9 fold in *TP53*^{wt} previously treated ones) (Figure 15B).

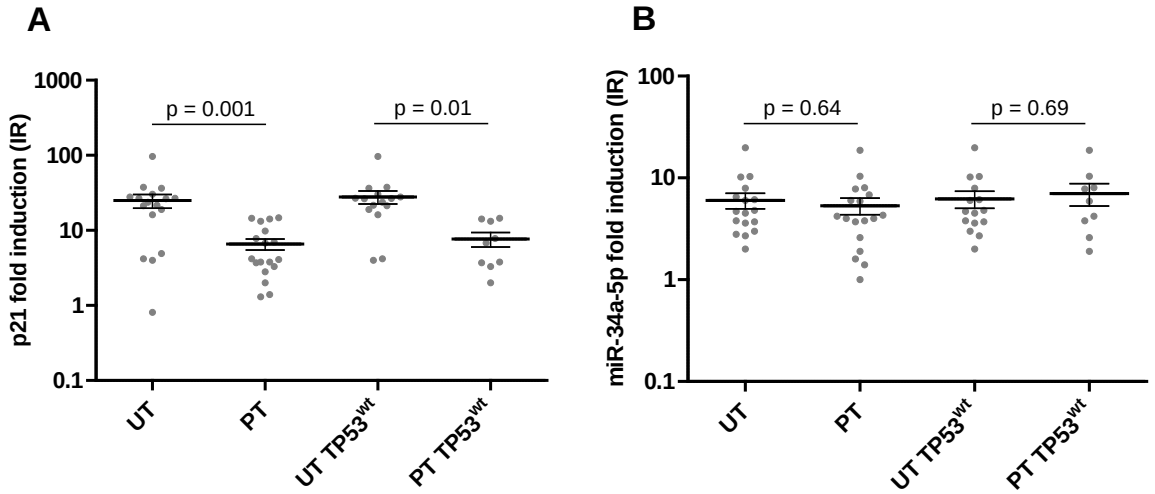

Figure 15**. DNA damage-triggered p21 and miR-34a-5p induction by patient treatment status. . (A)** p21 and **(B)** miR-34a-5p expression in previously untreated (UT) patients (n = 17) and patients having received prior therapy (PT) for CLL (n = 17) irrespective of genetic status, and of only *TP53*^{wt}, 11q disomic status (UT n = 15, PT n = 9). Means and standard errors are indicated. Target gene expression was normalized to RNU6B and referenced to a HeLa sample.

The identical RNA samples were used to screen for novel p53 targets by small RNA sequencing. For identification of p53 targets, *TP53*^{wt} patient's (n = 15, untreated) cells

were used for comparison to *TP53*$^{del/mut}$ samples (n = 10) to avoid impaired p53 pathway activity in previously treated *TP53*^{wt} patients.

3.3 Overview of RNA expression in primary CLL cells as captured by small RNA sequencing

For small RNA sequencing, total RNA was extracted from 82 CLL primary samples (35 patients, all treatments) and one pooled healthy B-cell control. RNA integrity numbers (RIN) as determined on an Agilent Bioanalyzer 2100 indicated that RNA was generally of sufficient quality (average RIN = 8.3, range 6.4-9.1, two samples below 7).

Applying the aforementioned experimental approach and data analysis pipeline, 1.98 billion reads were obtained from sequencing 84 small RNA libraries (= 82 + one technical replicate + healthy B-cells) (average 23.4 mio/sample) in total.

Section 3.3.1 provides an overview of the transcript landscape captured by sequencing and mapping of all high-quality, adaptor-trimmed reads of at least 15 nt length to a set of coding and non-coding RNA databases as listed in 2.6.1. Basal miRNAs expression profiles in non-treated samples are presented in 3.3.2.

3.3.1 RNA families detected by the approach

Figure 16 illustrates the representation of different RNA family's transcripts in the sequencing reads of at least 15 nt length. Ribosomal RNA, normally constituting 80-90% of cellular RNA[228], was efficiently depleted, representing only 2% of all sequencing reads. Interestingly, only 13% of all reads mapped to mature miRNA sequences, whereas snoRNA were covered by most reads (22%), followed by mRNA represented by 14%, down to lincRNA being covered by 1% of reads. 41% of reads did not map to any sequence of the curated set of reference databases, of which half (49%, i.e. 20% of total reads) were reads that did not map to the genome. In our selection of 17-25 nt long reads for miRNA expression analyses, 30% of reads mapped to mature miRNA (median; range 14 – 45%). Of the 1405 human mature miRNAs (miRBase v19), 1244 miRNAs were detected (≥ 1 read) in at least one CLL sample. We focused our analyses on miRNAs with an average of ≥ 5 reads across samples or a count of ≥ 10 in at least one sample.

Although our screen was targeted at small RNA sequences to enrich for miRNA, the data on mRNA and other ncRNA expression was also analysed.

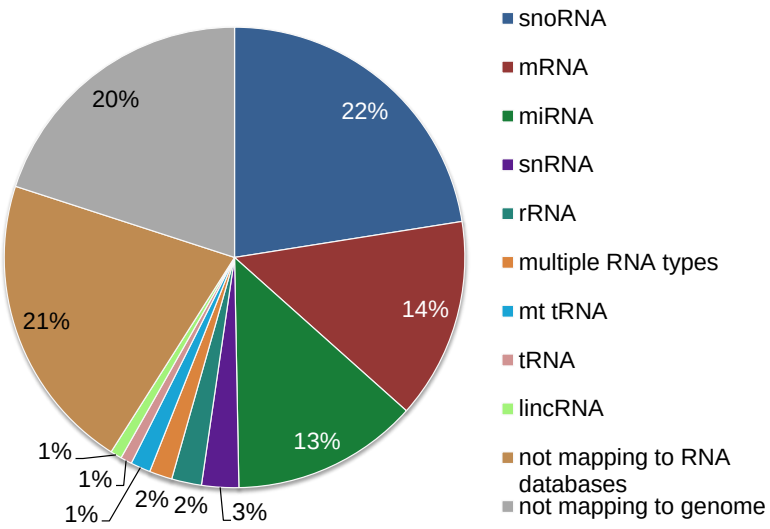

Figure 16. Expression of RNA subgroups detected by small RNA sequencing. Overview of read fractions mapping to different RNA families. Average values of n = 85 samples from 35 CLL patients and 1 pooled healthy B-cell sample. Relative abundance is expressed as percentage of total reads ≥15 nt. snoRNA = small nucleolar RNA; mRNA = messenger RNA); miRNA = mature microRNA, snRNA = small nuclear RNA; rRNA = ribosomal RNA; mt tRNA = mitochondrial transfer RNA; lincRNA = long intergenic ncRNA.

3.3.2 miRNA expression profiles at baseline

miRNA expression was quantified by mapping 17-25 nt long high quality reads to mature miRNA reference sequences of miRBase v19. Within this range of read lengths, isomiRs generated by 3' or 5' trimming of the miRNA reference sequence were subsumed in the total read count of the corresponding mature miRNA. For further analysis, read counts were corrected for batch effects between pilot and main screen, and normalized using DESeq2 in R.

After 24 hours in culture without treatment (i.e. at baseline), expression profiles were dominated by miR-21-5p, a miRNA frequently overexpressed in malignancies[229-231] (Figure 17). Together with miR-26a-5p, let-7g-5p and miR-101-3p, it accounted for 51% of total miRNA reads. Nine of the 10 most strongly expressed miRNAs were previously reported among the 10 most abundant miRNAs in primary CLL cells (all except for miR-148a-3p), although the top expressed miRNAs varied considerably between studies[227,232,233].

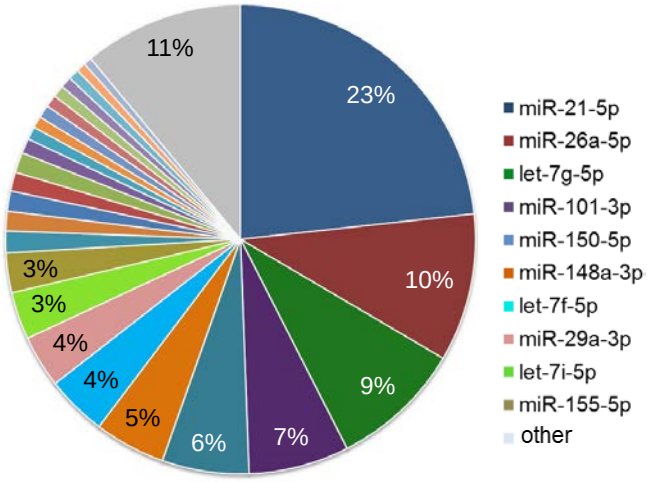

Figure 17. Basal miRNA expression profiles detected by small RNA sequencing. Relative abundance is expressed as percentage of total mature miRNA sequence reads. Median values of n = 35 samples cultured for 24 hours without treatment are provided. The top 10 most abundant miRNA and their contribution to the overall miRNA read count are specified. The top 25 miRNAs shown on the chart.

3.4 Identification of BCR signaling-dependent miRNA in CLL

The identification of miRNAs involved in BCR signaling was approached from different angles: Firstly, as *IGHV* mutational status is connected to BCR signaling capacity, miRNAs differentially expressed in *IGHV* mutated compared to *IGHV* unmutated samples at baseline were identified. Secondly, dependency of miRNA expression on BCR signaling was directly tested by inhibition of the signaling pathway at the step of Bruton's Tyrosine Kinase (BTK) using ibrutinib. Further, the correlation of miRNA expression profiles to *in vitro* ibrutinib sensitivity of primary CLL cells was assessed.

3.4.1 Baseline miRNA expression and *IGHV* status

To identify *IGHV* dependently expressed miRNA, the basal miRNA expression profiles of 35 CLL patient samples of known *IGHV* mutation status were evaluated. Seven miRNAs were significantly overexpressed in samples of unmutated *IGHV* as compared to mutated *IGHV*, five were downregulated (Table 4), pointing towards potential involvement in BCR signaling.

Table 4. miRNAs differentially expressed with respect to *IGHV* status. Identified from miRNA expression profiles of n = 35 primary CLL samples.

miRNA name	U-*IGHV*	M-*IGHV*	fold difference	p-value
***Higher in U*-IGHV**				
miR-574-3p	241	115	2.0	0.009
miR-184	30	9	3.3	0.009
miR-330-3p	112	67	1.7	0.009
miR-152	331	116	3.3	0.010
miR-574-5p	163	76	2.0	0.014
miR-9-5p	781	99	3.3	0.014
miR-155-5p	44517	30945	1.4	0.041
***Lower in U*-IGHV**				
miR-514a-3p	3	13	0.2	0.003
miR-29c-3p	1741	3736	0.5	0.009
miR-141-3p	89	186	0.5	0.010
miR-29c-5p	137	282	0.5	0.014
miR-4432	2	6	0.3	0.042

Normalized read counts are provided. U-*IGHV* = unmutated *IGHV*; M-*IGHV* = mutated *IGHV*. P-values were determined by Wald Test and corrected for multiple testing.

Table 5. miRNA signature for the classification of samples according to *IGHV* status.

Signature component	coefficient
miR-1246	0.10
miR-138-5p	-0.41
miR-144-3p	1.03
miR-151a-5p	1.11
miR-181a-2-3p	0.14
miR-181b-5p	1.29
miR-193b-3p	0.25
miR-29c-3p	1.34
miR-29c-5p	0.90
miR-365a-3p	0.67
miR-365b-3p	0.00
miR-4685-3p	2.67
miR-511	-0.72
miR-514a-3p	4.38
miR-654-3p	-1.60

Using an L1 penalized logistic regression model for the development of signatures for sample classification, a miRNA expression signature composed of 15 components was found to discriminate between *IGHV* mutated and *IGHV* unmutated samples (Table 5). The performance of this *IGHV* status predictor was tested by leave-one-out crossvalidation, displaying an accuracy of 82%. The regression model provides a weighted classification rule, i.e. the coefficient indicated in Table 5 represents the weight of the respective miRNA for the classification. The higher the positive coefficient, the more a high expression level of the respective miRNA argues for the sample being *IGHV* mutated (e.g. miR-514a-3p). On the contrary, expression of a miRNA with a negative indicated coefficient will argue for the sample being *IGHV* unmutated (e.g. miR-654-3p).

3.4.2 The impact of BTK inhibition on miRNA expression

The BTK inhibitor Ibrutinib was used for abrogating the BCR signaling pathway in primary PBMNCs of 12 CLL patients. After a 24 hour treatment with 1 µM ibrutinib *in vitro*, the great majority of miRNAs did not change in expression as illustrated in Figure

18. However, miR-320c and miR-1246 were found upregulated, while miR-484, miR-17-5p, miR-155-3p and miR-27a-5p were downregulated (Table 6).

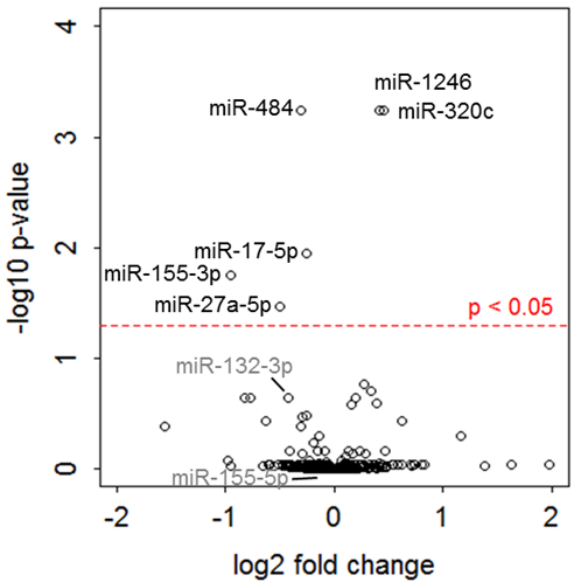

Figure 18. miRNA expression changes due to 1 µM ibrutinib treatment for 24 hours. Volcano plot displaying 397 expressed miRNAs, of which 6 are influenced by the treatment ($p < 0.05$). miR-155-3p/5p, miR-27a-5p, and miR-132 have previously been described as BCR signaling dependent[190,234]. P-values were determined by Wald Test and corrected for multiple testing.

Table 6. miRNAs differentially regulated upon ibrutinib treatment. Mean normalized read counts per group are provided. p-values were determined by Wald Test and Benjamini-Hochberg corrected. FC = fold change.

miRNA name	non-treated	24h ibrutinib	FC	p-value
upregulated				
miR-320c	80	108	1.4	5.8E-04
miR-1246	5587	7797	1.3	5.8E-04
downregulated				
miR-484	337	272	0.8	5.8E-04
miR-17-5p	4191	3440	0.8	0.011
miR-155-3p	21	10	0.5	0.018
miR-27a-5p	245	159	0.7	0.034

Whereas the expression changes caused by BCR signaling inhibition were subtle for most miRNAs, they were consistent across the samples (Figure 19).

qPCR validation was attempted for miR-320c, miR-1246, miR-484 and miR-155-3p regulation, using miR-155-5p expression which was not influenced by the treatment as

control. The inhibitory effect of BCR signaling abrogation on miR-155-3p could be validated (fold change in qRT-PCR 0.6, p = 0.01), just as the steady expression of miR-155-5p (fold change 1.3, p = 0.95). For the other candidates, the regulation as determined from the sequencing data was within the variability of the qRT-PCR assay.

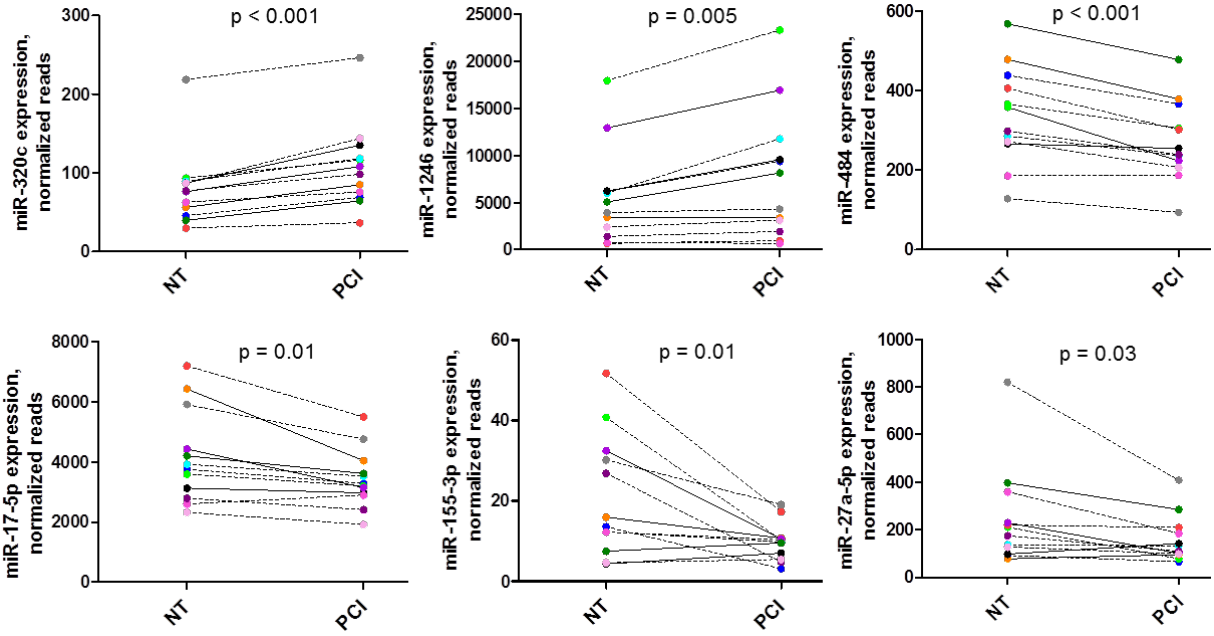

Figure 19. Expression of six ibrutinib-regulated miRNAs in 12 primary CLL samples in non-treated (NT) condition and after 24h with 1 µM ibrutinib (PCI). P-values were determined by two-sided Student's t-test. Dashed lines represent samples of unmutated *IGHV* status (n = 8), sold lines of mutated *IGHV* (n = 4) status. Every individual sample is encoded by one specific colour.

No regulation of ncRNA expression beyond mature miRNAs (e.g. tRNA, lincRNA, etc.) was observed.

3.4.3 Baseline miRNA expression and *in vitro* ibrutinib sensitivity

Abrogation of BCR signaling with ibrutinib induces apoptosis in CLL tumor cells, and does so in an *IGHV* status dependent manner[95,101]. This could also be observed after treating the screen samples with 1 µM ibrutinib for 48 hours *in vitro* and measuring cell viability with CellTiter-Glo®. As illustrated in Figure 20, viability – indicated by the level of cellular ATP - was decreased to 83% over all samples (median; n = 34) at this timepoint. For *IGHV* mutated samples, viability dropped to 89% (median; n = 15), whereas viability was decreased to 77% in *IGHV* unmutated samples (median; n = 19) (p = 0.006). Viability data were kindly provided by Leopold Sellner.

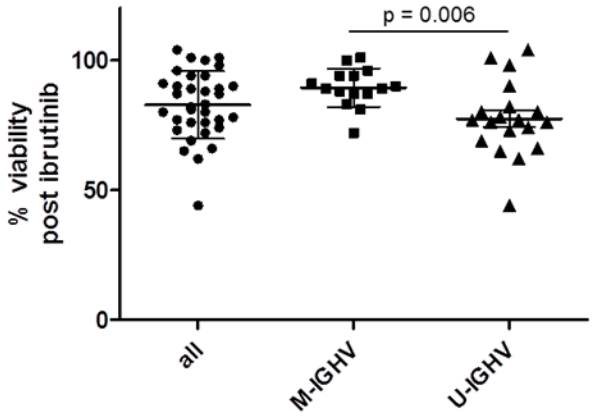

Figure 20. Cell viability post *in vitro* ibrutinib treatment, stratified by *IGHV* status. Cell viability in all samples (n = 34), and separated into mutated *IGHV* (n = 15) and unmutated *IGHV* (n = 19), after 48 hour treatment with 1 µM Ibrutinib as determined by ATP-measurement with CellTiter-Glo®. Referenced to non-treated samples; mean and SEM are indicated. P-value was determined by two-sided Student's t-test.

We asked whether basal expression levels of specific miRNAs correlate to, and putatively influence, the treatment efficiency *in vitro*. To this end, basal miRNA expression levels were tested for differential expression in regard to cellular viability after treatment with ibrutinib. Because of outliers, the results were additionally tested for robustness using Cook's distance measure. 10 miRNAs were found differentially expressed in regard to ibrutinib sensitivity, i.e. these miRNAs showed significant regulation upon 10% increase of cell viability post treatment (Figure 21 and Table 7). Of the 10, miR-23a, miR-23b and miR-24 are expressed from the same miRNA cluster. Three miRNAs, miR-574-5p, miR-155-5p and miR-4432 had been found to be *IGHV* status dependently expressed (refer to section 3.4.1). As miR-150-5p and miR-155-5p had been previously reported to regulate BCR signaling activity[233,235], the potential involvement of the 10 miRNAs in regulating BCR signaling was investigated. The highly expressed miRNAs miR-23b-3p, miR-150-5p, miR-24-3p, miR-23a-3p and miR-155-5p were selected for identification of potential mRNA targets. To identify mRNAs which were inversely co-regulated with the expression of these miRNAs, and at the same time predicted targets of the respective miRNA, mRNA expression data generated from small RNA sequencing (see also section 3.5.2), the Pearson correlation coefficient and the miRanda, miRWalk and TargetScan target prediction algorithms were used. For miR-150-5p, two potential mRNA targets were identified. The expression levels of the top hit, protein disulfide isomerase family A, member 6 (PDIA6) displayed a strong negative correlation to miR-150-5p expression ($R = -0.75$, $p = 0.002$) and was reported to be induced upon anti-IgM stimulation in CLL[59]. This opens up the possibility of BCR

signaling impairment by high miR-150-5p expression leading to ibrutinib resistance. The expression of Fc receptor-like protein 2 (FCRL2) correlated with and is targeted by miR-23a-3p (R = -0.68, p = 0.04). It is an inhibitor of BCR signaling[236] known to be downregulated in poor prognostic CLL[237]. It was also predicted to be targeted by miR-155-5p (R = -0.68, p = 0.06). For miR-574-5p, 20 predicted targets displayed inverse co-regulation (table S4), of which proto-oncogene PIM3, a serine/threonine kinase (R = -0.64, p = 0.01) and transcription factor forkhead box O4 (FOXO4, R = -0.54, p = 0.04) were previously implicated in regulating BCR signaling and/or survival[238-241].

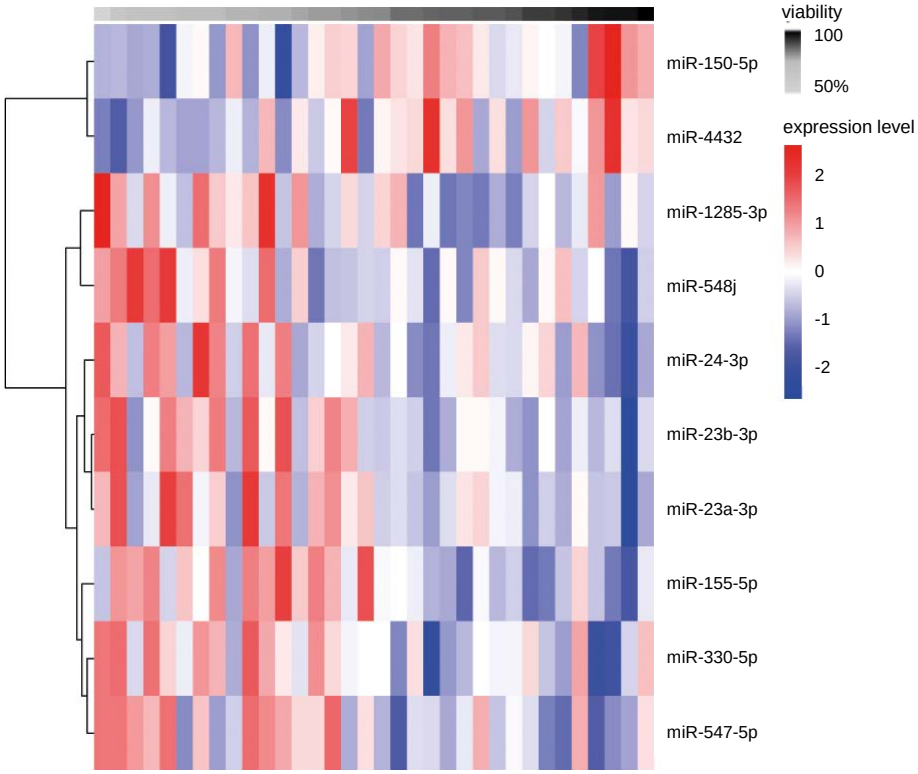

Figure 21. Hierarchical clustering of basal expression of miRNAs displaying robust differential expression in regard to CLL cell viability post *in vitro* ibrutinib treatment. miRNAs are presented in rows, CLL samples in columns. Median-centered, normalized expression levels are illustrated. Samples (n = 35) are sorted for cell viability post ibrutinib treatment (1 µM, 48 hours) as determined by CellTiter-Glo®.

The baseline miRNA expression profiles could not be used to reliably predict *in vitro* ibrutinib sensitivity though (R^2 = 0.2 for the correlation of observed viability after treatment to viability predicted using the L1 penalized linear regression model).

Table 7. miRNAs regulated with 10% increase of cell viability after 1 µM ibrutinib *in vitro.* n = 35 CLL samples. Normalized read counts and Benjamini-Hochberg corrected p-values are provided.

miRNA name	mean basal expression (reads)	Fold change	p-value
miR-23b-3p	1146	0.8	0.007
miR-4432	7	1.8	0.011
miR-150-5p	138529	1.2	0.011
miR-24-3p	7976	0.8	0.014
miR-23a-3p	3094	0.8	0.015
miR-548j	6	0.7	0.019
miR-574-5p	205	0.8	0.019
miR-155-5p	63468	0.9	0.029
miR-1285-3p	39	0.9	0.032
miR-330-5p	129	0.9	0.036

3.4.4 Summary of BCR-dependent miRNAs in CLL

The BCR signaling-dependent miRNA transcriptome in primary CLL was comprehensively assessed by small RNA sequencing. 12 miRNAs were found differentially expressed according to *IGHV* mutation status, which is a strong prognostic factor known to determine BCR signaling capacity. A miRNA signature made of 15 components predicted *IGHV* status with good accuracy (82%). By ibrutinib-mediated BCR signaling inhibition at the stage of BTK, six regulated miRNAs were identified: miR-320c and miR-1246 were induced, miR-484, miR-17-5p, miR-155-3p and miR-27a-5p were downregulated, implicating a role in BCR-signaling mediated support of cell survival. The basal expression of 10 miRNAs associated with *in vitro* sensitivity to ibrutinib treatment, and potentially influences BCR signaling capacity.

3.5 Identification of p53-dependent ncRNAs in primary CLL cells

The impaired transcriptional activity of mutant p53 was used to identify ncRNAs dependent on p53 function in primary leukemia cells by comparison of DNA-damage triggered induction in *TP53*^{wt} samples of previously untreated patients to *TP53*$^{del/mut}$ CLL.

Analyses were performed separately for mature miRNAs, presented in section 3.5.1, and other ncRNAs, presented in section 3.5.4. For the latter, p53-dependency was assessed by two approaches: Firstly, by qRT-PCR based assessment of the expression of long intergenic non-coding RNA p21 (lincRNA-p21), a known p53 target in other cancer entities[204]. Secondly, by analysis of small RNA sequencing data for ncRNAs displaying *TP53* status dependent induction after irradiation.

3.5.1 *TP53* status dependent miRNA induction

In the absence of DNA damage induction, no differentially expressed miRNAs were found in *TP53*^{wt} compared to *TP53*$^{del/mut}$, but the lower expression of miR-34a-5p in *TP53*$^{del/mut}$ (97 vs. 29 reads; p = 0.16) was confirmed. In an unsupervised hierarchical clustering, samples clustered by patient (data not shown), reflecting inter-patient heterogeneity.

Across all CLL samples, there was a strong correlation of miRNA expression in untreated versus irradiated CLL cells (median R^2 = 0.98), suggesting that the transcriptional profile is not altered for the great majority of miRNAs. An overview of irradiation-induced miRNA expression changes related to genetic and clinical parameters of our test cohort by unsupervised hierarchical clustering (Figure 21) demonstrated that the miRNA signature was not sufficient to identify the patient's genetic or treatment status, although most samples carrying *TP53*$^{del/mut}$ or del11q clustered together.

Subsequently, DNA damage triggered miRNA induction in *TP53*^{wt} was compared to *TP53*$^{del/mut}$ samples. A more dynamic expression change was observed in the p53 wild-type CLLs, where 36 miRNAs were regulated in response to DNA damage compared to 12 in the group with p53 loss/mutation (Table 8). While a set of miRNAs including miR-150-3p, miR-155-5p and miR-92a-3p was uniformly regulated in the genetic subgroups suggesting a p53-independent role upon DNA-damage, 23 miRNAs showed substantially different regulation in *TP53*^{wt} compared to *TP53*$^{del/mut}$ samples, albeit some at very low expression levels (Table 8, bold print). miR-34a-5p was the most strongly induced target in *TP53*^{wt} but not in *TP53*$^{del/mut}$ samples (4.3 fold, p < 0.001 vs. 2.9 fold, p < 0.001). Further, the expression of a set of miRNAs including miR-182-5p, miR-7-5p and miR-320d/c was found up-regulated after IR in *TP53*^{wt}, but not *TP53*$^{del/mut}$ samples, indicating

p53-dependent transcriptional regulation (see also S1). p53-dependent miR-34a-5p expression had been validated by qRT-PCR (Figure 14).

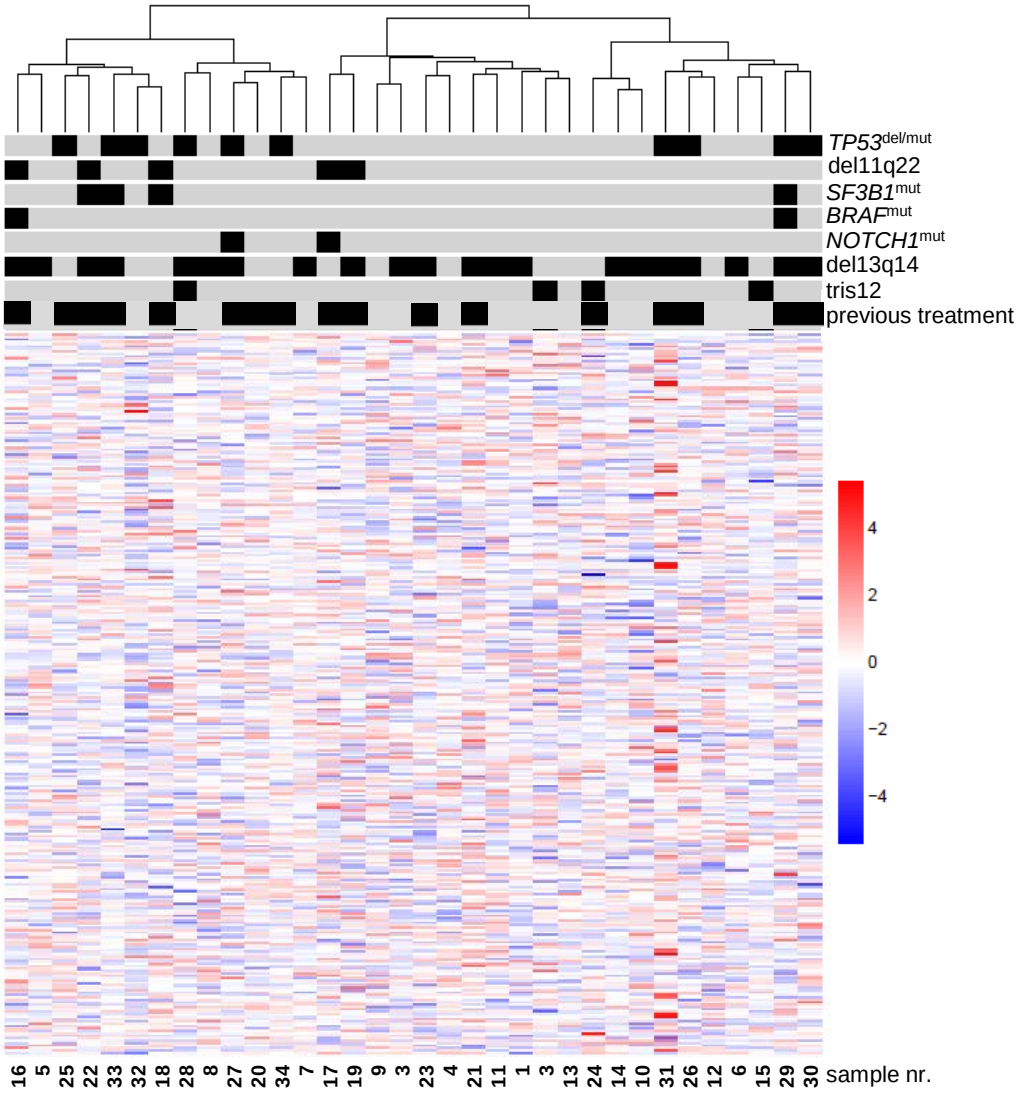

Figure 22. Unsupervised hierarchical clustering of IR-induced expression changes of the 300 most variably expressed miRNAs over 34 CLL patient samples. Genetic and clinical data are provided (grey = no, black = yes). Each row represents a miRNA, each column represents a sample. The colour scale illustrates the median-centered, relative expression change of a miRNA (red = higher, blue = lower than median).

Additionally, miR-7-5p and -320d regulation upon IR was successfully validated by qRT-PCR (median miR-7-5p *TP53*^{wt} (n = 10): 2.4 fold, p = .001; *TP53*$^{del/mut}$ (n = 6): 1.0 fold, p = .31; median miR-320d *TP53*^{wt} (n = 11): 1.7 fold, p = .01; *TP53*$^{del/mut}$ (n = 7): 1.0 fold, p = .37). Our data furthermore support a p53-dependent regulation of miR-320d family members miR-320c and miR-320b sharing the same seed sequence (Table 8).

Table 8A. miRNAs regulated upon DNA damage in *TP53*^{wt} (n = 15) CLL samples. miRNAs regulated upon IR in *TP53*^{wt} but not in *TP53*$^{del/mut}$ cases, or vice versa, are highlighted*. Mean normalized read counts 24h post NT (no treatment) or IR (irradiation) are provided. P-values are Benjamini-Hochberg corrected for multiple testing.

*miRNA selection criteria: A fold change (FC) difference of ≥0.3 between *TP53*^{wt} and *TP53*$^{del/mut}$, and a p-value of < 0.05 in at least one of both groups, and a difference in p-values of ≥ 1 $\log_{10}$.

miRNA	***TP53*^{wt}**		***TP53*$^{del/mut}$**		***TP53*^{wt}**	***TP53*$^{del/mut}$**	***TP53*^{wt}**	***TP53*$^{del/mut}$**
	NT	IR	NT	IR	FC	FC	p-value	p-value
miR-34a-5p	**97**	**370**	**29**	**115**	**4.3**	**2.9**	**4.3E-39**	**2.3E-04**
miR-150-3p	302	180	292	172	0.6	0.6	9.3E-18	1.3E-07
miR-182-5p	**98**	**158**	**149**	**170**	**1.6**	**1.2**	**6.7E-10**	**0.221**
miR-7-5p	**1218**	**1767**	**1508**	**1672**	**1.5**	**1.1**	**4.4E-08**	**0.671**
miR-155-5p	33921	47139	43778	54809	1.4	1.3	6.2E-07	3.6E-04
miR-320d	**39**	**69**	**59**	**57**	**1.7**	**1.0**	**7.6E-07**	**0.984**
miR-320c	**69**	**116**	**101**	**98**	**1.6**	**1.0**	**7.6E-07**	**0.990**
miR-21-3p	223	323	375	458	1.5	1.3	9.0E-07	0.026
miR-574-5p	**83**	**116**	**147**	**154**	**1.4**	**1.1**	**2.6E-05**	**0.918**
miR-9-5p	**115**	**167**	**1203**	**1299**	**1.5**	**1.1**	**8.4E-05**	**0.923**
miR-34a-3p	**1**	**4**	**0**	**1**	**8.4**	**8.7**	**8.6E-05**	**1.000**
miR-92a-3p	15619	18608	15648	18329	1.2	1.2	1.2E-04	0.221
miR-23a-3p	**1958**	**2496**	**2515**	**2546**	**1.3**	**1.0**	**1.2E-04**	**0.984**
miR-320b	**168**	**237**	**267**	**256**	**1.4**	**1.0**	**2.3E-04**	0.984
miR-186-5p	6295	5499	5903	5903	0.9	1.0	9.9E-06	0.984
miR-181d	**5**	**11**	**11**	**16**	**2.1**	**1.6**	**3.6E-04**	**0.501**
miR-29b-1-5p	**18**	**9**	**15**	**17**	**0.5**	**1.1**	**5.8E-04**	**0.936**
miR-24-3p	4276	5020	5773	6360	1.2	1.1	0.003	0.034
miR-1260b	**10**	**4**	**11**	**10**	**0.5**	**1.0**	**0.003**	**0.984**
miR-26a-2-3p	**129**	**75**	**92**	**78**	**0.6**	**0.9**	**0.004**	**0.921**
miR-339-5p	787	606	591	573	0.8	1.0	0.006	0.936
miR-181c-3p	**5**	**11**	**10**	**15**	**2.1**	**1.6**	**0.006**	**0.605**
miR-28-5p	1206	1027	1200	1204	0.8	1.0	0.009	0.990
miR-183-5p	29	39	37	43	1.4	1.4	0.009	0.501
miR-335-5p	487	415	486	475	0.8	1.0	0.012	0.936
miR-582-5p	**3**	**7**	**2**	**6**	**2.2**	**1.5**	**0.014**	**0.928**
miR-27a-5p	240	317	390	454	1.3	1.2	0.014	0.221
miR-15a-5p	**1266**	**1063**	**705**	**675**	**0.8**	**1.1**	**0.017**	**0.928**
miR-3653	**182**	**255**	**207**	**178**	**1.3**	**0.9**	0.020	0.928
miR-142-3p	25133	22119	21751	23157	0.9	1.1	0.020	0.928
miR-6724-5p	**5**	**3**	**4**	**3**	**0.4**	**0.8**	**0.021**	**1.000**
let-7i-5p	49359	58378	56522	60268	1.2	1.1	0.023	1.000
miR-27a-3p	16001	18532	19466	23169	1.2	1.2	0.035	0.006
miR-3609	**61**	**81**	**82**	**78**	**1.2**	**0.9**	**0.035**	**0.936**
miR-17-5p	3710	4538	3285	4696	1.2	1.4	0.035	1.3E-04
miR-339-3p	393	347	351	335	0.9	1.0	0.043	0.984

Table 8B. miRNAs regulated upon DNA damage in *TP53*$^{del/mut}$ CLL (n = 10) not listed in A. .

miRNA	*TP53*^{wt}		*TP53*$^{del/mut}$		*TP53*^{wt}	*TP53*$^{del/mut}$	*TP53*^{wt}	*TP53*$^{del/mut}$
	NT	IR	NT	IR	FC	FC	p-value	p-value
miR-18a-5p	**71**	**73**	**61**	**95**	**1.0**	**1.6**	**0.902**	**0.002**
miR-20a-5p	16613	18664	15483	19367	1.1	1.3	0.432	0.004
miR-155-3p	**14**	**17**	**19**	**36**	**1.2**	**1.8**	**0.578**	**0.011**
miR-1246	**8040**	**10090**	**12275**	**9635**	**1.2**	**0.8**	**0.213**	**0.025**
miR-22-3p	2733	2876	3037	3451	1.0	1.1	0.839	0.026

On the contrary, three miRNAs were regulated in the TP53 del/mut but not TP53wt samples (Table 8B), suggesting a p53-independent role in resistance to DNA damage-induced apoptosis.

3.5.2 Deriving insights into the regulation of long RNA transcripts from a small RNA sequencing screen

The small RNA sequencing reads had been mapped to a set of ncRNA families and mRNA (section 3.3.1). In order to investigate whether these expression data derived from fragments of longer RNAs would be informative, i.e. whether the fragment quantity would reflect the parent RNA expression and could be used for analyses, irradiation-induced mRNA expression changes in previously untreated *TP53*^{wt} were compared to *TP53*$^{del/mut}$ samples.

In the wild-type setting, 792 mRNA transcripts were found significantly regulated as opposed to 15 in p53 aberrant samples. Table 9 compares the 10 most strongly regulated mRNAs in the *TP53*^{wt} samples and well-established p53 targets Bax[242,243] and GADD45A[153,244] to their expression and induction in *TP53*$^{del/mut}$ CLLs. Key p53 targets MDM2 and CDKN1A (p21) ranked among the top five induced mRNAs in *TP53*^{wt}, but showed no significant induction in *TP53*$^{del/mut}$. The same regulation was also observed for Bax and GADD45A. In line with this, all of the top 10 regulated mRNAs displaying induction exclusively in the wild-type setting were known p53 targets (bold print; RPS19[206,208,243], MDM2[245], PLXNB2[246], TRIM22[243], CDKN1A[247,248], PCNA[153], TNFRSF10B[153], ASCC3[208], BBC3 (PUMA)[206,249]). *TP53* status dependent induction was not a bystander effect of higher RNA fragmentation in irradiated *TP53*^{wt} than *TP53*$^{del/mut}$ samples caused by higher apoptosis rates in *TP53*^{wt} (Figure 12), since the mean RIN for both *TP53* groups after IR was 8.2. The expression values of p21/CDKN1A post irradiation as determined by qRT-PCR and smRNA sequencing correlated well (R^2 = 0.65) over all samples.

These data strongly suggested that small RNA sequencing was representative even for longer transcripts.

Table 9. Top mRNAs induced in previously untreated *TP53*^{wt} compared to *TP53*$^{del/mut}$ samples 24 h post irradiation. Known p53 targets are marked by bold print. Mean normalized read counts and Benjamini-Hochberg corrected p-values are provided. NT = non-treated, IR = irradiated, FC = fold change.

Rank	mRNA name	*TP53*^{wt}		*TP53*$^{del/mut}$		*TP53*^{wt}	*TP53*$^{del/mut}$	*TP53*^{wt}	*TP53*$^{del/mut}$
		NT	IR	NT	IR	FC	FC	p-value	p-value
1	**RPS19**	**140**	**387**	**121**	**185**	**2.7**	**0.7**	**3.6E-40**	**0.015**
2	**MDM2**	**92**	**390**	**81**	**179**	**4.1**	**1.9**	**4.7E-40**	**0.178**
3	**PLXNB2**	**28**	**103**	**24**	**42**	**3.7**	**1.6**	**4.3E-22**	**0.154**
4	**TRIM22**	**61**	**144**	**64**	**78**	**2.3**	**1.1**	**7.2E-21**	**1.000**
5	**CDKN1A**	**10**	**44**	**11**	**21**	**4.5**	**1.9**	**1.1E-19**	**0.207**
6	**PCNA**	**17**	**50**	**19**	**27**	**2.8**	**1.4**	**2.1E-15**	**1.000**
7	**TNFRSF10B**	**34**	**80**	**33**	**41**	**2.3**	**1.2**	**8.9E-14**	**1.000**
8	EEF1A1	1139	1829	1249	1741	1.6	1.4	4.9E-13	5.2E-4
9	**ASCC3**	**72**	**132**	**70**	**84**	**1.8**	**1.2**	**1.5E-12**	**1.000**
10	**BBC3**	**9**	**29**	**7**	**14**	**3.2**	**1.7**	**1.8E-12**	**1.000**
17	**BAX**	**29**	**55**	**27**	**33**	**1.9**	**1.3**	**5.6E-9**	**1.000**
78	**GADD45A**	**11**	**21**	**9**	**14**	**2.0**	**1.6**	**6.6E-5**	**1.000**

3.5.3 Potential targets of p53-dependently regulated miRNAs in CLL

Target prediction for miR-34a-5p, miR-182-5p, miR-7-5p and miR-320c/d was performed in Ingenuity® (based on the TargetScan algorithm). Only mRNAs significantly downregulated after DNA damage in *TP53*^{wt} samples were analysed. Table 10 summarizes all predicted mRNA targets for which a role in cell proliferation and/or survival has been previously reported, and which were predicted to be targeted by the respective miRNA by at least one additional database tool (TarBase[250], miRanda[118], miRwalk[223], PicTar[251]). Induction of miR-182-5p, for example, correlates with a reduction of nuclear receptor subfamily 1, group D, member 2 (NR1D2) mRNA, which was suggested to negatively regulate p21 expression[252]. It further correlates with a downregulation of O-linked β-N-acetylglucosamine transferase (OGT) mRNA levels. OGT has been shown to affect the phosphorylation of ATM, fostering p53 activation[253]. Moreover, miR-182-5p induction correlates with reduction of cAMP-dependent protein kinase type I-alpha regulatory subunit 1 alpha (PRKAR1A) mRNA. PRKAR1A is overexpressed in a variety of tumors[254] and a loss of function was shown to cause apoptosis via BCL2[255].

Table 10. mRNAs predicted to be targeted by p53-dependent miRNAs upon DNA damage. Gene names of high confidence targets (TargetScan) are listed. FC, fold change after irradiation (5 Gy) in *TP53*^{wt} CLL.

miRNA name	FC	mRNA target (gene)	FC	Involved in proliferation/survival, reference
miRNA-34a-5p	4.3	E2F5	0.6	256,257
		MDM4	0.8	258,259
miR-182-5p	1.6	NR1D2	0.7	252
		OGT	0.8	253
		PRKAR1A	0.8	254,255
miR-7-5p	1.5	OGT	0.8	253
		PRKCB	0.8	260,261
miR-320c/d	1.7	NR1D2	0.7	252
		PCDH9	0.7	69
		PRKAR1A	0.8	254,255
		YWHAZ	0.8	**262**

3.5.4 p53 dependent long non-coding RNA induction

3.5.4.1 lincRNA-p21 in CLL

qRT-PCR quantification of lincRNA-p21 expression upon irradiation-triggered p53 activation revealed a significantly stronger induction in *TP53*^{wt} (n = 19, p = 0.005) than *TP53*$^{del/mut}$ CLL (n = 10, p = 0.08) (median 16.5 vs. 3.0 fold, p = 0.001), while samples with del11q displayed a medium induction (n = 5, p = 0.04, median 16.5 vs. 7.7 fold, p = 0.11) (Figure 23 A, B).

These results were validated in an independent cohort of 39 CLL patients (Figure 23 C, D). Brisk lincRNA-p21 induction was again observed after DNA damage in *TP53*^{wt} CLL (p < 0.001, median induction 16.3 fold) but not in p53 deficient CLL (p = 0.27, induction 1.3 fold; Figure 23 D).

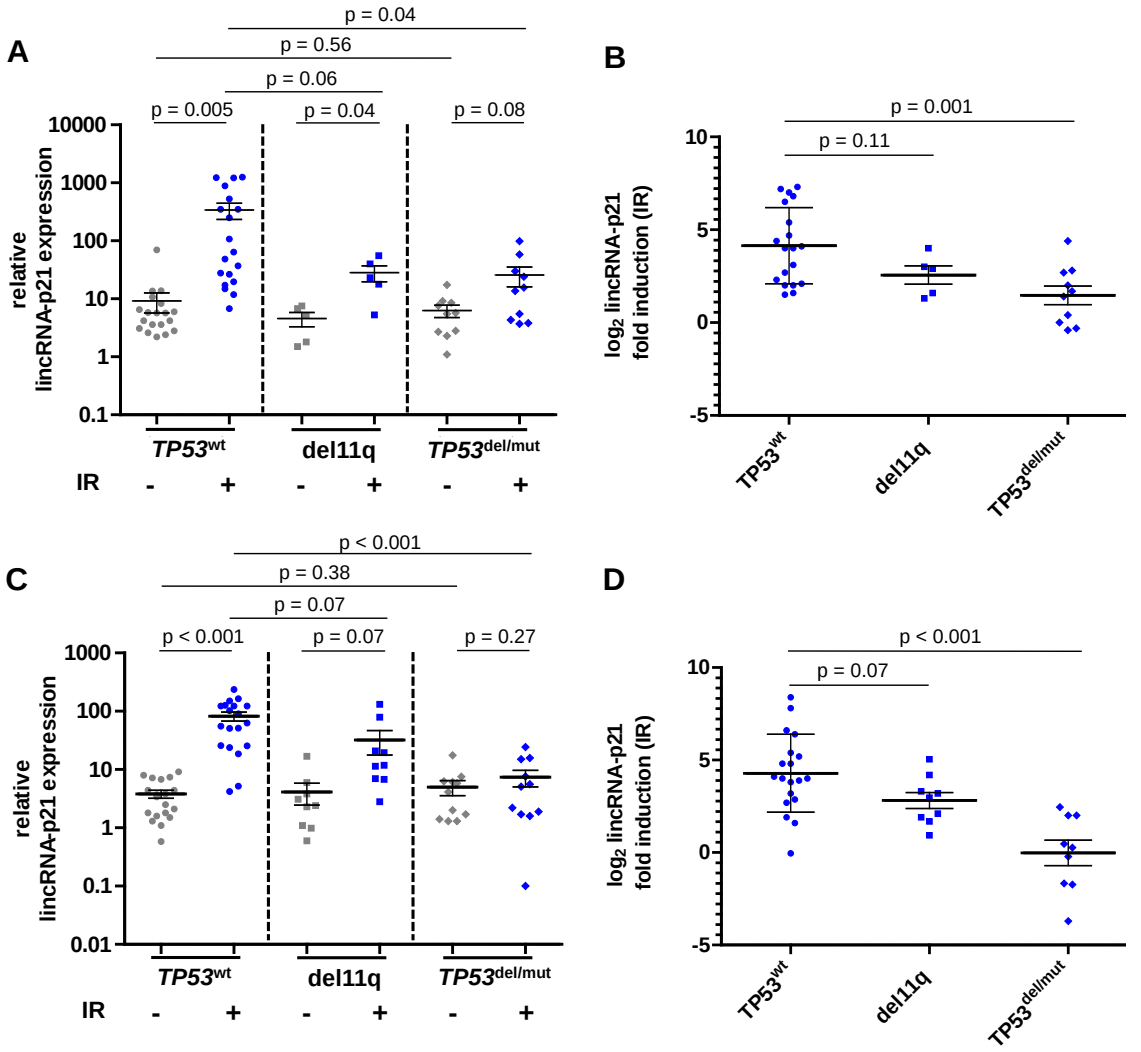

Figure 23. DNA damage triggered lincRNA-p21 induction in CLL. . (A, B) lincRNA-p21 expression in samples of n = 34 CLL patients left untreated for 24h or 24h post irradiation (IR, 5 Gy), grouped into *TP53*^{wt} and 11q23 disomic, *TP53*^{wt} with del11q23, and *TP53*$^{del/mut}$ as in Figure 14. **(C, D)** LincRNA-p21 induction in a validation cohort of CLL patients (n = 36). Median ± SEM are indicated.

We observed a strong correlation of lincRNA-p21 with induction of p21 and with reduction of cell viability due to apoptosis, a major endpoint of p53 activation (Figure 24 A, B).

Cp values across all samples post irradiation ranged between 29.0 and 35.6, indicating low expression.

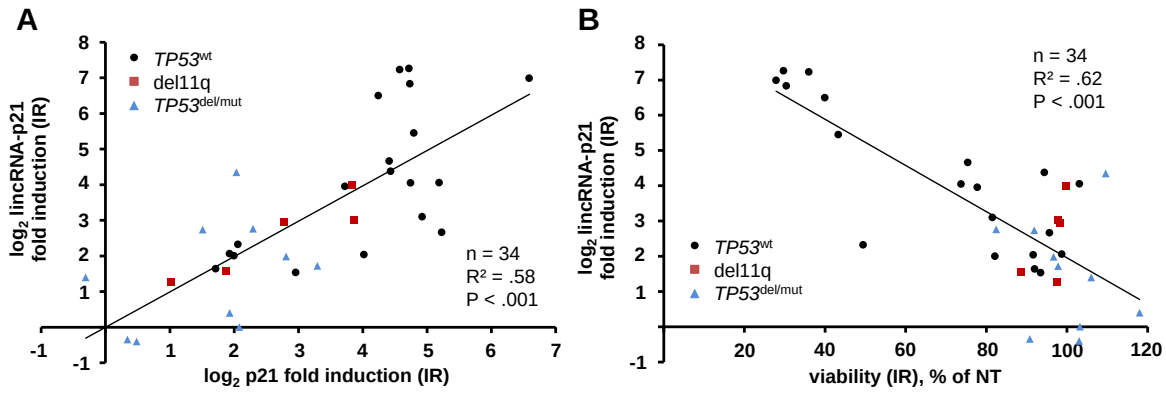

Figure 24. Correlation of DNA-damage triggered lincRNA-p21 induction with p21 induction and cell viability. (A) LincRNA-p21 vs. p21 expression after IR in the test cohort. Median ± SD are indicated. **(B)** Correlation of lincRNA-p21 induction with cellular viability as determined by double negativity in FACS Annexin V / PI staining of the test cohort samples.

To support p53-dependence of expression in the absence of DNA damage induction, primary CLL cells were exposed for 24 hours to 10 µM of the MDM2 inhibitor nutlin-3 selectively stabilizing p53. Likewise, nutlin-3 led to induction of lincRNA-p21 expression exclusively in *TP53*^{wt} (n = 7, median 5.3 fold), but not *TP53*$^{del/mut}$ samples (n = 3, median 1.1 fold) (Figure 25).

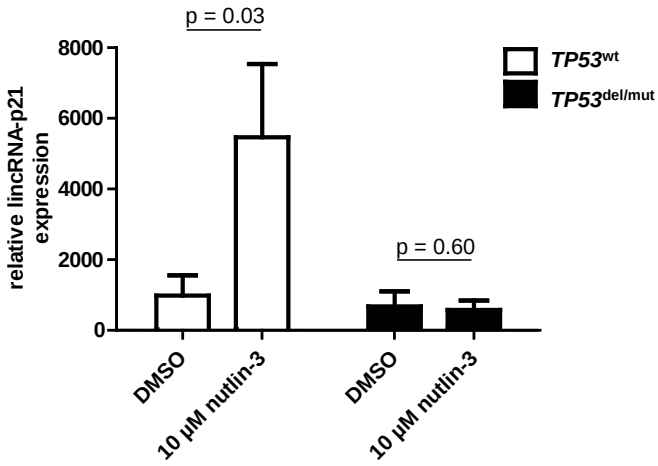

Figure 25. LincRNA-p21 expression 24 h post induction with 10 µM nutlin-3 or vehicle control in primary CLL samples. Expression was determined by qRT-PCR in n = 8 p53^{wt} samples and n = 3 p53$^{del/mut}$ samples. Means ± SEM are indicated.

3.5.2.3 NEAT1 in CLL

In order to identify p53-dependent ncRNAs beyond mature miRNAs, all reads ≥ 15 nt which did not correspond to mature miRNA sequences were mapped to a set of ncRNA

reference sequences curated from Ensembl 71, GtRNAdb[217], Rfam 11.0, and the piRNA cluster database[218]. From this, a list of DNA damage induced ncRNA in primary CLL was generated (Table 11). The precursor of miR-34a was the top IR-induced ncRNA. Directly following pre-miR-34a, two transcripts of NEAT1 (nuclear enriched abundant transcript 1), a lincRNA constituting a major component of the nuclear paraspeckles of mammalian cells[263], showed distinct p53-dependent induction after IR.

In total, three overlapping NEAT1 transcript sequences were captured - NEAT1-002 (1.8 kb), NEAT1-202 (1.5 kb) and NEAT1-001 (22.7 kb; Figure 26A) - originating from the 22.8 kb long *NEAT1* gene located on chromosome 11q13.1 (11:65,190,245-65,213,011 Ensembl GRCh37). In contrast to NEAT1-002 and NEAT-202, NEAT1-001 was not found regulated by DNA damage (mean fold change $TP53^{wt}$ 1.1, p = 0.32; $TP53^{del/mut}$ 1.0, p = 0.99). DNA damage-triggered NEAT1-202 and NEAT1-002 induction in previously untreated $TP53^{wt}$ was significantly stronger than in $TP53^{del/mut}$ samples ($TP53^{wt}$ mean NEAT1-202/NEAT1-002 induction 2.0/1.8 fold, p < 0.001; $TP53^{del/mut}$ mean NEAT1-202/NEAT1-002 induction 1.3/1.3 fold, p = 0.22/0.03; Table 11 and Figure 26 B, C). NEAT1-202 and NEAT1-002 normalized read counts over all samples strongly correlated (R^2 = 0.91), which was expected due to high sequence similarity of the transcripts.

Table 11. Top 10 ncRNAs induced in previously untreated $TP53^{wt}$ compared to $TP53^{del/mut}$ samples 24 h post irradiation. Mature miRNAs were excluded. Mean normalized read counts and Benjamini-Hochberg corrected p-values are provided. FC = fold change.

RNA name	$TP53^{wt}$		$TP53^{del/mut}$		$TP53^{wt}$	$TP53^{del/mut}$	$TP53^{wt}$	$TP53^{del/mut}$
	NT	IR	NT	IR	FC	FC	p-value	p-value
pre-miR-34a	200	853	70	314	4.6	3.5	1.07E-34	2.50E-07
NEAT1-202	40	84	41	52	2.0	1.3	8.43E-24	0.222
NEAT1-002	61	115	58	77	1.8	1.3	5.04E-17	0.025
trna8-LysCTT	358	642	354	401	1.8	1.1	5.12E-11	0.811
tRNA	385	669	397	460	1.7	1.1	5.12E-11	0.444
trna30-LysCTT	703	1036	771	880	1.5	1.2	1.58E-10	0.201
trna119-LysCTT	4063	5796	4212	6176	1.4	1.4	4.00E-09	2.29E-16
trna10-LysCTT	5366	8067	5003	7175	1.5	1.4	4.97E-07	4.84E-13
trna13-LysCTT	8107	12173	7243	9670	1.5	1.4	1.24E-06	2.01E-07
trna1-SeC(e)TCA	343	584	215	315	1.7	1.4	1.68E-06	0.085

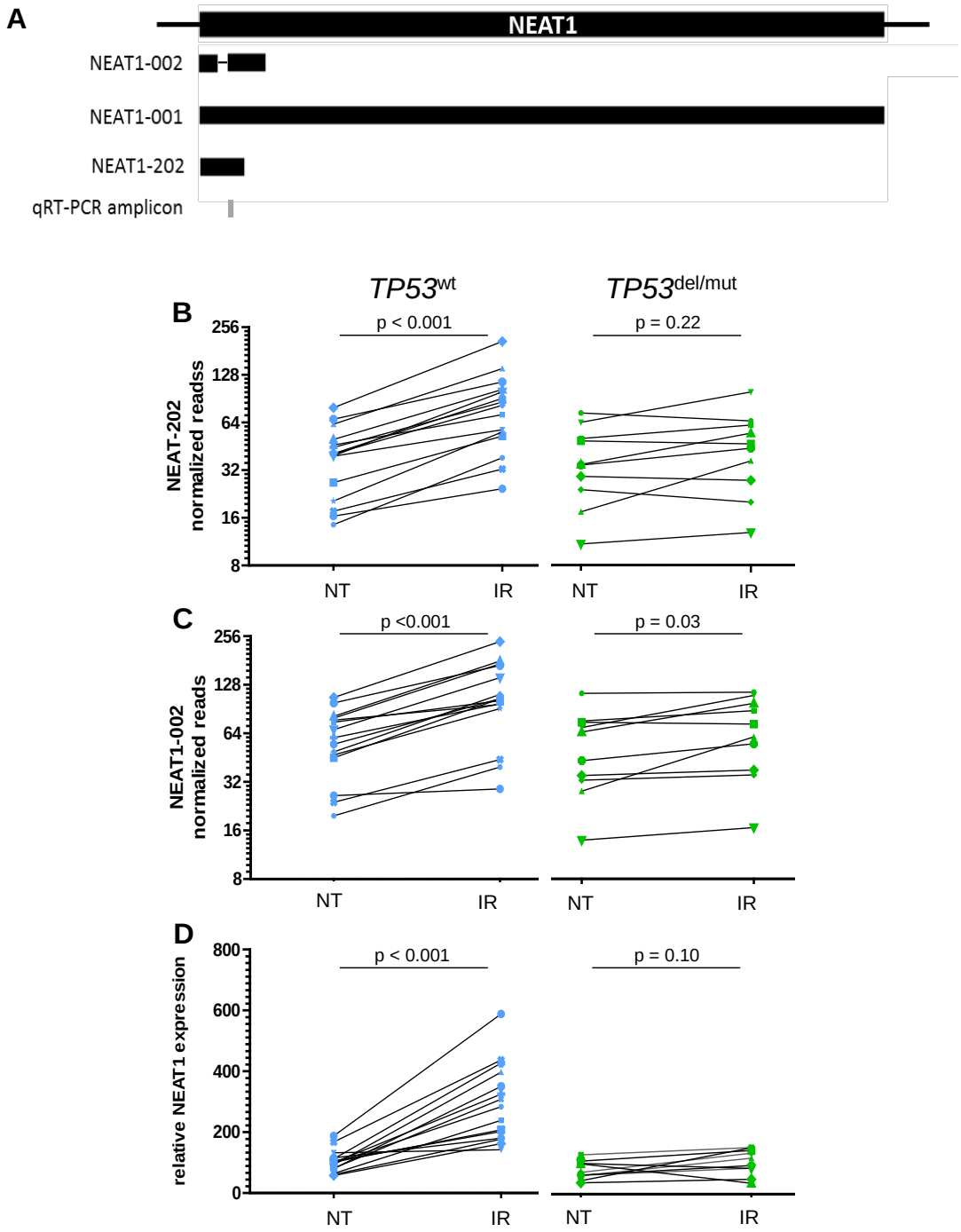

Figure 26. NEAT1 induction upon DNA damage in primary CLL cells. (A) NEAT1 transcripts as originating from the 22.77 kb long *NEAT1* gene on chromosome 11q as in Ensembl GRCh37. Localization of the qRT-PCR amplicon is indicated. **(B, C)** NEAT1-202 and NEAT1-002 expression as determined by sequencing (see Table 11) in non-treated (NT) and irradiated (IR) samples of *TP53*^{wt} and *TP53*$^{del/mut}$ status, and **(D)** as determined by qRT-PCR in identical samples. In B and C, P-values were calculated using the Wald test and corrected for multiple testing. In D, two-sided Student's t-test was applied.

NEAT1 expression levels were validated by qRT-PCR detecting an amplicon in the 5' end of the 2nd exon of NEAT1-002, i.e. detecting all three NEAT1 transcripts (Figure 26 A, D and Figure 27). As in the sequencing data, NEAT1 expression after IR was significantly higher in *TP53*^{wt} than *TP53*$^{del/mut}$ samples ($p < 0.001$, Figure 27 A). Cp values of irradiated samples ranged between 19.5 and 23.7, indicating high NEAT1 expression. Thus, the moderate average induction of 2.8-fold (qRT-PCR) in *TP53*^{wt} samples reflected a strong addition in NEAT1 transcript amount upon DNA damage.

Samples harboring del11q displayed a tendency towards diminished NEAT1 induction as illustrated in Figure 27 A, B (*TP53*^{wt} median 2.9 fold; del11q 1.9 fold; *TP53*$^{mut/del}$ 1.3 fold).

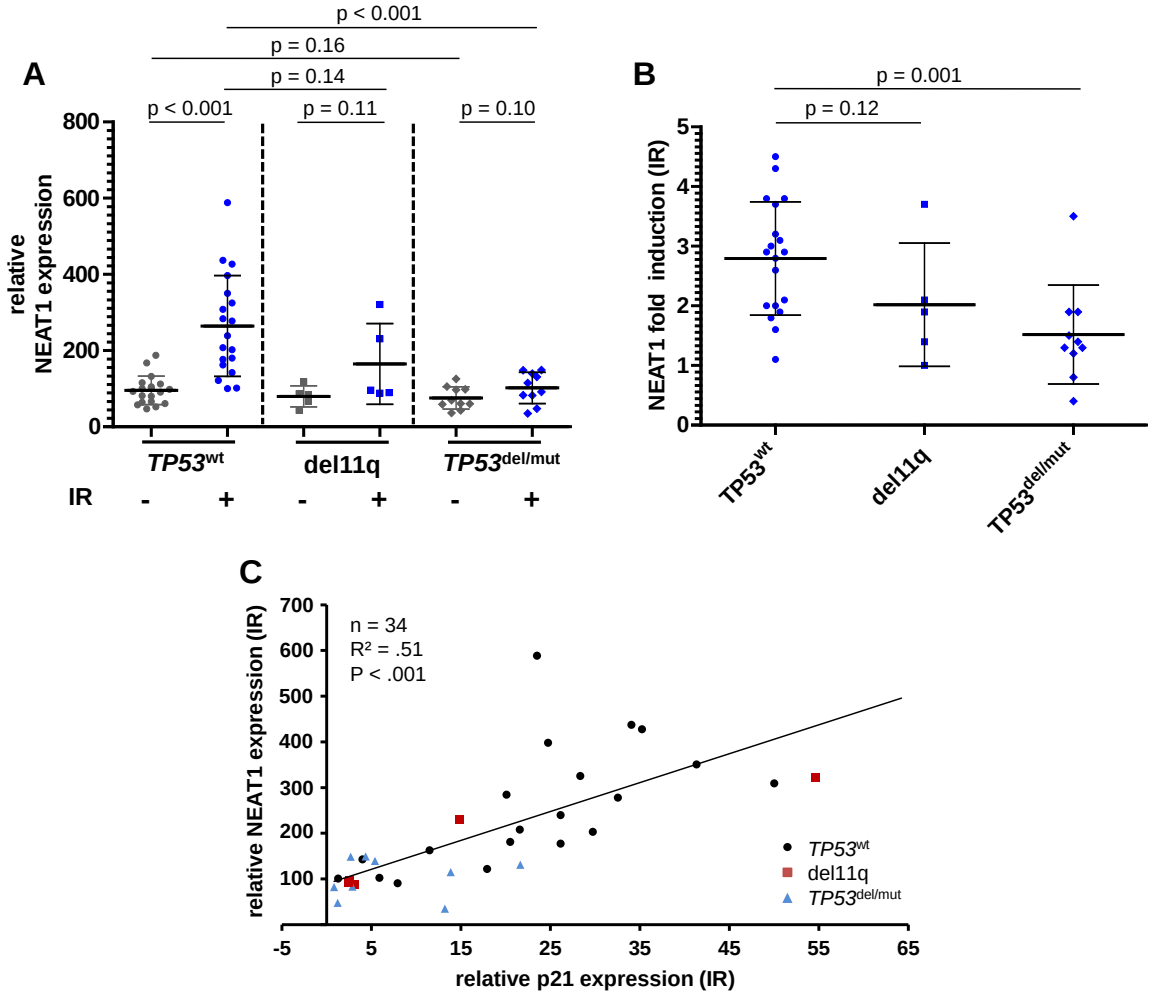

Figure 27. NEAT1 expression 24 hours after irradiation (IR) or no treatment (NT) of primary CLL cells. (A) NEAT1 expression at NT state or post IR, stratified by *TP53* and 11q status. **(B)** DNA damage-triggered NEAT1 induction stratified by *TP53* and 11q status. P-values were calculated by two-sided Student's t-test. **(C)** Correlation of NEAT1 and p21 expression in irradiated samples. All data were generated by qRT-PCR.

The level of NEAT1 and p21 expression after DNA damage strongly correlated (Figure 27 C), indicating a common regulatory mechanism. The correlation of NEAT1 expression to the fraction of apoptotic cells was low ($R^2 = 0.19$, $p = 0.28$; data not shown).

Targeted activation of p53 by nutlin-3 treatment of primary CLL cells induced cellular apoptosis in *TP53*^{wt} samples ($p < 0.001$) but not in the presence of *TP53* aberrations ($p = 0.35$). At the same time, NEAT1 expression was induced in *TP53*^{wt} ($p < 0.001$) but not *TP53*$^{del/mut}$ samples ($p = 0.30$) (Figure 28), confirming p53-dependent regulation.

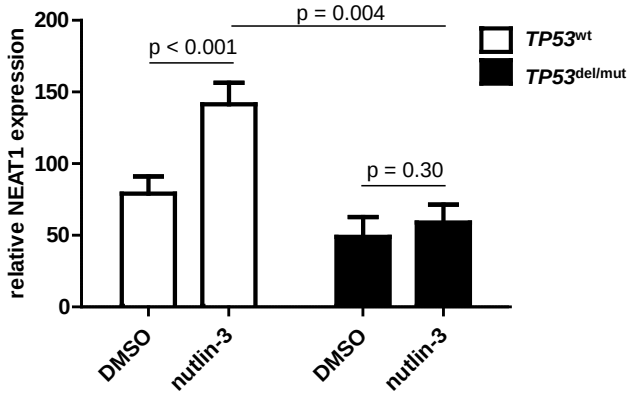

Figure 28. NEAT1 expression 24 h post induction with 10 µM nutlin-3 or vehicle control in primary CLL samples. Expression was determined by qRT-PCR in n = 10 *TP53*^{wt} samples and n = 5 *TP53*$^{del/mut}$ samples. Means ± SEM are indicated.

3.5.5 Comparison of p53 pathway activity in treated and untreated *TP53* wild-type CLL

TP53 aberrations in CLL associate with relapse after therapy, but not all relapsed CLL patients carry mutant p53[264,47]. To determine factors causing poor therapy response in the wild-type setting, p53 pathway activity was assessed in nine previously treated, high-risk *TP53*^{wt} CLLs and compared to samples of *TP53*^{wt} patients who had not received prior therapy for CLL.

In treated *TP53*^{wt} CLLs, only three miRNAs were regulated upon IR-induced p53 activation: miR-34a-5p (fold change (FC) 4.1, $p < 0.001$), miR-150-3p (FC 0.7, $p = 0.002$) and miR-21-3p (FC 1.3, $p = 0.03$). This is in contrast to the dynamic response observed in samples of *TP53*^{wt}, untreated patients, where 36 miRNAs were regulated (Table 8). The expression of p53 targets miR-182-5p, miR-7-5p and miR-320d/c was unchanged upon DNA damage in *TP53*^{wt} high-risk patient samples (miR-182-5p FC 1.3, $p = 0.68$; miR-7-5p FC 1.1, $p = 0.84$; miR-320d FC 0.9, $p = 0.97$, miR-320c FC 1.0, $p = 0.98$). Similarly, treated *TP53*^{wt} CLLs displayed reduced lincRNA-p21 and NEAT1 induction

(Figure 29, PT median 4.2 fold and 2.0 fold, respectively) compared to untreated (UT) *TP53*^{wt} CLLs (median 20.7 fold and 2.9 fold, respectively; p = 0.03 for lincRNA-p21 and p = 0.01 for NEAT1). This was independent from the treated *TP53*^{wt} patients' *ATM* status, as lincRNA-p21 induction was diminished to 7.9 fold (median) also in disomic 11q and wild-type *ATM* samples (p = 0.17, Figure 29 A). This was comparable for NEAT1, where induction in the high-risk group with *ATM* aberrations was 2.0 fold (n = 6), just as for *ATM* normal samples (median 2.0 fold, n = 3; p = 0.60), both being far lower than the induction in 11q disomic *ATM*^{wt}, *TP53*^{wt} samples of untreated patients. This is in keeping with the observations for p21 (refer to section 3.2). Together, this points towards impaired p53 pathway activity in treated *TP53*^{wt} high-risk CLLs, which is independent from aberrations of *ATM*.

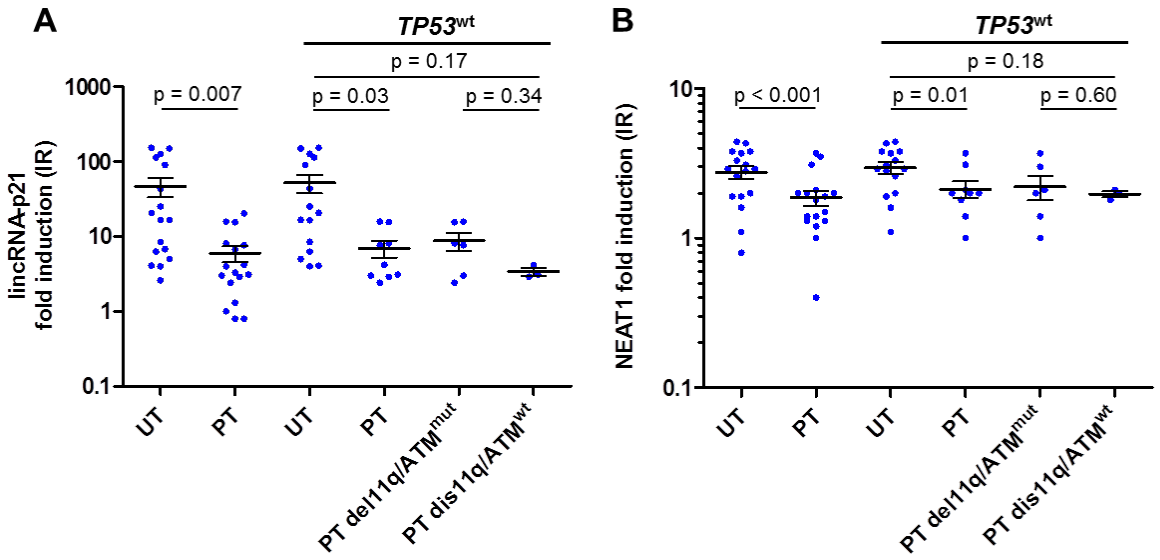

Figure 29. Induction of lincRNA-p21 and NEAT1 in CLL stratified by patient treatment, *TP53* and *ATM* status. (A) lincRNA-p21 fold induction and **(B)** NEAT1 fold induction in CLL-PBMNCs 24 hours post 5 Gy irradiation stratified by patient treatment status, indicating samples derived from patients that were previously untreated (UT), or had received prior therapy (PT) for CLL. The four groups on the right display *TP53*^{wt} samples only, stratified by treatment (UT = 15, PT = 9) and ATM status (aberrant n = 6; normal n = 3). The PT *TP53*^{wt} patients had all relapsed within 26 months after therapy. Means and standard errors are indicated. P-values were calculated by Student's t-test.

To explore possible mechanisms of p53 deactivation in treated *TP53*^{wt} patients, baseline miRNA profiles were compared between untreated *TP53*^{wt} and treated, high-risk *TP53*^{wt} CLLs. After additional testing for robustness using Cook's distance measure, miR-1285-3p and let-7b-5p were found higher expressed in samples from treated patients (fold difference 1.9 and 2.2, p < 0.05). Interestingly, miR-1285-3p was reported to target p53

mRNA[265]. However, no direct correlation between baseline miR-1285-3p expression and p53 activity indicated by IR-triggered p21 induction was observed (n = 35, R^2 = 0.05). Still, *TP53*^{wt} high-risk patient samples expressing high miR-1285-3p (> median) displayed a tendency towards lower p21 induction (average 5.8 fold) than low expressing samples (average 10.1 fold, p = 0.22). Let-7b is predicted to target the mRNA of p53 and *TP53* regulating kinase (miRanda, miRWalk and TargetScan). Again, no direct correlation of basal expression to p21 induction post irradiation was found (R^2 = 0.04). High (> median) let-7b-5p expressing samples showed only slightly lower p21 induction than low let-7b-5p (< median) expressors (6.0 vs. 9.1, p = 0.40). In addition, basal non-miRNA ncRNA expression was compared between previously untreated *TP53*^{wt} patients and treated *TP53*^{wt} patients. As displayed in table S5, nine transcripts were differentially expressed, whereas for none of them, a function in the p53 pathway has been previously reported. In conclusion, no overexpression of a known ncRNA repressor of the p53 pathway was found in treated, high-risk *TP53*^{wt} patients.

3.6 p53 dependency of lincRNA-p21 and NEAT1 expression in the Burkitt's Lymphoma (BL) cell line model

To assess lincRNA-p21 and NEAT1 regulation in other lymphoma subtypes, a large set of Burkitt's Lymphoma derived B-cell lines of disparate *TP53* status was chosen. In this model, p53-dependency of NEAT1 and lincRNA-p21 was investigated in more detail.

3.6.1 lincRNA-p21 and NEAT1 induction in BL cell lines

Induction dynamics of lincRNA-p21 and NEAT1 expression in response to IR-mediated DNA damage were studied in a set of 11 genetically unmodified Burkitt's lymphoma cell lines, of which six were *TP53*^{wt}, seven *TP53*^{mut} (table S2) as illustrated in Figure 30.

In analogy to the observations in CLL, lincRNA-p21 was induced 24 hours post 5 Gy IR in the *TP53*^{wt} cell lines only, while none of the *TP53*^{mut} cell lines showed an increase in expression (Figure 30 A), supporting a direct regulation by p53. The induction observed in the wild-type setting was heterogeneous, ranging from 22.0 fold (BL-7) to 1.9 fold (Seraphine).

NEAT1 induction was more subtle and did not separate the cell lines by *TP53* mutation status as clearly (Figure 30 B). Still, at 24 hours after IR, *TP53*^{wt} displayed a clear tendency towards higher NEAT1 induction (mean 2.5 fold) than *TP53*^{mut} cell lines (mean 1.1 fold) (p = 0.07).

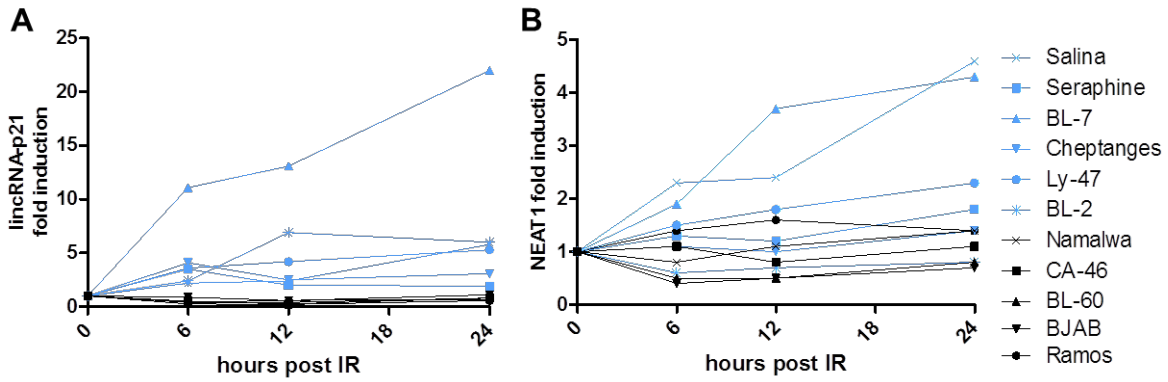

Figure 30. Time course of lincRNA-p21 and NEAT1 induction in *TP53*^{wt} and *TP53*^{mut} Burkitt's Lymphoma cell lines. (A) lincRNA-p21 and **(B)** NEAT1 induction in *TP53*^{wt} (blue) and *TP53*^{mut} (black) Burkitt's Lymphoma cell lines after 5 Gy irradiation (IR) was monitored for up to 24 hours (h). Expression levels are relative to the non-irradiated sample (normalized to lamin B1) determined by qRT-PCR.

3.6.2 NEAT1 and lincRNA-p21 expression in BL cell line models of controlled p53 expression

To finally prove p53-dependency of NEAT1 and lincRNA-p21 expression, modified Salina and Seraphine cells (p53^{wt}) with p53 expression controlled by shRNA mediated knockdown (p53^{kd}, Salina) or CRISPR/Cas9 mediated p53 knockout (p53^{ko}, Seraphine) as well as p53 mutant Namalwa (p53^{mut}) were used. The cell lines were exposed to nutlin-3 for 6 or 24 hours or treated with vehicle control. A concentration- and time-dependent, nutlin-3 triggered induction of p53 protein levels was observed in the wild-type setting (Figure 31).

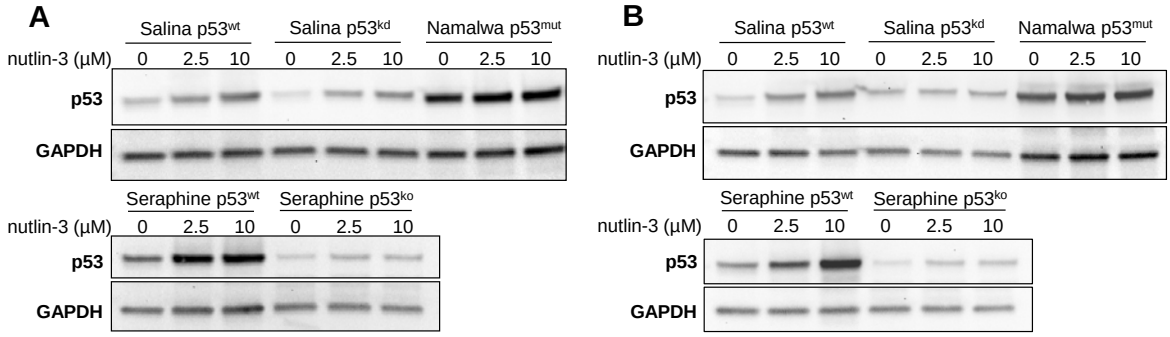

Figure 31. Effect of nutlin-3 treatment on p53 expression in BL cell lines of defined p53 status. (A) p53 and expression after 6 h treatment with 0-10 µM nutlin-3 determined by Western Blot. **(B)** p53 expression after 24 h treatment with 0-10 µM nutlin-3. GAPDH served as loading control.

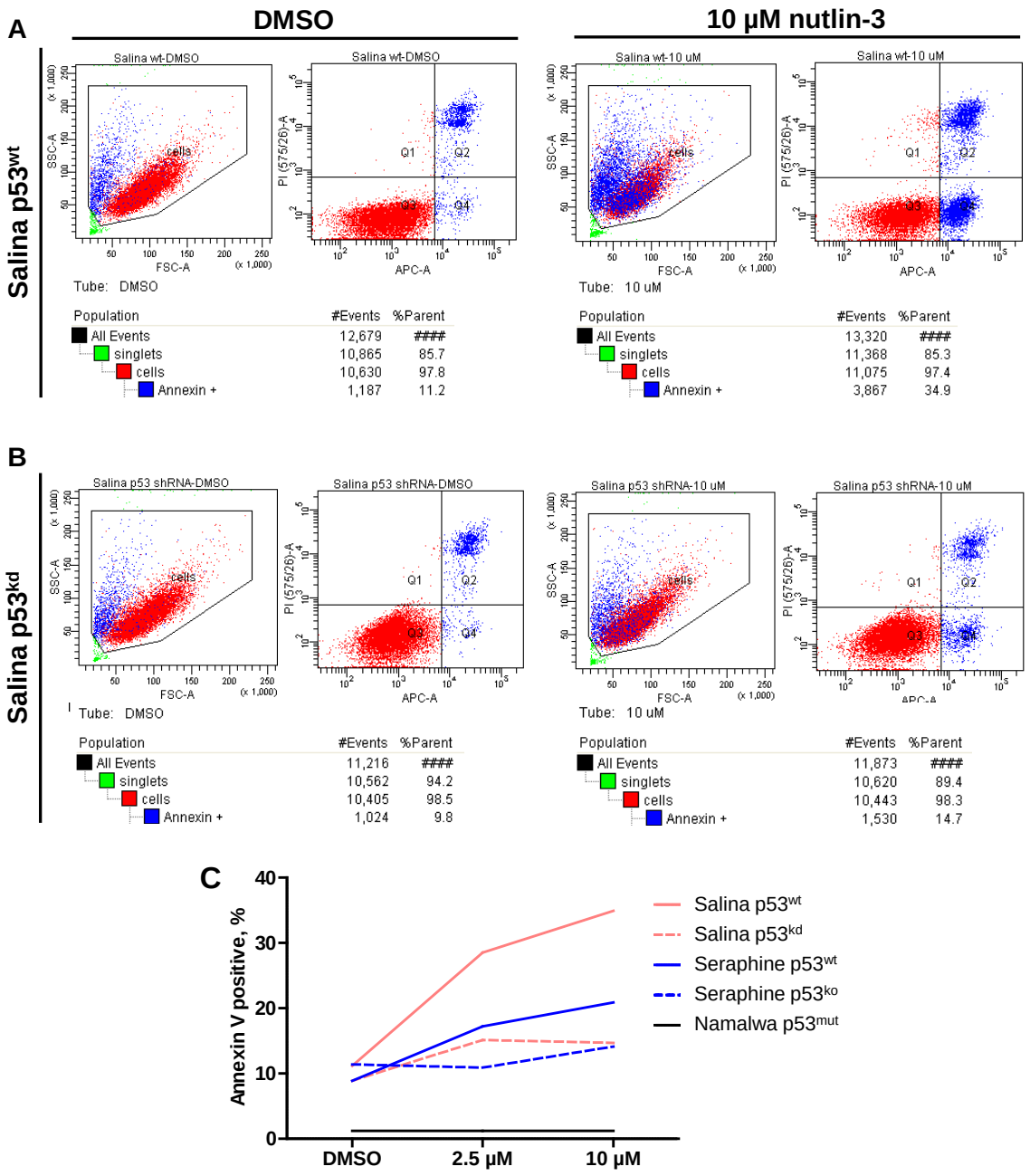

Figure 32. Effect of nutlin-3 treatment on apoptosis in BL cell lines of defined p53 status. Wild-type p53 ($p53^{wt}$), p53 mutation ($p53^{mut}$), shRNA-mediated p53 knockdown ($p53^{kd}$) or CRISPR/Cas9 mediated knockout ($p53^{ko}$) cell lines were subjected to treatment with nutlin-3 or solvent control (DMSO). The fraction of apoptotic cells was measured by APC-coupled Annexin V staining in FACS. **(A)** Exemplary scatter plots displaying the fraction of apoptotic cells (blue) post 24 h DMSO solvent control or 10 µM nutlin-3 in Salina $p53^{wt}$ and **(B)** Salina $p53^{kd}$ cells. **(C)** Summary of nutlin-3 concentration dependent fraction of apoptotic, Annexin V positive cells in FACS after 24 h for all cell lines.

Simultaneously, the fraction of apoptotic cells increased as determined by FACS (Figure 32 C). p53 modified or mutant cell lines displayed no ($p53^{kd}$, $p53^{mut}$) or subtle ($p53^{ko}$)

nutlin-triggered p53 stabilization. Residual p53 expression in the $p53^{ko}$ cells was attributable to the pooled nature of the approach; the knockout was present in 80% of cells as confirmed by 454 sequencing. p53 mutant Namalwa displayed strong overexpression of (non-functional) p53, as expected. Induction of apoptosis in these p53 aberrant cell lines was negligible.

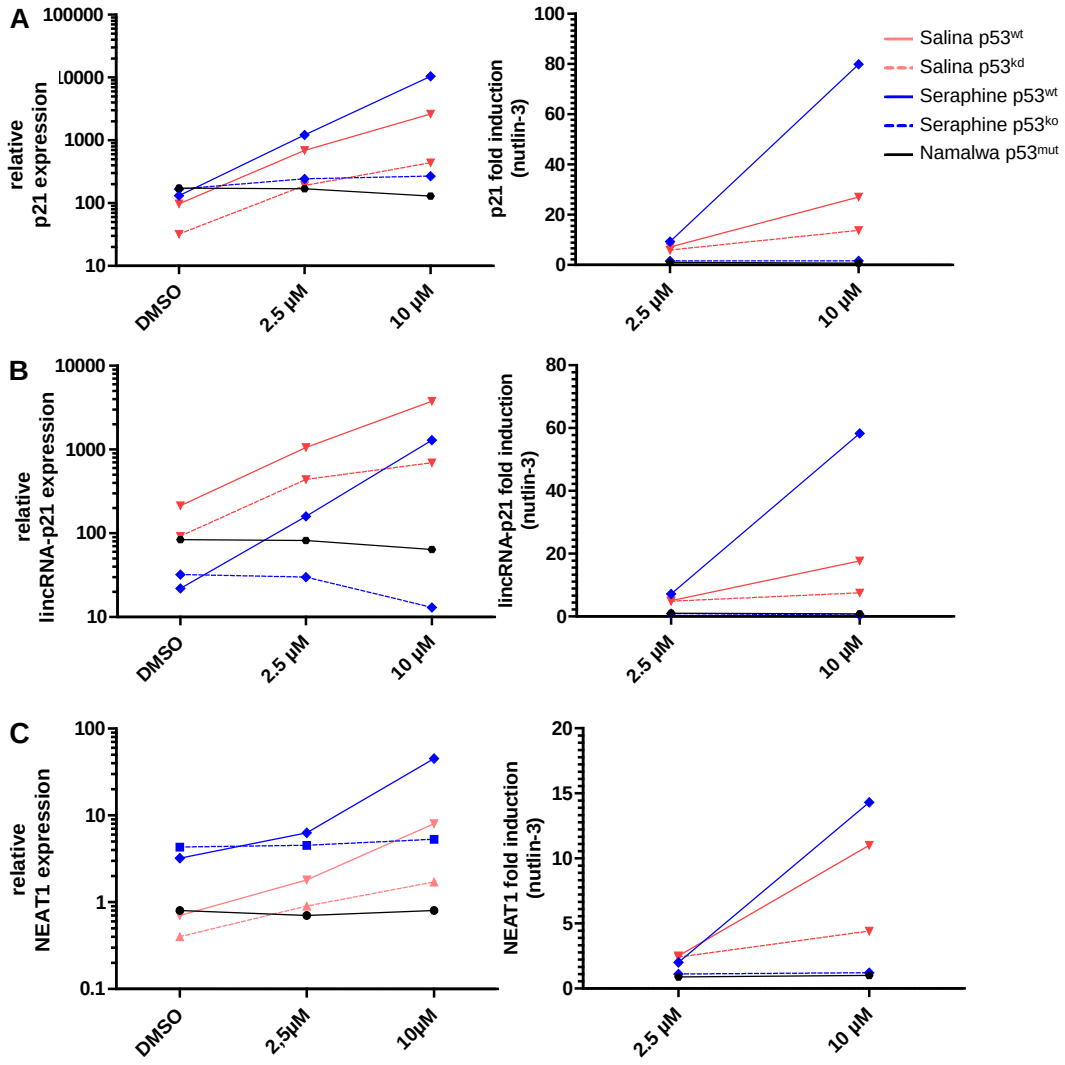

Figure 33. Expression of p21, lincRNA-p21 and NEAT1 upon nutlin-3 treatment of primary CLL and BL cell lines. (A) Expression and fold induction of p21, **(B)** lincRNA-p21 and **(C)** NEAT1 after 24 hours of treatment with 0-10 µM nutlin-3 as assessed by qRT-PCR. Values were normalized to Lamin B1 and referenced to a HeLa sample. Induction was calculated as fold change compared to solvent control (DMSO). The legend in A is applicable to all panels of this figure.

Induction of p21, lincRNA-p21 and, most importantly, NEAT1 were monitored by qRT-PCR. Their expression levels tightly correlated to those of p53 (Figure 31). Apoptosis induction strongly correlated with induction of NEAT1 (R^2 = 0.75), and moderately with

induction of lincRNA-p21 (R^2 = 0.32) and p21 (R^2 = 0.35). For all three RNAs, nutlin-3 triggered induction was pronounced in the Seraphine and Salina $p53^{wt}$ cell lines and reduced in the p53 knockdown / $p53^{ko}$ and $p53^{mut}$ cells. These data strongly suggest a role of p53 in regulating lincRNA-p21 and NEAT1 transcription not only in primary CLL cells, but also in cellular models of Burkitt's Lymphoma.

3.6.3 Assessment of p53 binding to the NEAT1 promoter

To determine whether p53 binds to the NEAT1 promoter and to rule out indirect regulation of NEAT1 expression by a p53 target, we made use of the Burkitt's lymphoma cell line models of controlled p53 expression. 24 hours upon treatment with 10 µM nutlin-3, Séraphine $p53^{wt}$ and isogenic $p53^{ko}$ cells were harvested, DNA was sheared to 300-400 bp (Figure 34 A) and subjected to ChIP with p53 antibodies. Subsequently, the NEAT1 promoter sequence was amplified by PCR, using self-designed primers targeting a published p53 binding site upstream of NEAT1[206]. As displayed in Figure 34 B, p53 was found to bind to the NEAT1 promoter in the $p53^{wt}$ cells, whereas no binding was observed in the $p53^{ko}$ cells which served as negative control. Binding to the p21 promoter was used as positive control, showing the identical pattern with the exception of a contamination detected in the no-antibody control.

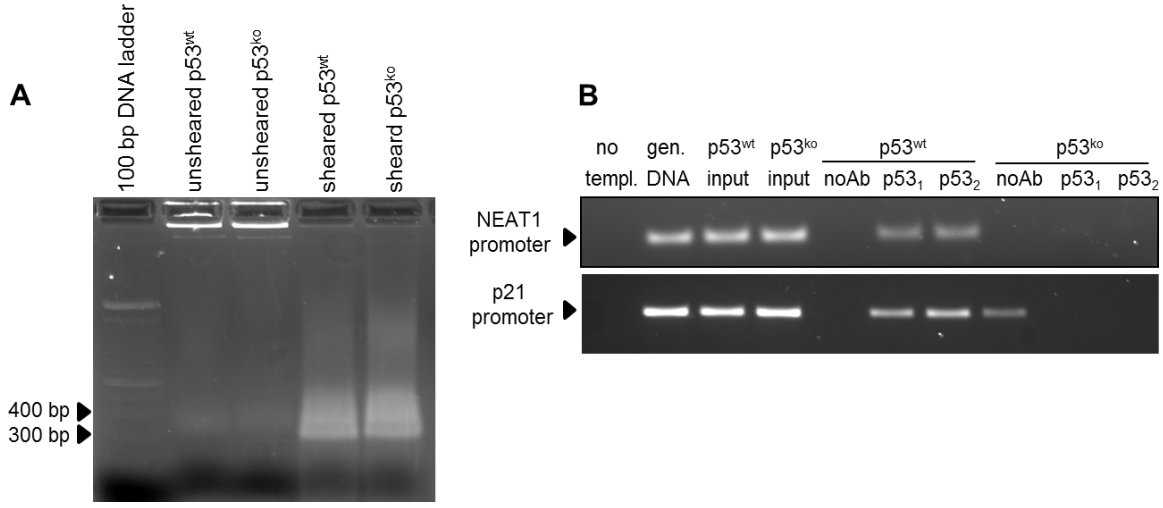

Figure 34. ChIP-PCR for p53 binding in the promoter regions of NEAT1 and p21. Séraphine $p53^{wt}$ and $p53^{ko}$ cells treated with 10 µM nutlin-3 were used for ChIP. **(A)** 1.5% agarose gel showing high molecular weight DNA in unsheared samples, and successful shearing to 300 - 400 bp in the samples used for ChIP. **(B)** Products of qRT-PCR for the NEAT1 promoter region (137 nt) and p21 promoter region (positive control, 214 nt) were run on a 3% agarose gel. qRT-PCR products from a reaction run without template, with genomic DNA and without antibody selection ('input') served as controls. p53 antibodies from Santa Cruz (SC, $p53_1$) and BD ($p53_2$) were tested. Samples incubated with no antibody (noAb) were additional controls.

Combined with the data provided in section 3.6.2 this provides strong evidence for p53 binding to the NEAT1 promoter, which results in transcriptional activation and expression of the *NEAT1* gene.

3.6.4 Summary of p53-dependent ncRNAs in CLL and BL

By small RNA sequencing-based comparison of miRNA induction in *TP53*^{wt} and *TP53*$^{del/mut}$ primary samples after DNA damage, miR-34a-5p was confirmed as prime p53 target in CLL. A set of potential novel p53 targets was suggested including miR-182-5p, miR-7-5p and miR-320c/d, which show irradiation-triggered induction only in the wild-type setting. In addition, this work's data demonstrated p53-dependent lincRNA-p21 and NEAT1 regulation in primary CLL upon irradiation and nutlin-3 treatment. Figure 35 provides an overview of DNA damage triggered expression changes of the top p53-dependent RNAs assessed. In this hierarchical clustering, all *TP53*$^{del/mut}$ samples and most previously treated, high-risk *TP53*^{wt} samples cluster together.

In BL cell lines genetically modified for controlled p53 expression, both lincRNA-p21 and NEAT1 displayed *TP53* status dependent induction upon nutlin-3, and direct p53 binding to the NEAT1 promoter was confirmed by ChIP-PCR.

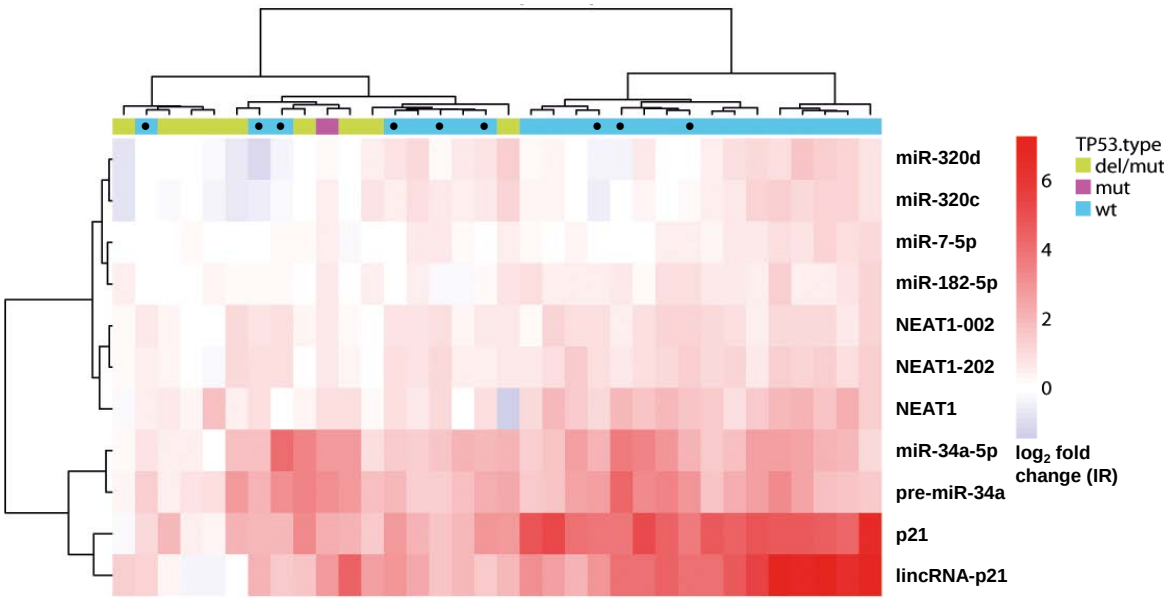

Figure 35. Unsupervised hierarchical clustering of p53 targets identified in primary CLL samples. The heatmap summarizes the irradiation (IR)-triggered fold induction of p53 targets (rows) NEAT1, lincRNA-p21 and p21 as determined by qRT-PCR, and NEAT1-002, NEAT1-202, miR-182-5p, miR-7-5p, miR-320d/c, miR-34a-5p and miR-34a precursor (pre-miR34a) as determined by sequencing for all samples of our test cohort (n = 34, columns). *TP53* status of the samples is indicated. (●) Denotes previously treated *TP53*^{wt} patients who had relapsed after chemotherapy.

4 Discussion

The BCR- and p53 signaling pathways are key determinants of B-CLL tumor cell survival. BCR signaling is constitutively active in CLL cells[56,83,84], eliciting survival supporting effects, while p53 is frequently deleted and/or mutated, leading to impaired tumor cell apoptosis and treatment resistance[42,78]. The involvement of ncRNAs in mediating these pro-survival and apoptotic effects is not well understood. To identify ncRNA networks dependent on BCR signaling and p53 pathway activation in primary CLL, a small RNA sequencing and analysis platform was established.

Investigations of miRNA expression in primary CLL established the link between miRNA deregulation and cancer[53]. More extensive screens on miRNA expression in CLL have relied on quantification by microarray and qRT-PCR array technologies[53,160,166-169,190,266,267] confining the assessment of target RNA expression to sequences covered by the respective array. In contrast, sequencing based miRNA quantification allows the analyses to be continuously adapted to employ the most current reference databases for read mapping. The few studies that implemented RNA sequencing to quantify miRNA expression in CLL either used reference databases which contained still a limited number of sequences[188,268], or were confined to a small number of CLL samples analysed (less than 10)[188,227,232]. This study therefore set out to use small RNA sequencing for a comprehensive quantification of miRNA expression in 35 primary CLL samples with a focus on dynamic expression upon BCR signaling inhibition or p53 activation.

By sequencing 82 samples from 35 CLL patients, 1244 mature miRNAs were detected. This greatly exceeds the 157 miRNAs detected by Landgraf *et al.*[227] or the 256 miRNAs found expressed by Jima *et al.*[232], who applied a similar analysis pipeline. In line with Jima *et al.*, sequencing reads were mapped to the miRBase human reference sequences requesting perfect sequence identity. In contrast though, analyses for the present study did not exclude reads with more than 5 genomic matches. The challenge of dealing with multiple mapping reads was met by selecting only reads of 17 – 25 nt length for statistical analyses of miRNA expression, thereby excluding short sequences likely to map to the genome multiple times.

After selecting ~15 to 35 nt RNA molecules for sequencing during library preparation, only 13% of reads generated corresponded to mature miRNA sequences, whereas 41% were not found in the RNA databases used (which did not include e.g. transponsons, non-lincRNA lncRNA and miRNA precursor sequences) or did not map to the genome. Considering the abundance of transposon transcripts and RNA splicing and editing, this percentage of non-mapping reads was expected. A considerable fraction of sequences

originated from transcripts > 50 nt, although 50 bp sequencing was performed. These possibly represent fragments originating from RNA degradation in the sample set (average RIN = 8.3). Unexpectedly, these sequences proved to be highly useful and informative.

At baseline, miRNA expression in CLL was dominated by miR-21-5p, which accounted for 25% of all miRNA reads and is frequently found overexpressed in malignancies[229-231]. Eight of the 10 most strongly expressed miRNAs reported here were previously listed among the most abundant in primary CLL cells[188], supporting the results of this work. Comparisons of baseline miRNA expression between CLL and normal CD19 positive B-cells have been performed extensively[53,160,168,269] and are therefore mentioned in this thesis only to evaluate the chosen sequencing approach. Interestingly, of those 10 most highly expressed miRNAs, miR-21-5p, miR-101-3p, miR-150-5p and miR-155-5p are known to be overrepresented in CLL versus normal B-cells isolated from peripheral blood[188] and were confirmed in the present study. This overrepresentation was not observed in a comparison to miRNA expression in normal CD5+ memory B-cells[168] though, emphasizing the impact of the 'normal counterpart' chosen for profiling of aberrant miRNA expression.

4.1 miRNA expression profiles predict *IGHV* status and associate with *in vitro* ibrutinib sensitivity

The BCR signaling pathway is constitutively activated in freshly isolated B-CLL cells[55,84,270], supporting tumor cell survival[91,101] and providing an attractive drug target[95,271]. In this work, miRNAs involved in BCR signaling and response to inhibition by ibrutinib treatment *in vitro* were investigated, as they may play a role in BCR-signaling mediated CLL cell survival. To this end, *IGHV* status dependent miRNAs and miRNAs directly regulated upon *in vitro* ibrutinib treatment were identified, and miRNAs associated with treatment response were reported.

Analyzing the basal expression of 35 primary CLL samples, 12 miRNAs were found differentially regulated based on *IGHV* status. Of those, the higher expression of miR-155-5p and the lower expression of miR-29c-3p/5p in U-*IGHV* samples is in keeping with previous reports[166,188,189,269]. This study additionally found miR-547, -184, -330, -153 and -9 upregulated, and miR-514a, -141 and -4432 downregulated in U-*IGHV* samples. The pro-proliferative roles of miR-9 observed in mixed-lineage leukemia-arranged leukemia[272], of miR-330 in glioblastoma[273], of miR-153 in prostate cancer[274] and of miR-184 in squameous cell carcinoma[275] are in line with higher expression in U-*IGHV* CLL. However, the targets of one miRNA are numerous and depend on cell type and

physiologic state, so that contrary findings exist[276-278]. A predictor encompassing the expression profiles of 15 miRNAs was calculated in this work, which was able to discriminate between M-*IGHV* and U-*IGHV* samples with 82% accuracy. Using miRNA expression profiles presents a potential alternative to *IGHV* sequencing as has been previously suggested[187]. However, the level of accuracy seen in this study does not support a substitution of sequencing by miRNA profiling in this cohort.

Ibrutinib, a covalent inhibitor of Bruton's tyrosine kinase (BTK) downstream of the BCR, leads to abrogation of CLL cell survival and has recently been approved for the treatment of relapsed CLL[95,279]. The basal expression of 10 miRNAs was found to differ based on *in vitro* ibrutinib sensitivity in 34 CLL samples. This included miR-574-5p, miR-24-3p, miR-23a-3p and miR-155-5p, implicating a correlation between low baseline sample viability and high ibrutinib sensitivity. miR-155-5p, miR-24 and miR-23b were previously described as higher expressed in U-*IGHV*[166]*.* miR-330-3p was added to this group, reflecting the established link between *IGHV* status and ibrutinib sensitivity.

Samples expressing high miR-155-5p levels displayed particularly good ibrutinib sensitivity *in vitro*. Interestingly, high miR-155-5p levels associate with adverse clinical patient outcome and were demonstrated to enhance responsiveness to BCR ligation in CLL[280], supporting CLL cell survival. Therefore, enhanced BCR signaling in miR-155-5p high expressing CLL could contribute to ibrutinib sensitivity of these samples. In contrast, high basal miR-150-5p levels mediated resistance to ibrutinib *in vitro*. Interestingly, miR-150 was described to target FOXP1 (forkhead box P1) and GRB1 (GRB2-associated binding protein 1), enhancers of BCR signaling[233]. High miR-150-5p levels associated with low FOXP1 expression also in this work, and additionally with low PDIA6 expression, which is predicted to be targeted by miR-150-5p and is induced upon BCR stimulation in CLL[59]. The negative impact of miR-150 on BCR signaling activity may explain the low effectivity of ibrutinib, which targets the same pathway. These two examples suggested that also other miRNAs associating with ibrutinib sensitivity could regulate BCR signaling activity and CLL cell survival. First support for this hypothesis was provided by observations of a negative correlation of miR-23a-3p (low in ibrutinib resistant samples) and FCRL2 expression. Predicted miR-23a-3p target FCRL2 is a transmembrane molecule specifically expressed in B lineage cells, is overexpressed in CLL with good prognosis[237] and inhibits BCR signaling by recruitment of the inhibitory tyrosine phosphatase SHP-1 to the BCR[236]. Low miR-23a-3p expression could reduce BCR signaling activity via accumulation of FCRL2, contributing to ibrutinib resistance. Likewise, the expression of miR-574-5p (low in resistant samples) and its predicted target PIM3 inversely correlated. The kinase PIM3 is essential for CLL tumor cell survival[281]. Low miR-574-5p levels could therefore support cell survival and mediate

ibrutinib resistance through de-repression of PIM3 in CLL. These hypotheses provide an interesting starting point for further experimental work.

4.2 BTK inhibition identifies a set of five BCR signaling-dependent miRNAs

Until recently, regulation of miRNA expression by the complex BCR signaling cascade remained poorly investigated[282]. To identify BCR signaling dependent miRNAs, ibrutinib was used as a tool to abrogate BCR signaling in primary CLL. BCR signaling-induced miRNA expression was previously investigated by Pede *et al.*[190], who evaluated the transcriptional response (mRNA, miRNA) of primary CLL cells upon anti-IgM mediated BCR stimulation *in vitro* using hybridization arrays and qRT-PCR. Stimulation with anti-IgM targeting the BCR poses an unphysiological trigger to the receptor and it appeared more meaningful to inhibit steady-state, cell-autonomous BCR signaling[55] for this work.

Sequencing data analyses revealed an induction of miR-320c and miR-1246, while miR-484, miR-17-5p, miR-155-3p and miR-27a-5p were downregulated. The p53-dependent induction of miR-320c observed upon DNA damage (refer to section 3.5.1) suggests that this regulation reflects ibrutinib treatment-induced apoptosis rather than a direct effect of BTK blockage. miR-155-3p has been found induced in the study of Pede *et al*., in line with our data. The miR-212/132-3p cluster was the only other miRNA regulated after BCR stimulation in their experiments. Interestingly, a reduction in miR-212 and miR-132-3p expression was observed in this work, albeit the expression levels were extremely low. This questions the biological relevance of the published miR-212/132-3p induction upon BCR signaling.

The repression of oncogenic miR-17-5p upon BTK inhibition is in keeping with ibrutinib's effects of abrogating CLL cell survival and proliferation. Overexpression of the miR-17~92 cluster is known to induce lymphoma-/leukemogenesis in transgenic mice[283] and has been described to amplify BCR signaling in diffuse large B-cell lymphoma by augmenting BCR downstream target activation including PLCγ2 phosphorylation and calcium flux[284]. The present work suggests a role of miR-17-5p in BCR signaling also in CLL, acting to support tumor cell survival and proliferation.

Previously, miR-155-5p expression was suggested to be BCR dependent as implied by the coexistence of miR-155-5p overexpression and over-active BCR signaling in CLL vs. healthy B-cells[181,269,285] and an induction of miR-155-5p after BCR stimulation of healthy B-cells and Burkitt's Lymphoma cell lines[269,286]. Neither Pede *et al*. nor this work found miR-155-5p expression to be BCR signaling dependent. However, an association between high miR-155-5p expression, high ibrutinib sensitivity and U-*IGHV* status was

apparent. Therefore, this study rather supports miR-155-5p as a recently suggested enhancer[280] than as a target of CLL B-cell receptor signaling.

For miR-484 and miR-1246 no connection to BCR signaling or support of cell survival has been previously reported.

In general, very subtle regulations of miRNA expression upon BTK inhibition were observed (0.5 to 1.4 fold), indicating a low level of baseline BCR signaling activity. This suggests that inhibiting baseline, cell-autonomous BCR signaling without applying extrinsic BCR stimulation comes at the expense of low downstream regulation amplitudes and the possibility of missing BCR signaling targets. Additionally, ibrutinib has been shown to act *in vitro* within 8 hours as read out by CD69 expression, cell viability and caspase-3 activation[100], so a shorter incubation time (e.g. 12 hours) might enrich the results for more immediate BCR signaling targets.

4.3 miR-182, miR-7 and miR-320d/c are novel p53-dependent miRNAs in CLL

miRNA targets of p53 were previously reported for various cellular models and cancer entities. They will not be reviewed here for their sheer number, but were recently summarized by Hermeking[287]. It needs to be kept in mind though, that the set of functional p53 targets will vary with the cell type and the type of stress applied to trigger p53 activation[208,288]. In CLL, several studies have gathered associative data of basal miRNA expression levels and 17p status[169,191,266]. However, a direct regulation of aberrantly expressed miRNAs by p53, as can be demonstrated by analysis of miRNA expression changes upon p53 activation, was not investigated.

Upon DNA damage, higher rates of apoptosis and expression of key p53 targets p21 and miR-34a-5p was observed in *TP53*^{wt} than in del11q than in *TP53*$^{del/mut}$ samples. Further, miR-34a-5p expression was already significantly lower in *TP53*$^{del/mut}$ than *TP53*^{wt} already at baseline. This was in line with previous data[70,116,170,289] and affirmed the capability of the experimental approach chosen.

Quantification of miRNA expression dynamics upon DNA damage demonstrated a more dynamic overall response to irradiation-triggered p53 induction in *TP53*^{wt} than *TP53*$^{del/mut}$ samples. Still, a few miRNAs including miR-150-3p, miR-155-5p and miR-21-3p were found regulated in both sample groups, implying a role in DNA damage response independent of p53. miR-34a-5p, miR-182-5p, miR-7-5p and miR-320d/c were identified as the top five p53-dependent miRNAs. The miRNAs were checked for shared sequences, and a false-positive induction caused by a random RNA fragment mapping to all of them was excluded. Interestingly, for the four last-mentioned, basal expression

levels were higher in *TP53*$^{del/mut}$ than *TP53*^{wt} samples, which is in contrast to miR-34a-5p and seems counter-intuitive when considering p53-dependency. However, *TP53* status dependent miRNA induction was validated by qRT-PCR for miR-7-5p and miR-320d (in addition to miR-34a-5p). Previous observations support p53-dependent expression of these miRNAs. miR-182-5p has been described as p53 target in lung, breast and colon cancer cell lines[193,290], and its anti-proliferative activity was demonstrated in renal cell carcinoma[291]. For miR-7-5p, a p53 binding site was identified in close proximity to miR-7-2[206], and an anti-proliferative, cell cycle arresting[292,293] function in solid cancers underlines its tumor suppressive role and supports p53-dependent transcription. Experimentally validated targets of miR-7-5p include members of the AKT pathway (IRS-1 and 2) in glioblastoma[294] and transcriptional repressor YY1 (yin yang 1) in colorectal cancer[292] to induce apoptosis and inhibit cell proliferation. miR-320d/c/b display high sequence homology, similar regulation and belong to the miR-320 family sharing the same seed sequence. For miR-320, no direct functional link to p53 has been established to date, although p53 binding sites in proximity to miR-320c and b were reported[207]. Zhang *et al.*[295] found miR-320 in regions with DNA copy number loss in three different types of solid cancer (breast, ovarian, melanoma), and Schepeler *et al.*[296] established miR-320 as independent predictor in colon tumors, where high expression correlated with a longer progression-free survival. In summary, this suggests a role of miR-182-5p, miR-7-5p and miR-320d/c in apoptosis and inhibition of cell proliferation as part of the p53 pathway in primary CLL, a connection which was uncovered by this work.

Eighteen further miRNAs displayed p53-dependent expression, of which miR-34a-3p (as part of pre-miR-34a) and miR-15a-5p are published p53 targets in CLL[70,116,297]. p53 has been shown to activate transcription of mir-155[195], and was reported to bind in the proximity of mir-9-2[207], mir-23a[206-208], mir-29b[208] and mir-26a-2[208] in various cell lines. Functional studies of their p53-dependence are lacking.

Interestingly, irradiation-triggered induction of oncogenic miR-17~92 cluster members (miR-17, miR-18a and miR-20a but not miR-92a) was stronger in *TP53*$^{del/mut}$ than *TP53*^{wt} samples. This could result from a decreased miR-17~92 repression by p53[298]. Similarly, miR-155-3p was stronger induced in *TP53*$^{del/mut}$ than than *TP53*^{wt} samples. Considering its downregulation after survival-abrogating ibrutinib treatment, it could confer a survival advantage to *TP53*$^{del/mut}$ cells, although its rather low expression is to be beared in mind.

Table 12 summarizes miRNAs that were previously reported to display significantly different basal expression levels between 17p13 disomic and 17p13 deleted patients. This work's data support and confirm p53-dependency of miR-34a-5p expression, since lower basal levels were observed in del17p patients and a higher DNA-damage triggered induction was seen in *TP53*^{wt} than *TP53*$^{del/mut}$. Along the same lines, evidence for p53-

dependency of miR-15a suppression is provided by a significant IR-mediated suppression exclusively in the wild-type setting. In contrast, this work's results suggest that the lower expression of miR-151a-3p, miR-29c, miR-181b and miR-497 in del17p is a p53-independent effect, possibly resulting from the deletion of another gene on 17p, as no regulation is observed upon p53 induction. This can be underlined for miR-497, which itself is located on 17p approximately 200 kb centromeric of *TP53* and hit by 17p deletions as a 'bystander'[266]. For miR-17-5p and miR-155-5p, DNA damage triggered induction independent of *TP53* status suggests a p53-independent role in the DNA damage response.

Table 12. p53 dependence of miRNAs with reported differential basal expression in deleted versus disomic 17p in CLL. Observed data were derived from the small RNA sequencing screen on 15 tumor samples from previously untreated *TP53*^{wt} and 10 *TP53*$^{del/mut}$ patients. FC = fold change. IR = irradiation, 5 Gy (cell harvest 24h thereafter). P-values were Benjamini-Hochberg corrected.

miRNA name	Reported level in del17p	Observed FC del vs. disomic 17p	p-value	Regulation by IR in *TP53*^{wt}	p-value	Regulation by IR in *TP53*$^{del/mut}$	p-value
miR-34a-5p	Low[115,167,189,262]	0.3	0.16	4.3	4.3E-39	2.9	2.3E-04
miR-151a-3p	Low[169]	0.2	0.16	1.0	0.91	1.0	0.99
miR-29c	Low[167,189]	0.6	0.51	1.0	0.77	1.0	0,94
miR-17-5p	Low[191]	0.9	0.90	1.2	0.03	1.4	1.3E-04
miR-181b	Low[266]	1.1	0.94	1.1	0.21	1.1	0.94
miR-497	Low[266]	1.1	0.95	0.9	0.81	0.9	0.98
miR-155-5p	High[266]	1.4	0.43	1.4	6.2E-07	1.3	3.6E-04
miR-21-5p	High[266]	1.2	0.70	0.9	0.28	1.0	0.93
miR-15a	High[266]	0.7	0.75	0.8	0.02	1.1	0.93

Detailed insight into the biological role of miRNAs can only be gained through characterization of their mRNA target genes, which enables the discovery of their mechanism of action. A targeted quantification of mRNA expression was not part of this work. However, 13% of the small RNA reads generated here mapped to mRNA sequences. Those reads are expected to be fragments arising from RNA degradation, which was present at low levels after RNA isolation as indicated by an average RNA integrity number of 8.3. In these fragments, a clear *TP53* status dependent induction of key p53 transcriptional targets including MDM2, p21, Bax, Puma and GADD45A was observed. This suggested that their levels were representative of the expression of

longer parent transcripts, enabling the identification of p53-dependent long (non-coding) RNA transcripts from this dataset.

Accordingly, for the top five p53-dependent miRNAs (miR-34a-5p, miR-182-5p, miR-7-5p, miR-320d/c), predicted mRNA targets displaying an IR-triggered regulation inverse to the miRNA expression dynamics were identified. This provides a starting point for experimental validation and subsequent functional analyses.

4.4 p53-dependent long non-coding RNAs identified in primary CLL and BL cell lines

4.4.1 p53-dependent lincRNA-p21 expression in CLL and BL

The present work demonstrates a very low expression of lincRNA-p21 in CLL, which is strongly induced upon p53 induction by irradiation or nutlin-3 treatment in p53 wild-type samples only. Induction of apoptosis, p21 and lincRNA-p21 were shown to closely correlate. *TP53* status dependency of lincRNA-p21 induction was confirmed in a set of Burkitt's Lymphoma cell lines. p53 knockdown or CRISPR/Cas9-mediated p53 knockout abolished lincRNA-p21 induction, proving direct p53-dependency. These data argue for a role of lincRNA-p21 in the p53 pathway in CLL and lymphoma albeit the question remains, whether this is limited to a co-activation of *p21*[299], or whether it is (additionally) acting beyond on a plethora of downstream targets of the p53 pathway[205]. The present experiments were not designed to dissect the independence of p21 and lincRNA-p21 transcription.

Long non-coding RNAs have been implicated in the p53 network as regulators and effectors of p53. Only a handful of lncRNA p53 targets have been described in more detail, and the relevance to CLL biology remained unknown. LincRNA-p21 was one of the first lncRNA p53 targets to be characterized in mouse endothelial fibroblasts[204]. It obtained its name for its proximity to the neighboring *p21* gene, but was proposed to be transcribed independently from *p21*[204] to mediate transcriptional suppression (e.g. of stat3, cyclin D2, cyclin dependent kinase 4) downstream of p53 via several mechanisms in *trans*[205]. Very recently, lincRNA-p21 was shown to activate *p21* transcription in *cis*, acting primarily as a locus-restricted coactivator for p53-mediated *p21* expression, which contrasts previous findings[299]. p53-dependent transcription of lincRNA-p21 was confirmed in various solid cancer cell lines (HCT-116[300], HeLa and MCF-7[301]). In primary human material, lincRNA-p21 was found at decreased levels in plasma of CLL patients as opposed to healthy individuals[302], and decreased in colon tumor versus normal colonic tissue[300], which is consistent with a tumor-suppressive function.

4.4.2 p53-dependent NEAT1 expression in CLL and BL

NEAT1 (nuclear enriched abundant transcript 1) clearly emerged as potential p53 target from sequencing-based analysis of non-coding RNA expression other than mature miRNA. More precisely, of the three NEAT1 transcripts in the reference database (Ensembl GRCh37), the largely overlapping NEAT1-002 and -202 transcripts (~1.7 and ~1.5 kb) were found induced. *TP53* status dependent NEAT1 induction was validated by qRT-PCR. Since the discovery of NEAT1, confirmed transcript sizes and numbers have been subject to numerous changes, amounting to five since the latest Ensembl update in August 2014 (Emsembl GRCh38). This discussion will consider aggregated NEAT1 expression as determined by qRT-PCR (Figure 26 A).

p53-dependence of NEAT1 expression was further supported by a close correlation to p21 expression and *TP53* status dependent response to nutlin-3 treatment in primary CLL. TP53 dependent expression was confirmed in genetically modified Burkitt's lymphoma cell lines displaying controlled p53 activity, and a p53 ChIP-PCR experiment finally demonstrated direct, *TP53* status dependent binding of p53 to the NEAT1 promoter sequence.

NEAT1 is a lincRNA widely expressed across cell types upon differentiation[303], where it localizes to the nucleus. It is an essential architectural component of paraspeckles, relatively newly identified ribonucleoprotein bodies that are found in the interchromatin space of mammalian cells upon differentiation[263,304-306]. NEAT1 is the only RNA component in human paraspeckles, building a scaffold for 40 co-localized proteins[307]. Knockdown of NEAT1 led to paraspeckle loss[263], demonstrating that its RNA, but not the associated proteins, is the rate-limiting molecule for paraspeckle formation. In mice, paraspeckles were non-essential in unstressed conditions[308]. As NEAT1 upregulation was observed upon proteasomal inhibition, serum starvation, acidosis and HIV infection *in vitro,* a role in the cellular stress response has been suggested[213,309].

Binding of p53 to the NEAT1 promoter has been observed in two previous large-scale p53 ChIP-Seq studies: Botcheva *et al.*[206] reported the NEAT1 promoter as novel p53 binding site in a human lung fibroblast cell line, which was confirmed in mouse endothelial fibroblasts[310]. It was not until very recently though, that p53 binding at this locus was demonstrated to be functional, i.e. induce transcription of the nearby *NEAT1* gene[209]. The present work now demonstrates a stress-induced transcriptional activation of NEAT1 by p53 in leukemia and lymphoma. In light of the aforementioned, this poses the question about the role of NEAT1 upregulation upon p53 activation in the DNA damage response or, asked differently, the role of NEAT1 in mediating p53 pathway function.

Paraspeckles can influence gene expression through three mechanisms: On the one hand, they control nuclear retention of mRNAs containing inverted repeats (*Alu* elements) that form double-stranded RNA regions subject to adenosine-to-inosine (A-to-I) editing by ADARs (adenosine deaminases acting on RNA), ultimately resulting in translational repression[304]. On the other hand, they counter-regulate the function of paraspeckle-localizing proteins, which normally regulate distinct nuclear processes outside the paraspeckles, as recently demonstrated for SFPQ (splicing factor proline/glutamine-rich)[311,312]. Thirdly, NEAT1 has been described to bind to active chromatin sites, its localization being subject to transcriptional status rather than homology to the DNA sequence. It was speculated, that NEAT1 could play a structural role in the organization of nuclear bodies at highly transcribed loci, although it remained unclear how this would impact on gene expression profiles[313].

Considering the role of NEAT1 in the control of hyperedited mRNA expression, p53 activation potentially impacts on the expression of hundreds of genes containing *Alu* repeats in their 3'-UTRs that undergo A-to-I editing. The impact of p53-mediated translational repression via NEAT1-mediated nuclear retention of (hyperedited) mRNA could be characterized by screening the subcellular localization of mRNA and corresponding protein levels after p53 activation. Thereby, NEAT1 overexpression could explain repressive effects seen upon p53 activation[314], whose mechanisms remain largely unknown[142,315]. Another potential connection between p53 and NEAT1 expression emerges from the re-localization of paraspeckle proteins from the nucleoplasm into the paraspeckles upon NEAT1 overexpression[263,311,312]. In the nucleoplasm, these proteins serve diverse functions including transcriptional control, RNA processing and DNA repair[311,316]. Interestingly, upon DNA damage, the paraspeckle proteins SFPQ, NONO (non-POU domain-containing octamer-binding protein) and FUS (fused in sarcoma) are rapidly recruited to the damaged sites, where the SFPQ supports homology-directed double-strand break repair[317,318]. In line with this observation, reduced SFPQ expression conferred cellular sensitivity to DNA damaging agents. A combination of SFPQ depletion with a deletion of *Rad51d* (catalyzing homologous pairing between single- and double-stranded DNA) resulted in a lethal phenotype as would be expected from a disruption of homologous recombination (HR)[318]. FUS depletion diminished double-strand break repair by HR and non-homologous end joining (NHEJ)[77]. Similarly, paraspeckle protein RBM14 (RNA binding motif protein 14) was shown to stimulate DNA repair by controlling the NHEJ pathway. Accordingly, its upregulation caused radio resistance in glioblastima[319]. It is tempting to hypothesize that p53-mediated NEAT1 induction would sequester SFPQ, FUS and RBM14 away from their sites of action, resulting in a

disruption of HR and NHEJ, tilting the p53-response from DNA damage repair to apoptosis.

However, considering NEAT1 is also induced upon direct p53 activation by nutlin-3 in absence of DNA damage, it would be expected to regulate responses beyond DNA damage repair. A connection between p53 activation, NEAT1 induction and inhibition of paraspeckle protein activity or nuclear export of A-to-I edited RNA to apoptosis as suggested here has not been established and opens an interesting field of study.

In summary, this work confirmed miR-34a as prime p53 target and identified several novel p53 targets in CLL including miR-182-5p, miR-7-5p and miR-320d/c. While some reports indicating p53-dependency of miR-182-5p, miR-7-5p in other entities exist, this context is novel for miR-320d/c. With the exception of miR-15a and miR-34a, miRNAs previously reported to associate with p53 aberrations in CLL were regulated

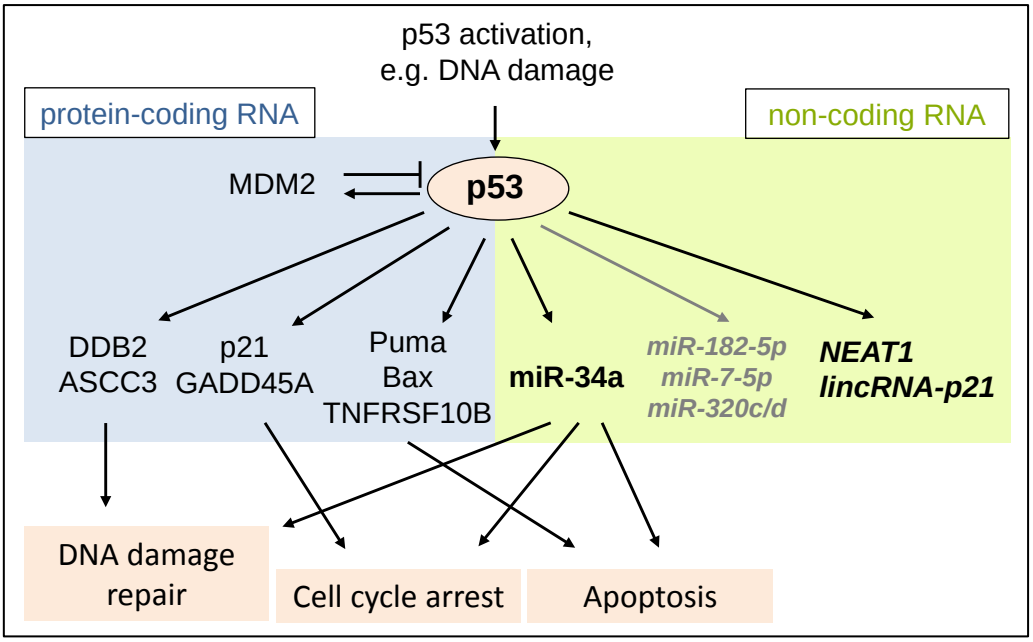

Figure 36. Summary of p53 targets identified in CLL. miR-34a-5p was confirmed as non-coding p53 target. miR-182-5p, miR-7-5p and miR-320c/d are *newly* suggested targets in CLL, which are induced less strongly. NEAT1 and lincRNA-p21 are novel long non-coding p53 targets in CLL and Burkitt's lymphoma. The roles of the newly identified ncRNAs in mediating the outcome of p53 activation needs further study. In addition, a selection of known p53 targets also found in this work is presented. MDM2, mouse double minute 2 homolog; DDB2, damage-specific DNA binding protein 2; ASCC3, activating signal cointegrator 1 complex subunit 3, GADD45A, growth arreast and DNA-damage-inducible alpha; Puma, p53 upregulated modulator of apoptosis; BCL-2 associated X protein; TNFRSF10B, tumor necrosis factor receptor superfamily, member 10B.

independently of *TP53* status. Beyond miRNA, the smRNA sequencing dataset reflected the p53-dependency of key p53 targets including MDM2, p21, Bax and Puma, and was therefore used to evaluate long ncRNA expression. The lincRNAs NEAT1 and lincRNA-p21 were found p53-dependently induced in CLL and Burkitt's lymphoma. Considering the high expression levels of NEAT1 and the absence of a previous link to cancer chemoresistance, it appeared a particularly interesting target. p53 binding to the promoter sequence of NEAT1 was demonstrated. The function of NEAT1 upon p53 induction remains unknown. However, NEAT1 binding partners were previously implied to be critical for DNA damage repair, suggesting a role for p53-induced NEAT1 in tilting the balance from damage repair to apoptosis. A graphical summary is provided in Figure 36.

4.5 CLL high-risk patients display p53 pathway impairment independent of *TP53* and *ATM* aberrations

The reasons for chemorefractoriness in CLL patients displaying wild-type, disomic *TP53* and ATM are not well understood. By analysis of irradiation-triggered induction of p21, lincRNA-p21, NEAT1, miR-182-5p, miR-7-5p and miR-320d/c to assess p53 signaling activity in samples of *TP53*^{wt}, previously treated 'high-risk' patients, a pattern similar to p53 pathway inactivation was found despite disomic wild-type p53 and ATM. In this setting of impaired p53 activity, miR-34a-5p induction was not reduced in the high-risk group, which might be due to p53-independent, alternative regulation, whose existence has been previously suggested[193,320,321]. While p53 pathway inactivation offers an explanation for the observed chemorefractoriness, no reason for p53 inactivation could be found on the basis of ncRNA regulation, i.e. no aberrant expression of ncRNAs reported to target p53 pathway members were identified. Thus, the mechanism underlying impaired p53 pathway activity in this patient group warrants further study. However, the development of high-risk disease can (additionally) be caused by deregulation of tumor suppressors and oncogenes other than p53, as recently suggested by the identification of genetic aberrations affecting *BIRC3* (Baculoviral IAP repeat containing 3) and *FAT1* (protocadherin Fat 1), which closely associated with chemorefractoriness in *TP53*^{wt} CLL[322,323].

5 Conclusion and Perspective

Active B-cell receptor signaling supports the survival of CLL tumor cells, and p53 aberrations are known to confer resistance towards apoptosis, mediating poor prognosis. We hypothesized that by modulating the BCR- and p53 signaling pathways, miRNAs and other ncRNAs could be identified that play important roles in mediating their outcome, and are critical to survival or apoptosis of CLL tumor cells.

In this work, small RNA sequencing was applied to assess ncRNA expression in CLL at unprecedented resolution. miRNAs were identified that are *IGHV* mutation status dependently expressed, regulated upon abrogation of BCR signaling and/or show basal expression levels associated with *in vitro* ibrutinib sensitivity. All of those are potentially involved in supporting CLL cell survival. Direct BCR signaling dependent expression was demonstrated for miR-320c, miR-1246, miR-484, miR-17-5p, miR-155-3p and miR-27a-5p. Their influence on tumor cell survival would be most interesting to investigate further by targeted modulation of expression levels.

The emphasis of this work was put on the identification of p53-dependent ncRNAs. By analyzing ncRNA expression changes upon DNA damage-triggered p53 induction, a set of miRNAs were discovered as novel p53 targets in CLL. Beyond known prominent p53 target miRNA-34a these included miR-182-5p, miR-7-5p and miR-320d/c. Experimentally validating the suggested mRNA targets of those miRNAs will be critical to understand underlying functional mechanisms and evaluate their potential for miRNA-based therapies. Importantly, the present work demonstrates p53-dependent induction of lincRNA-p21 and NEAT1 in CLL and Burkitt's lymphoma, providing first evidence of p53-dependent long non-coding RNA regulation in these entities. p53-dependent induction of lincRNA NEAT1, a key component of nuclear paraspeckles, is intriguing, and the involvement of paraspeckles in p53-dependent apoptosis opens a new field of study.

These findings extend the network of p53-regulated genes in CLL and lymphoma. Subsequent work will need to elucidate the functional roles of the newly identified p53 targets.

References

1. Alberts B. JA, Lewis J., Raff M., Roberts K., Walter P. Molecular Biology of the cell, 4th edition. *Garland Science*. 2002(New York).
2. Hanahan D, Weinberg RA. The hallmarks of cancer. *Cell*. 2000;100(1):57-70.
3. Hanahan D, Weinberg RA. Hallmarks of cancer: the next generation. *Cell*. 2011;144(5):646-674.
4. Croce CM. Oncogenes and cancer. *N Engl J Med*. 2008;358(5):502-511.
5. Knudson AG. Two genetic hits (more or less) to cancer. *Nat Rev Cancer*. 2001;1(2):157-162.
6. Feinberg AP, Tycko B. The history of cancer epigenetics. *Nat Rev Cancer*. 2004;4(2):143-153.
7. Esteller M. Epigenetics in cancer. *N Engl J Med*. 2008;358(11):1148-1159.
8. Sherr CJ. Principles of tumor suppression. *Cell*. 2004;116(2):235-246.
9. Croce CM, Thierfelder W, Erikson J, et al. Transcriptional activation of an unrearranged and untranslocated c-myc oncogene by translocation of a C lambda locus in Burkitt. *Proc Natl Acad Sci U S A*. 1983;80(22):6922-6926.
10. Dang CV. c-Myc target genes involved in cell growth, apoptosis, and metabolism. *Mol Cell Biol*. 1999;19(1):1-11.
11. Harris AW, Pinkert CA, Crawford M, Langdon WY, Brinster RL, Adams JM. The E mu-myc transgenic mouse. A model for high-incidence spontaneous lymphoma and leukemia of early B cells. *J Exp Med*. 1988;167(2):353-371.
12. Eischen CM, Weber JD, Roussel MF, Sherr CJ, Cleveland JL. Disruption of the ARF-Mdm2-p53 tumor suppressor pathway in Myc-induced lymphomagenesis. *Genes Dev*. 1999;13(20):2658-2669.
13. Schuster C, Berger A, Hoelzl MA, et al. The cooperating mutation or "second hit" determines the immunologic visibility toward MYC-induced murine lymphomas. *Blood*. 2011;118(17):4635-4645.
14. Knudson AG, Jr. Mutation and cancer: statistical study of retinoblastoma. *Proc Natl Acad Sci U S A*. 1971;68(4):820-823.
15. Nevins JR. The Rb/E2F pathway and cancer. *Hum Mol Genet*. 2001;10(7):699-703.
16. Willis A, Jung EJ, Wakefield T, Chen X. Mutant p53 exerts a dominant negative effect by preventing wild-type p53 from binding to the promoter of its target genes. *Oncogene*. 2004;23(13):2330-2338.
17. Kastan MB, Lim DS. The many substrates and functions of ATM. *Nat Rev Mol Cell Biol*. 2000;1(3):179-186.
18. Parkin J, Cohen B. An overview of the immune system. *Lancet*. 2001;357(9270):1777-1789.
19. van Gent DC, Hoeijmakers JH, Kanaar R. Chromosomal stability and the DNA double-stranded break connection. *Nat Rev Genet*. 2001;2(3):196-206.
20. Kuppers R. Mechanisms of B-cell lymphoma pathogenesis. *Nat Rev Cancer*. 2005;5(4):251-262.
21. Rajewsky K. Clonal selection and learning in the antibody system. *Nature*. 1996;381(6585):751-758.
22. Klein U, Dalla-Favera R. Germinal centres: role in B-cell physiology and malignancy. *Nat Rev Immunol*. 2008;8(1):22-33.
23. Campo E, Swerdlow SH, Harris NL, Pileri S, Stein H, Jaffe ES. The 2008 WHO classification of lymphoid neoplasms and beyond: evolving concepts and practical applications. *Blood*. 2011;117(19):5019-5032.
24. Fisher SG, Fisher RI. The epidemiology of non-Hodgkin's lymphoma. *Oncogene*. 2004;23(38):6524-6534.

25. Siegel R, Naishadham D, Jemal A. Cancer statistics, 2012. *CA Cancer J Clin*. 2012;62(1):10-29.
26. Chiorazzi N, Ferrarini M. Cellular origin(s) of chronic lymphocytic leukemia: cautionary notes and additional considerations and possibilities. *Blood*. 2011;117(6):1781-1791.
27. Seifert M, Sellmann L, Bloehdorn J, et al. Cellular origin and pathophysiology of chronic lymphocytic leukemia. *J Exp Med*. 2012;209(12):2183-2198.
28. Damle RN, Wasil T, Fais F, et al. Ig V gene mutation status and CD38 expression as novel prognostic indicators in chronic lymphocytic leukemia. *Blood*. 1999;94(6):1840-1847.
29. Hamblin TJ, Davis Z, Gardiner A, Oscier DG, Stevenson FK. Unmutated Ig V(H) genes are associated with a more aggressive form of chronic lymphocytic leukemia. *Blood*. 1999;94(6):1848-1854.
30. Rickert RC. New insights into pre-BCR and BCR signalling with relevance to B cell malignancies. *Nat Rev Immunol*. 2013;13(8):578-591.
31. Dreyling M, Amador V, Callanan M, et al. Update on the molecular pathogenesis and targeted approaches of mantle cell lymphoma: summary of the 12th annual conference of the European Mantle Cell Lymphoma Network. *Leuk Lymphoma*. 2014:1-11.
32. Kraus M, Alimzhanov MB, Rajewsky N, Rajewsky K. Survival of resting mature B lymphocytes depends on BCR signaling via the Igalpha/beta heterodimer. *Cell*. 2004;117(6):787-800.
33. Lam KP, Kuhn R, Rajewsky K. In vivo ablation of surface immunoglobulin on mature B cells by inducible gene targeting results in rapid cell death. *Cell*. 1997;90(6):1073-1083.
34. Burger JA, Ghia P, Rosenwald A, Caligaris-Cappio F. The microenvironment in mature B-cell malignancies: a target for new treatment strategies. *Blood*. 2009;114(16):3367-3375.
35. Johnson PW, Watt SM, Betts DR, et al. Isolated follicular lymphoma cells are resistant to apoptosis and can be grown in vitro in the CD40/stromal cell system. *Blood*. 1993;82(6):1848-1857.
36. Kurtova AV, Balakrishnan K, Chen R, et al. Diverse marrow stromal cells protect CLL cells from spontaneous and drug-induced apoptosis: development of a reliable and reproducible system to assess stromal cell adhesion-mediated drug resistance. *Blood*. 2009;114(20):4441-4450.
37. Burger JA, Tsukada N, Burger M, Zvaifler NJ, Dell'Aquila M, Kipps TJ. Blood-derived nurse-like cells protect chronic lymphocytic leukemia B cells from spontaneous apoptosis through stromal cell-derived factor-1. *Blood*. 2000;96(8):2655-2663.
38. Burger JA. Nurture versus nature: the microenvironment in chronic lymphocytic leukemia. *Hematology Am Soc Hematol Educ Program*. 2011;2011:96-103.
39. Kuppers R. B cells under influence: transformation of B cells by Epstein-Barr virus. *Nat Rev Immunol*. 2003;3(10):801-812.
40. Thorley-Lawson DA, Gross A. Persistence of the Epstein-Barr virus and the origins of associated lymphomas. *N Engl J Med*. 2004;350(13):1328-1337.
41. Young LS, Rickinson AB. Epstein-Barr virus: 40 years on. *Nat Rev Cancer*. 2004;4(10):757-768.
42. Zenz T, Mertens D, Kuppers R, Dohner H, Stilgenbauer S. From pathogenesis to treatment of chronic lymphocytic leukaemia. *Nat Rev Cancer*. 2010;10(1):37-50.
43. Rozman C, Montserrat E. Chronic lymphocytic leukemia. *N Engl J Med*. 1995;333(16):1052-1057.
44. Dores GM, Anderson WF, Curtis RE, et al. Chronic lymphocytic leukaemia and small lymphocytic lymphoma: overview of the descriptive epidemiology. *Br J Haematol*. 2007;139(5):809-819.
45. Hallek M, Cheson BD, Catovsky D, et al. Guidelines for the diagnosis and treatment of chronic lymphocytic leukemia: a report from the International Workshop on Chronic

Lymphocytic Leukemia updating the National Cancer Institute-Working Group 1996 guidelines. *Blood*. 2008;111(12):5446-5456.
46. Stilgenbauer S, Bullinger L, Lichter P, Dohner H, German CLLSGCll. Genetics of chronic lymphocytic leukemia: genomic aberrations and V(H) gene mutation status in pathogenesis and clinical course. *Leukemia*. 2002;16(6):993-1007.
47. Stilgenbauer S, Zenz T. Understanding and managing ultra high-risk chronic lymphocytic leukemia. *Hematology Am Soc Hematol Educ Program*. 2010;2010:481-488.
48. Dohner H, Stilgenbauer S, Benner A, et al. Genomic aberrations and survival in chronic lymphocytic leukemia. *N Engl J Med*. 2000;343(26):1910-1916.
49. Rossi D, Fangazio M, Gaidano G. The spectrum of genetic defects in chronic lymphocytic leukemia. *Mediterr J Hematol Infect Dis*. 2012;4(1):e2012076.
50. Rossi D, Bruscaggin A, Spina V, et al. Mutations of the SF3B1 splicing factor in chronic lymphocytic leukemia: association with progression and fludarabine-refractoriness. *Blood*. 2011;118(26):6904-6908.
51. Puente XS, Pinyol M, Quesada V, et al. Whole-genome sequencing identifies recurrent mutations in chronic lymphocytic leukaemia. *Nature*. 2011;475(7354):101-105.
52. Wahlfors J, Hiltunen H, Heinonen K, Hamalainen E, Alhonen L, Janne J. Genomic hypomethylation in human chronic lymphocytic leukemia. *Blood*. 1992;80(8):2074-2080.
53. Calin GA, Dumitru CD, Shimizu M, et al. Frequent deletions and down-regulation of micro- RNA genes miR15 and miR16 at 13q14 in chronic lymphocytic leukemia. *Proc Natl Acad Sci U S A*. 2002;99(24):15524-15529.
54. Widhopf GF, 2nd, Rassenti LZ, Toy TL, Gribben JG, Wierda WG, Kipps TJ. Chronic lymphocytic leukemia B cells of more than 1% of patients express virtually identical immunoglobulins. *Blood*. 2004;104(8):2499-2504.
55. Duhren-von Minden M, Ubelhart R, Schneider D, et al. Chronic lymphocytic leukaemia is driven by antigen-independent cell-autonomous signalling. *Nature*. 2012;489(7415):309-312.
56. Herishanu Y, Perez-Galan P, Liu D, et al. The lymph node microenvironment promotes B-cell receptor signaling, NF-kappaB activation, and tumor proliferation in chronic lymphocytic leukemia. *Blood*. 2011;117(2):563-574.
57. Krober A, Seiler T, Benner A, et al. V(H) mutation status, CD38 expression level, genomic aberrations, and survival in chronic lymphocytic leukemia. *Blood*. 2002;100(4):1410-1416.
58. Rossi D, Spina V, Bomben R, et al. Association between molecular lesions and specific B-cell receptor subsets in chronic lymphocytic leukemia. *Blood*. 2013;121(24):4902-4905.
59. Guarini A, Chiaretti S, Tavolaro S, et al. BCR ligation induced by IgM stimulation results in gene expression and functional changes only in IgV H unmutated chronic lymphocytic leukemia (CLL) cells. *Blood*. 2008;112(3):782-792.
60. Chen L, Huynh L, Apgar J, et al. ZAP-70 enhances IgM signaling independent of its kinase activity in chronic lymphocytic leukemia. *Blood*. 2008;111(5):2685-2692.
61. Cruse JM, Lewis RE, Webb RN, Sanders CM, Suggs JL. Zap-70 and CD38 as predictors of IgVH mutation in CLL. *Exp Mol Pathol*. 2007;83(3):459-461.
62. Wiestner A, Rosenwald A, Barry TS, et al. ZAP-70 expression identifies a chronic lymphocytic leukemia subtype with unmutated immunoglobulin genes, inferior clinical outcome, and distinct gene expression profile. *Blood*. 2003;101(12):4944-4951.
63. Roos G, Krober A, Grabowski P, et al. Short telomeres are associated with genetic complexity, high-risk genomic aberrations, and short survival in chronic lymphocytic leukemia. *Blood*. 2008;111(4):2246-2252.
64. Damle RN, Temburni S, Calissano C, et al. CD38 expression labels an activated subset within chronic lymphocytic leukemia clones enriched in proliferating B cells. *Blood*. 2007;110(9):3352-3359.

65. Damle RN, Temburni S, Banapour T, et al. T-cell independent, B-cell receptor-mediated induction of telomerase activity differs among IGHV mutation-based subgroups of chronic lymphocytic leukemia patients. *Blood*. 2012;120(12):2438-2449.
66. Cimmino A, Calin GA, Fabbri M, et al. miR-15 and miR-16 induce apoptosis by targeting BCL2. *Proc Natl Acad Sci U S A*. 2005;102(39):13944-13949.
67. Stilgenbauer S, Zenz T, Winkler D, et al. Subcutaneous alemtuzumab in fludarabine-refractory chronic lymphocytic leukemia: clinical results and prognostic marker analyses from the CLL2H study of the German Chronic Lymphocytic Leukemia Study Group. *J Clin Oncol*. 2009;27(24):3994-4001.
68. Austen B, Powell JE, Alvi A, et al. Mutations in the ATM gene lead to impaired overall and treatment-free survival that is independent of IGVH mutation status in patients with B-CLL. *Blood*. 2005;106(9):3175-3182.
69. Guarini A, Marinelli M, Tavolaro S, et al. ATM gene alterations in chronic lymphocytic leukemia patients induce a distinct gene expression profile and predict disease progression. *Haematologica*. 2012;97(1):47-55.
70. Zenz T, Habe S, Denzel T, et al. Detailed analysis of p53 pathway defects in fludarabine-refractory chronic lymphocytic leukemia (CLL): dissecting the contribution of 17p deletion, TP53 mutation, p53-p21 dysfunction, and miR34a in a prospective clinical trial. *Blood*. 2009;114(13):2589-2597.
71. Rossi D, Rasi S, Fabbri G, et al. Mutations of NOTCH1 are an independent predictor of survival in chronic lymphocytic leukemia. *Blood*. 2012;119(2):521-529.
72. Mansouri L, Cahill N, Gunnarsson R, et al. NOTCH1 and SF3B1 mutations can be added to the hierarchical prognostic classification in chronic lymphocytic leukemia. *Leukemia*. 2013;27(2):512-514.
73. Jeromin S, Weissmann S, Haferlach C, et al. SF3B1 mutations correlated to cytogenetics and mutations in NOTCH1, FBXW7, MYD88, XPO1 and TP53 in 1160 untreated CLL patients. *Leukemia*. 2013.
74. Schnaiter A, Paschka P, Rossi M, et al. NOTCH1, SF3B1 and TP53 mutations in fludarabine-refractory CLL patients treated with alemtuzumab: results from the CLL2H trial of the GCLLSG. *Blood*. 2013.
75. Dicker F, Herholz H, Schnittger S, et al. The detection of TP53 mutations in chronic lymphocytic leukemia independently predicts rapid disease progression and is highly correlated with a complex aberrant karyotype. *Leukemia*. 2009;23(1):117-124.
76. Rossi D, Cerri M, Deambrogi C, et al. The prognostic value of TP53 mutations in chronic lymphocytic leukemia is independent of Del17p13: implications for overall survival and chemorefractoriness. *Clin Cancer Res*. 2009;15(3):995-1004.
77. Mastrocola AS, Kim SH, Trinh AT, Rodenkirch LA, Tibbetts RS. The RNA-binding protein fused in sarcoma (FUS) functions downstream of poly(ADP-ribose) polymerase (PARP) in response to DNA damage. *J Biol Chem*. 2013;288(34):24731-24741.
78. Dreger P, Corradini P, Kimby E, et al. Indications for allogeneic stem cell transplantation in chronic lymphocytic leukemia: the EBMT transplant consensus. *Leukemia*. 2007;21(1):12-17.
79. Wan Y, Wu CJ. SF3B1 mutations in chronic lymphocytic leukemia. *Blood*. 2013;121(23):4627-4634.
80. Arruga F, Gizdic B, Serra S, et al. Functional impact of NOTCH1 mutations in chronic lymphocytic leukemia. *Leukemia*. 2014;28(5):1060-1070.
81. Zucchetto A, Caldana C, Benedetti D, et al. CD49d is overexpressed by trisomy 12 chronic lymphocytic leukemia cells: evidence for a methylation-dependent regulation mechanism. *Blood*. 2013;122(19):3317-3321.
82. Goodnow CC, Sprent J, Fazekas de St Groth B, Vinuesa CG. Cellular and genetic mechanisms of self tolerance and autoimmunity. *Nature*. 2005;435(7042):590-597.

83. Ferreira PG, Jares P, Rico D, et al. Transcriptome characterization by RNA sequencing identifies a major molecular and clinical subdivision in chronic lymphocytic leukemia. *Genome Res*. 2013.
84. Ringshausen I, Schneller F, Bogner C, et al. Constitutively activated phosphatidylinositol-3 kinase (PI-3K) is involved in the defect of apoptosis in B-CLL: association with protein kinase Cdelta. *Blood*. 2002;100(10):3741-3748.
85. Johnson TA, Rassenti LZ, Kipps TJ. Ig VH1 genes expressed in B cell chronic lymphocytic leukemia exhibit distinctive molecular features. *J Immunol*. 1997;158(1):235-246.
86. Stamatopoulos K, Belessi C, Moreno C, et al. Over 20% of patients with chronic lymphocytic leukemia carry stereotyped receptors: Pathogenetic implications and clinical correlations. *Blood*. 2007;109(1):259-270.
87. Stevenson FK, Caligaris-Cappio F. Chronic lymphocytic leukemia: revelations from the B-cell receptor. *Blood*. 2004;103(12):4389-4395.
88. Chiorazzi N, Rai KR, Ferrarini M. Chronic lymphocytic leukemia. *N Engl J Med*. 2005;352(8):804-815.
89. Binder M, Muller F, Frick M, et al. CLL B-cell receptors can recognize themselves: alternative epitopes and structural clues for autostimulatory mechanisms in CLL. *Blood*. 2013;121(1):239-241.
90. Burger JA, Quiroga MP, Hartmann E, et al. High-level expression of the T-cell chemokines CCL3 and CCL4 by chronic lymphocytic leukemia B cells in nurselike cell cocultures and after BCR stimulation. *Blood*. 2009;113(13):3050-3058.
91. Bernal A, Pastore RD, Asgary Z, et al. Survival of leukemic B cells promoted by engagement of the antigen receptor. *Blood*. 2001;98(10):3050-3057.
92. Petlickovski A, Laurenti L, Li X, et al. Sustained signaling through the B-cell receptor induces Mcl-1 and promotes survival of chronic lymphocytic leukemia B cells. *Blood*. 2005;105(12):4820-4827.
93. Quiroga MP, Balakrishnan K, Kurtova AV, et al. B-cell antigen receptor signaling enhances chronic lymphocytic leukemia cell migration and survival: specific targeting with a novel spleen tyrosine kinase inhibitor, R406. *Blood*. 2009;114(5):1029-1037.
94. Hendriks RW, Yuvaraj S, Kil LP. Targeting Bruton's tyrosine kinase in B cell malignancies. *Nat Rev Cancer*. 2014;14(4):219-232.
95. Byrd JC, Furman RR, Coutre SE, et al. Targeting BTK with ibrutinib in relapsed chronic lymphocytic leukemia. *N Engl J Med*. 2013;369(1):32-42.
96. Petro JB, Rahman SM, Ballard DW, Khan WN. Bruton's tyrosine kinase is required for activation of IkappaB kinase and nuclear factor kappaB in response to B cell receptor engagement. *J Exp Med*. 2000;191(10):1745-1754.
97. Craxton A, Jiang A, Kurosaki T, Clark EA. Syk and Bruton's tyrosine kinase are required for B cell antigen receptor-mediated activation of the kinase Akt. *J Biol Chem*. 1999;274(43):30644-30650.
98. Tomlinson MG, Woods DB, McMahon M, et al. A conditional form of Bruton's tyrosine kinase is sufficient to activate multiple downstream signaling pathways via PLC Gamma 2 in B cells. *BMC Immunol*. 2001;2:4.
99. Honigberg LA, Smith AM, Sirisawad M, et al. The Bruton tyrosine kinase inhibitor PCI-32765 blocks B-cell activation and is efficacious in models of autoimmune disease and B-cell malignancy. *Proc Natl Acad Sci U S A*. 2010;107(29):13075-13080.
100. Herman SE, Gordon AL, Hertlein E, et al. Bruton tyrosine kinase represents a promising therapeutic target for treatment of chronic lymphocytic leukemia and is effectively targeted by PCI-32765. *Blood*. 2011;117(23):6287-6296.
101. Ponader S, Chen SS, Buggy JJ, et al. The Bruton tyrosine kinase inhibitor PCI-32765 thwarts chronic lymphocytic leukemia cell survival and tissue homing in vitro and in vivo. *Blood*. 2012;119(5):1182-1189.

102. Herman SE, Mustafa RZ, Gyamfi JA, et al. Ibrutinib inhibits B-cell receptor and NF-kappaB signaling and reduces tumor proliferation in tissue-resident cells of patients with chronic lymphocytic leukemia. *Blood*. 2014.
103. Furman RR, Sharman JP, Coutre SE, et al. Idelalisib and Rituximab in Relapsed Chronic Lymphocytic Leukemia. *N Engl J Med*. 2014.
104. Markham A. Idelalisib: First Global Approval. *Drugs*. 2014.
105. Herman SE, Barr PM, McAuley EM, Liu D, Wiestner A, Friedberg JW. Fostamatinib inhibits B-cell receptor signaling, cellular activation and tumor proliferation in patients with relapsed and refractory chronic lymphocytic leukemia. *Leukemia*. 2013;27(8):1769-1773.
106. Suljagic M, Longo PG, Bennardo S, et al. The Syk inhibitor fostamatinib disodium (R788) inhibits tumor growth in the Emu- TCL1 transgenic mouse model of CLL by blocking antigen-dependent B-cell receptor signaling. *Blood*. 2010;116(23):4894-4905.
107. Vousden KH, Lane DP. p53 in health and disease. *Nat Rev Mol Cell Biol*. 2007;8(4):275-283.
108. Vogelstein B, Lane D, Levine AJ. Surfing the p53 network. *Nature*. 2000;408(6810):307-310.
109. Riley T, Sontag E, Chen P, Levine A. Transcriptional control of human p53-regulated genes. *Nat Rev Mol Cell Biol*. 2008;9(5):402-412.
110. Bieging KT, Mello SS, Attardi LD. Unravelling mechanisms of p53-mediated tumour suppression. *Nat Rev Cancer*. 2014;14(5):359-370.
111. Wade M, Li YC, Wahl GM. MDM2, MDMX and p53 in oncogenesis and cancer therapy. *Nat Rev Cancer*. 2013;13(2):83-96.
112. Gonzalez D, Martinez P, Wade R, et al. Mutational status of the TP53 gene as a predictor of response and survival in patients with chronic lymphocytic leukemia: results from the LRF CLL4 trial. *J Clin Oncol*. 2011;29(16):2223-2229.
113. Zenz T, Eichhorst B, Busch R, et al. TP53 mutation and survival in chronic lymphocytic leukemia. *J Clin Oncol*. 2010;28(29):4473-4479.
114. Zenz T, Krober A, Scherer K, et al. Monoallelic TP53 inactivation is associated with poor prognosis in chronic lymphocytic leukemia: results from a detailed genetic characterization with long-term follow-up. *Blood*. 2008;112(8):3322-3329.
115. de Vries A, Flores ER, Miranda B, et al. Targeted point mutations of p53 lead to dominant-negative inhibition of wild-type p53 function. *Proc Natl Acad Sci U S A*. 2002;99(5):2948-2953.
116. Zenz T, Mohr J, Eldering E, et al. miR-34a as part of the resistance network in chronic lymphocytic leukemia. *Blood*. 2009;113(16):3801-3808.
117. Friedman RC, Farh KK, Burge CB, Bartel DP. Most mammalian mRNAs are conserved targets of microRNAs. *Genome Res*. 2009;19(1):92-105.
118. John B, Enright AJ, Aravin A, Tuschl T, Sander C, Marks DS. Human MicroRNA targets. *PLoS Biol*. 2004;2(11):e363.
119. Bartel DP. MicroRNAs: target recognition and regulatory functions. *Cell*. 2009;136(2):215-233.
120. Lee RC, Feinbaum RL, Ambros V. The C. elegans heterochronic gene lin-4 encodes small RNAs with antisense complementarity to lin-14. *Cell*. 1993;75(5):843-854.
121. Esquela-Kerscher A, Slack FJ. Oncomirs - microRNAs with a role in cancer. *Nat Rev Cancer*. 2006;6(4):259-269.
122. van Rooij E, Kauppinen S. Development of microRNA therapeutics is coming of age. *EMBO Mol Med*. 2014;6(7):851-864.
123. Winter J, Jung S, Keller S, Gregory RI, Diederichs S. Many roads to maturity: microRNA biogenesis pathways and their regulation. *Nat Cell Biol*. 2009;11(3):228-234.
124. Erhard F, Haas J, Lieber D, et al. Widespread context dependency of microRNA-mediated regulation. *Genome Res*. 2014;24(6):906-919.

125. Salmena L, Poliseno L, Tay Y, Kats L, Pandolfi PP. A ceRNA hypothesis: the Rosetta Stone of a hidden RNA language? *Cell*. 2011;146(3):353-358.
126. Sumazin P, Yang X, Chiu HS, et al. An extensive microRNA-mediated network of RNA-RNA interactions regulates established oncogenic pathways in glioblastoma. *Cell*. 2011;147(2):370-381.
127. Djebali S, Davis CA, Merkel A, et al. Landscape of transcription in human cells. *Nature*. 2012;489(7414):101-108.
128. Consortium EP. An integrated encyclopedia of DNA elements in the human genome. *Nature*. 2012;489(7414):57-74.
129. Carninci P, Kasukawa T, Katayama S, et al. The transcriptional landscape of the mammalian genome. *Science*. 2005;309(5740):1559-1563.
130. Guttman M, Amit I, Garber M, et al. Chromatin signature reveals over a thousand highly conserved large non-coding RNAs in mammals. *Nature*. 2009;458(7235):223-227.
131. Hung T, Wang Y, Lin MF, et al. Extensive and coordinated transcription of noncoding RNAs within cell-cycle promoters. *Nat Genet*. 2011;43(7):621-629.
132. Heward JA, Lindsay MA. Long non-coding RNAs in the regulation of the immune response. *Trends Immunol*. 2014;35(9):408-419.
133. Derrien T, Johnson R, Bussotti G, et al. The GENCODE v7 catalog of human long noncoding RNAs: analysis of their gene structure, evolution, and expression. *Genome Res*. 2012;22(9):1775-1789.
134. David L, Huber W, Granovskaia M, et al. A high-resolution map of transcription in the yeast genome. *Proc Natl Acad Sci U S A*. 2006;103(14):5320-5325.
135. Neil H, Malabat C, d'Aubenton-Carafa Y, Xu Z, Steinmetz LM, Jacquier A. Widespread bidirectional promoters are the major source of cryptic transcripts in yeast. *Nature*. 2009;457(7232):1038-1042.
136. Cabili MN, Trapnell C, Goff L, et al. Integrative annotation of human large intergenic noncoding RNAs reveals global properties and specific subclasses. *Genes Dev*. 2011;25(18):1915-1927.
137. Clark BS, Blackshaw S. Long non-coding RNA-dependent transcriptional regulation in neuronal development and disease. *Front Genet*. 2014;5:164.
138. Kung JT, Colognori D, Lee JT. Long noncoding RNAs: past, present, and future. *Genetics*. 2013;193(3):651-669.
139. Guttman M, Rinn JL. Modular regulatory principles of large non-coding RNAs. *Nature*. 2012;482(7385):339-346.
140. Penny GD, Kay GF, Sheardown SA, Rastan S, Brockdorff N. Requirement for Xist in X chromosome inactivation. *Nature*. 1996;379(6561):131-137.
141. Lee JT, Davidow LS, Warshawsky D. Tsix, a gene antisense to Xist at the X-inactivation centre. *Nat Genet*. 1999;21(4):400-404.
142. Khalil AM, Guttman M, Huarte M, et al. Many human large intergenic noncoding RNAs associate with chromatin-modifying complexes and affect gene expression. *Proc Natl Acad Sci U S A*. 2009;106(28):11667-11672.
143. Tsai MC, Manor O, Wan Y, et al. Long noncoding RNA as modular scaffold of histone modification complexes. *Science*. 2010;329(5992):689-693.
144. Dvinge H, Git A, Graf S, et al. The shaping and functional consequences of the microRNA landscape in breast cancer. *Nature*. 2013;497(7449):378-382.
145. Lujambio A, Lowe SW. The microcosmos of cancer. *Nature*. 2012;482(7385):347-355.
146. Volinia S, Galasso M, Costinean S, et al. Reprogramming of miRNA networks in cancer and leukemia. *Genome Res*. 2010;20(5):589-599.
147. Jansson MD, Lund AH. MicroRNA and cancer. *Mol Oncol*. 2012;6(6):590-610.

148. Watashi K, Yeung ML, Starost MF, Hosmane RS, Jeang KT. Identification of small molecules that suppress microRNA function and reverse tumorigenesis. *J Biol Chem*. 2010;285(32):24707-24716.
149. Yang CH, Yue J, Pfeffer SR, et al. MicroRNA-21 Promotes Glioblastoma Tumorigenesis by Down-regulating Insulin-like Growth Factor-binding Protein-3 (IGFBP3). *J Biol Chem*. 2014;289(36):25079-25087.
150. Scherr M, Elder A, Battmer K, et al. Differential expression of miR-17~92 identifies BCL2 as a therapeutic target in BCR-ABL-positive B-lineage acute lymphoblastic leukemia. *Leukemia*. 2014;28(3):554-565.
151. Calin GA, Pekarsky Y, Croce CM. The role of microRNA and other non-coding RNA in the pathogenesis of chronic lymphocytic leukemia. *Best Pract Res Clin Haematol*. 2007;20(3):425-437.
152. Baer C, Claus R, Plass C. Genome-Wide Epigenetic Regulation of miRNAs in Cancer. *Cancer Res*. 2013;73(2):473-477.
153. Baer C, Claus R, Frenzel LP, et al. Extensive Promoter DNA Hypermethylation and Hypomethylation Is Associated with Aberrant MicroRNA Expression in Chronic Lymphocytic Leukemia. *Cancer Res*. 2012;72(15):3775-3785.
154. Suzuki H, Maruyama R, Yamamoto E, Kai M. Epigenetic alteration and microRNA dysregulation in cancer. *Front Genet*. 2013;4:258.
155. Bandres E, Agirre X, Bitarte N, et al. Epigenetic regulation of microRNA expression in colorectal cancer. *Int J Cancer*. 2009;125(11):2737-2743.
156. Kim K, Lee HC, Park JL, et al. Epigenetic regulation of microRNA-10b and targeting of oncogenic MAPRE1 in gastric cancer. *Epigenetics*. 2011;6(6):740-751.
157. Kumar MS, Lu J, Mercer KL, Golub TR, Jacks T. Impaired microRNA processing enhances cellular transformation and tumorigenesis. *Nat Genet*. 2007;39(5):673-677.
158. Allegra D, Bilan V, Garding A, et al. Defective DROSHA processing contributes to downregulation of MiR-15/-16 in chronic lymphocytic leukemia. *Leukemia*. 2013.
159. Torrezan GT, Ferreira EN, Nakahata AM, et al. Recurrent somatic mutation in DROSHA induces microRNA profile changes in Wilms tumour. *Nat Commun*. 2014;5:4039.
160. Calin GA, Liu CG, Sevignani C, et al. MicroRNA profiling reveals distinct signatures in B cell chronic lymphocytic leukemias. *Proc Natl Acad Sci U S A*. 2004;101(32):11755-11760.
161. Yanaihara N, Caplen N, Bowman E, et al. Unique microRNA molecular profiles in lung cancer diagnosis and prognosis. *Cancer Cell*. 2006;9(3):189-198.
162. Rosenfeld N, Aharonov R, Meiri E, et al. MicroRNAs accurately identify cancer tissue origin. *Nat Biotechnol*. 2008;26(4):462-469.
163. Schultz NA, Dehlendorff C, Jensen BV, et al. MicroRNA biomarkers in whole blood for detection of pancreatic cancer. *JAMA*. 2014;311(4):392-404.
164. Shen J, Liu Z, Todd NW, et al. Diagnosis of lung cancer in individuals with solitary pulmonary nodules by plasma microRNA biomarkers. *BMC Cancer*. 2011;11:374.
165. Schwarzenbach H, Nishida N, Calin GA, Pantel K. Clinical relevance of circulating cell-free microRNAs in cancer. *Nat Rev Clin Oncol*. 2014;11(3):145-156.
166. Calin GA, Ferracin M, Cimmino A, et al. A MicroRNA signature associated with prognosis and progression in chronic lymphocytic leukemia. *N Engl J Med*. 2005;353(17):1793-1801.
167. Moussay E, Wang K, Cho JH, et al. MicroRNA as biomarkers and regulators in B-cell chronic lymphocytic leukemia. *Proc Natl Acad Sci U S A*. 2011;108(16):6573-6578.
168. Negrini M, Cutrona G, Bassi C, et al. microRNAome expression in chronic lymphocytic leukemia: comparison with normal B cell subsets and correlations with prognostic and clinical parameters. *Clin Cancer Res*. 2014.
169. Rosa Visone LZR, 2 Angelo Veronese,1,3 Cristian Taccioli,1 Stefan Costinean,1 Baltazar D. Aguda,4, Stefano Volinia MF, 3 Jeff Palatini,1 Veronica Balatti,1 Hansjuerg Alder,1 Massimo

Negrini,3 Thomas J. Kipps,2, Croce1 aCM. Karyotype-specific microRNAsignature in chronic lymphocytic leukemia. *Blood*. 2009;114:3872-3879.
170. Dufour A, Palermo G, Zellmeier E, et al. Inactivation of TP53 correlates with disease progression and low miR-34a expression in previously treated chronic lymphocytic leukemia patients. *Blood*. 2013.
171. Li XJ, Ren ZJ, Tang JH. MicroRNA-34a: a potential therapeutic target in human cancer. *Cell Death Dis*. 2014;5:e1327.
172. Bader AG. miR-34 - a microRNA replacement therapy is headed to the clinic. *Front Genet*. 2012;3:120.
173. Esteller M. Non-coding RNAs in human disease. *Nat Rev Genet*. 2011;12(12):861-874.
174. Gupta RA, Shah N, Wang KC, et al. Long non-coding RNA HOTAIR reprograms chromatin state to promote cancer metastasis. *Nature*. 2010;464(7291):1071-1076.
175. Prensner JR, Iyer MK, Sahu A, et al. The long noncoding RNA SChLAP1 promotes aggressive prostate cancer and antagonizes the SWI/SNF complex. *Nat Genet*. 2013;45(11):1392-1398.
176. Gutschner T, Diederichs S. The Hallmarks of Cancer: A long non-coding RNA point of view. *RNA Biol*. 2012;9(6):703-719.
177. Yildirim E, Kirby JE, Brown DE, et al. Xist RNA is a potent suppressor of hematologic cancer in mice. *Cell*. 2013;152(4):727-742.
178. Ji P, Diederichs S, Wang W, et al. MALAT-1, a novel noncoding RNA, and thymosin beta4 predict metastasis and survival in early-stage non-small cell lung cancer. *Oncogene*. 2003;22(39):8031-8041.
179. Xu C, Yang M, Tian J, Wang X, Li Z. MALAT-1: a long non-coding RNA and its important 3' end functional motif in colorectal cancer metastasis. *Int J Oncol*. 2011;39(1):169-175.
180. Calin GA, Liu CG, Ferracin M, et al. Ultraconserved regions encoding ncRNAs are altered in human leukemias and carcinomas. *Cancer Cell*. 2007;12(3):215-229.
181. Eis PS, Tam W, Sun L, et al. Accumulation of miR-155 and BIC RNA in human B cell lymphomas. *Proc Natl Acad Sci U S A*. 2005;102(10):3627-3632.
182. Stilgenbauer S, Nickolenko J, Wilhelm J, et al. Expressed sequences as candidates for a novel tumor suppressor gene at band 13q14 in B-cell chronic lymphocytic leukemia and mantle cell lymphoma. *Oncogene*. 1998;16(14):1891-1897.
183. Garding A, Bhattacharya N, Claus R, et al. Epigenetic upregulation of lncRNAs at 13q14.3 in leukemia is linked to the In Cis downregulation of a gene cluster that targets NF-kB. *PLoS Genet*. 2013;9(4):e1003373.
184. Hu Y, Chen HY, Yu CY, et al. A long non-coding RNA signature to improve prognosis prediction of colorectal cancer. *Oncotarget*. 2014;5(8):2230-2242.
185. Zhang S, Chen S, Yang G, et al. Long Noncoding RNA HOTAIR as an Independent Prognostic Marker in Cancer: A Meta-Analysis. *PLoS One*. 2014;9(8):e105538.
186. Qi P, Du X. The long non-coding RNAs, a new cancer diagnostic and therapeutic gold mine. *Mod Pathol*. 2013;26(2):155-165.
187. Calin GA, Ferracin M, Croce CM, al. e. A miRNA signature associated with prognosis and progression in CLL. *N Engl J Med*. 2005.
188. Fulci V, Chiaretti S, Goldoni M, et al. Quantitative technologies establish a novel microRNA profile of chronic lymphocytic leukemia. *Blood*. 2007;109(11):4944-4951.
189. Papakonstantinou N, Ntoufa S, Chartomatsidou E, et al. Differential microRNA profiles and their functional implications in different immunogenetic subsets of chronic lymphocytic leukemia. *Mol Med*. 2013;19:115-123.
190. Pede V, Rombout A, Vermeire J, et al. CLL cells respond to B-Cell receptor stimulation with a microRNA/mRNA signature associated with MYC activation and cell cycle progression. *PLoS One*. 2013;8(4):e60275.

191. Mraz M, Malinova K, Kotaskova J, et al. miR-34a, miR-29c and miR-17-5p are downregulated in CLL patients with TP53 abnormalities. *Leukemia*. 2009;23(6):1159-1163.
192. He L, He X, Lim LP, et al. A microRNA component of the p53 tumour suppressor network. *Nature*. 2007;447(7148):1130-1134.
193. Chang TC, Wentzel EA, Kent OA, et al. Transactivation of miR-34a by p53 broadly influences gene expression and promotes apoptosis. *Mol Cell*. 2007;26(5):745-752.
194. Raver-Shapira N, Marciano E, Meiri E, et al. Transcriptional activation of miR-34a contributes to p53-mediated apoptosis. *Mol Cell*. 2007;26(5):731-743.
195. Tarasov V, Jung P, Verdoodt B, et al. Differential regulation of microRNAs by p53 revealed by massively parallel Sequencing - miR-34a is a p53 target that induces apoptosis and G(1)-arrest. *Cell Cycle*. 2007;6(13):1586-1593.
196. Bommer GT, Gerin I, Feng Y, et al. p53-mediated activation of miRNA34 candidate tumor-suppressor genes. *Curr Biol*. 2007;17(15):1298-1307.
197. Sun F, Fu H, Liu Q, et al. Downregulation of CCND1 and CDK6 by miR-34a induces cell cycle arrest. *FEBS Lett*. 2008;582(10):1564-1568.
198. Tazawa H, Tsuchiya N, Izumiya M, Nakagama H. Tumor-suppressive miR-34a induces senescence-like growth arrest through modulation of the E2F pathway in human colon cancer cells. *Proc Natl Acad Sci U S A*. 2007;104(39):15472-15477.
199. Chen Y, Zhu X, Zhang X, Liu B, Huang L. Nanoparticles modified with tumor-targeting scFv deliver siRNA and miRNA for cancer therapy. *Mol Ther*. 2010;18(9):1650-1656.
200. Yamakuchi M, Lotterman CD, Bao C, et al. P53-induced microRNA-107 inhibits HIF-1 and tumor angiogenesis. *Proc Natl Acad Sci U S A*. 2010;107(14):6334-6339.
201. Sachdeva M, Zhu S, Wu F, et al. p53 represses c-Myc through induction of the tumor suppressor miR-145. *Proc Natl Acad Sci U S A*. 2009;106(9):3207-3212.
202. Hu W, Chan CS, Wu R, et al. Negative regulation of tumor suppressor p53 by microRNA miR-504. *Mol Cell*. 2010;38(5):689-699.
203. Morachis JM, Murawsky CM, Emerson BM. Regulation of the p53 transcriptional response by structurally diverse core promoters. *Genes Dev*. 2010;24(2):135-147.
204. Huarte M, Guttman M, Feldser D, et al. A large intergenic noncoding RNA induced by p53 mediates global gene repression in the p53 response. *Cell*. 2010;142(3):409-419.
205. Yoon JH, Abdelmohsen K, Srikantan S, et al. LincRNA-p21 suppresses target mRNA translation. *Mol Cell*. 2012;47(4):648-655.
206. Botcheva K, McCorkle SR, McCombie WR, Dunn JJ, Anderson CW. Distinct p53 genomic binding patterns in normal and cancer-derived human cells. *Cell Cycle*. 2011;10(24):4237-4249.
207. Nikulenkov F, Spinnler C, Li H, et al. Insights into p53 transcriptional function via genome-wide chromatin occupancy and gene expression analysis. *Cell Death Differ*. 2012;19(12):1992-2002.
208. Menendez D, Nguyen TA, Freudenberg JM, et al. Diverse stresses dramatically alter genome-wide p53 binding and transactivation landscape in human cancer cells. *Nucleic Acids Res*. 2013;41(15):7286-7301.
209. Schlereth K, Heyl C, Krampitz AM, et al. Characterization of the p53 cistrome--DNA binding cooperativity dissects p53's tumor suppressor functions. *PLoS Genet*. 2013;9(8):e1003726.
210. Zhang A, Xu M, Mo YY. Role of the lncRNA-p53 regulatory network in cancer. *J Mol Cell Biol*. 2014.
211. Subramanian M, Jones MF, Lal A. Long Non-Coding RNAs Embedded in the Rb and p53 Pathways. *Cancers (Basel)*. 2013;5(4):1655-1675.
212. Sun S, Xu MZ, Poon RT, Day PJ, Luk JM. Circulating Lamin B1 (LMNB1) biomarker detects early stages of liver cancer in patients. *J Proteome Res*. 2010;9(1):70-78.
213. Zhang Q, Chen CY, Yedavalli VS, Jeang KT. NEAT1 long noncoding RNA and paraspeckle bodies modulate HIV-1 posttranscriptional expression. *MBio*. 2013;4(1):e00596-00512.

214. Mattia M, Gottifredi V, McKinney K, Prives C. p53-Dependent p21 mRNA elongation is impaired when DNA replication is stalled. *Mol Cell Biol*. 2007;27(4):1309-1320.
215. Te Raa GD, Malcikova J, Mraz M, et al. Assessment of TP53 functionality in chronic lymphocytic leukaemia by different assays; an ERIC-wide approach. *Br J Haematol*. 2014.
216. Castro F, Dirks WG, Fahnrich S, Hotz-Wagenblatt A, Pawlita M, Schmitt M. High-throughput SNP-based authentication of human cell lines. *Int J Cancer*. 2013;132(2):308-314.
217. Chan PP, Lowe TM. GtRNAdb: a database of transfer RNA genes detected in genomic sequence. *Nucleic Acids Res*. 2009;37(Database issue):D93-97.
218. Rosenkranz D, Zischler H. proTRAC--a software for probabilistic piRNA cluster detection, visualization and analysis. *BMC Bioinformatics*. 2012;13:5.
219. Ernst P, Glatting KH, Suhai S. A task framework for the web interface W2H. *Bioinformatics*. 2003;19(2):278-282.
220. Anders S, Huber W. Differential expression analysis for sequence count data. *Genome Biol*. 2010;11(10):R106.
221. McCarthy DJ, Chen Y, Smyth GK. Differential expression analysis of multifactor RNA-Seq experiments with respect to biological variation. *Nucleic Acids Res*. 2012;40(10):4288-4297.
222. Smyth GK. Limma: linear models for microarray data. in: Bioinformatics and Computational Biology Solutions using R and Bioconductor, R Gentleman, V Carey, S Dudoit, R Irizarry, W Huber (eds.). *Springer, New York*. 2005:397-420.
223. Dweep H, Sticht C, Pandey P, Gretz N. miRWalk--database: prediction of possible miRNA binding sites by "walking" the genes of three genomes. *J Biomed Inform*. 2011;44(5):839-847.
224. Lewis BP, Burge CB, Bartel DP. Conserved seed pairing, often flanked by adenosines, indicates that thousands of human genes are microRNA targets. *Cell*. 2005;120(1):15-20.
225. Jima DD, Zhang J, Jacobs C, et al. Deep sequencing of the small RNA transcriptome of normal and malignant human B cells identifies hundreds of novel microRNAs. *Blood*. 2010;116(23):e118-127.
226. Schotte D, Akbari Moqadam F, Lange-Turenhout EA, et al. Discovery of new microRNAs by small RNAome deep sequencing in childhood acute lymphoblastic leukemia. *Leukemia*. 2011;25(9):1389-1399.
227. Landgraf P, Rusu M, Sheridan R, et al. A mammalian microRNA expression atlas based on small RNA library sequencing. *Cell*. 2007;129(7):1401-1414.
228. O'Neil D, Glowatz H, Schlumpberger M. Ribosomal RNA depletion for efficient use of RNA-seq capacity. *Curr Protoc Mol Biol*. 2013;Chapter 4:Unit 4 19.
229. Iorio MV, Ferracin M, Liu CG, et al. MicroRNA gene expression deregulation in human breast cancer. *Cancer Res*. 2005;65(16):7065-7070.
230. Chan JA, Krichevsky AM, Kosik KS. MicroRNA-21 is an antiapoptotic factor in human glioblastoma cells. *Cancer Res*. 2005;65(14):6029-6033.
231. Volinia S, Calin GA, Liu CG, et al. A microRNA expression signature of human solid tumors defines cancer gene targets. *Proc Natl Acad Sci U S A*. 2006;103(7):2257-2261.
232. Jima DD, Zhang J, Jacobs C, et al. Deep sequencing of the small RNA transcriptome of normal and malignant human B cells identifies hundreds of novel microRNAs. *Blood*. 2010;116(23):e118-127.
233. Mraz M, Chen L, Rassenti LZ, et al. MicroRNA-150 contributes to the proficiency of B-cell receptor signaling in chronic lymphocytic leukemia by regulating expression of GAB1 and FOXP1 genes. *Blood*. 2014.
234. Thai TH, Calado DP, Casola S, et al. Regulation of the germinal center response by microRNA-155. *Science*. 2007;316(5824):604-608.
235. Cui B, Chen L, Zhang S, et al. MicroRNA-155 influences B-cell receptor signaling and associates with aggressive disease in chronic lymphocytic leukemia. *Blood*. 2014;124(4):546-554.
236. Jackson TA, Haga CL, Ehrhardt GR, Davis RS, Cooper MD. FcR-like 2 Inhibition of B cell receptor-mediated activation of B cells. *J Immunol*. 2010;185(12):7405-7412.

237. Huttmann A, Klein-Hitpass L, Thomale J, et al. Gene expression signatures separate B-cell chronic lymphocytic leukaemia prognostic subgroups defined by ZAP-70 and CD38 expression status. *Leukemia*. 2006;20(10):1774-1782.
238. Krishnan N, Pan H, Buckley DJ, Buckley A. Prolactin-regulated pim-1 transcription: identification of critical promoter elements and Akt signaling. *Endocrine*. 2003;20(1-2):123-130.
239. Morishita D, Katayama R, Sekimizu K, Tsuruo T, Fujita N. Pim kinases promote cell cycle progression by phosphorylating and down-regulating p27Kip1 at the transcriptional and posttranscriptional levels. *Cancer Res*. 2008;68(13):5076-5085.
240. Sykes SM, Lane SW, Bullinger L, et al. AKT/FOXO signaling enforces reversible differentiation blockade in myeloid leukemias. *Cell*. 2011;146(5):697-708.
241. Downing JR. A new FOXO pathway required for leukemogenesis. *Cell*. 2011;146(5):669-670.
242. Miyashita T, Reed JC. Tumor suppressor p53 is a direct transcriptional activator of the human bax gene. *Cell*. 1995;80(2):293-299.
243. Wei CL, Wu Q, Vega VB, et al. A global map of p53 transcription-factor binding sites in the human genome. *Cell*. 2006;124(1):207-219.
244. Yarosh DB, Alas L, Kibitel J, O'Connor A, Carrier F, Fornace AJ, Jr. Cyclobutane pyrimidine dimers in UV-DNA induce release of soluble mediators that activate the human immunodeficiency virus promoter. *J Invest Dermatol*. 1993;100(6):790-794.
245. Y Barak TJ, R Haffner, and M Oren. mdm2 expression is induced by wild type p53 activity. *EMBO J*. 1993;12(2):461–468.
246. Wu Y, Lin JC, Piluso LG, et al. Phosphorylation of p53 by TAF1 inactivates p53-dependent transcription in the DNA damage response. *Mol Cell*. 2014;53(1):63-74.
247. el-Deiry WS, Kern SE, Pietenpol JA, Kinzler KW, Vogelstein B. Definition of a consensus binding site for p53. *Nat Genet*. 1992;1(1):45-49.
248. el-Deiry WS, Tokino T, Velculescu VE, et al. WAF1, a potential mediator of p53 tumor suppression. *Cell*. 1993;75(4):817-825.
249. Han J, Flemington C, Houghton AB, et al. Expression of bbc3, a pro-apoptotic BH3-only gene, is regulated by diverse cell death and survival signals. *Proc Natl Acad Sci U S A*. 2001;98(20):11318-11323.
250. Vergoulis T, Vlachos IS, Alexiou P, et al. TarBase 6.0: capturing the exponential growth of miRNA targets with experimental support. *Nucleic Acids Res*. 2012;40(Database issue):D222-229.
251. Krek A, Grun D, Poy MN, et al. Combinatorial microRNA target predictions. *Nat Genet*. 2005;37(5):495-500.
252. Grechez-Cassiau A, Rayet B, Guillaumond F, Teboul M, Delaunay F. The circadian clock component BMAL1 is a critical regulator of p21WAF1/CIP1 expression and hepatocyte proliferation. *J Biol Chem*. 2008;283(8):4535-4542.
253. Zhong J, Martinez M, Sengupta S, et al. Quantitative Phosphoproteomics Reveals Crosstalk Between Phosphorylation and O-GlcNAc in the DNA Damage Response Pathway. *Proteomics*. 2014.
254. Loilome W, Juntana S, Namwat N, et al. PRKAR1A is overexpressed and represents a possible therapeutic target in human cholangiocarcinoma. *Int J Cancer*. 2011;129(1):34-44.
255. Gangoda L, Doerflinger M, Srivastava R, et al. Loss of Prkar1a leads to Bcl-2 family protein induction and cachexia in mice. *Cell Death Differ*. 2014;21(11):1815-1824.
256. DeGregori J, Leone G, Miron A, Jakoi L, Nevins JR. Distinct roles for E2F proteins in cell growth control and apoptosis. *Proc Natl Acad Sci U S A*. 1997;94(14):7245-7250.
257. Gaubatz S, Lindeman GJ, Ishida S, et al. E2F4 and E2F5 play an essential role in pocket protein-mediated G1 control. *Mol Cell*. 2000;6(3):729-735.
258. Francoz S, Froment P, Bogaerts S, et al. Mdm4 and Mdm2 cooperate to inhibit p53 activity in proliferating and quiescent cells in vivo. *Proc Natl Acad Sci U S A*. 2006;103(9):3232-3237.

259. Marine JC, Francoz S, Maetens M, Wahl G, Toledo F, Lozano G. Keeping p53 in check: essential and synergistic functions of Mdm2 and Mdm4. *Cell Death Differ*. 2006;13(6):927-934.
260. Lutzny G, Kocher T, Schmidt-Supprian M, et al. Protein kinase c-beta-dependent activation of NF-kappaB in stromal cells is indispensable for the survival of chronic lymphocytic leukemia B cells in vivo. *Cancer Cell*. 2013;23(1):77-92.
261. Bluwstein A, Kumar N, Leger K, et al. PKC signaling prevents irradiation-induced apoptosis of primary human fibroblasts. *Cell Death Dis*. 2013;4:e498.
262. Nishimura Y, Komatsu S, Ichikawa D, et al. Overexpression of YWHAZ relates to tumor cell proliferation and malignant outcome of gastric carcinoma. *Br J Cancer*. 2013;108(6):1324-1331.
263. Clemson CM, Hutchinson JN, Sara SA, et al. An architectural role for a nuclear noncoding RNA: NEAT1 RNA is essential for the structure of paraspeckles. *Mol Cell*. 2009;33(6):717-726.
264. Zenz T, Gribben JG, Hallek M, Dohner H, Keating MJ, Stilgenbauer S. Risk categories and refractory CLL in the era of chemoimmunotherapy. *Blood*. 2012;119(18):4101-4107.
265. Bottcher S, Ritgen M, Fischer K, et al. Minimal residual disease quantification is an independent predictor of progression-free and overall survival in chronic lymphocytic leukemia: a multivariate analysis from the randomized GCLLSG CLL8 trial. *J Clin Oncol*. 2012;30(9):980-988.
266. Rossi S, Shimizu M, Barbarotto E, et al. microRNA fingerprinting of CLL patients with chromosome 17p deletion identify a miR-21 score that stratifies early survival. *Blood*. 2010;116(6):945-952.
267. Moussay E, Palissot V, Vallar L, et al. Determination of genes and microRNAs involved in the resistance to fludarabine in vivo in chronic lymphocytic leukemia. *Mol Cancer*. 2010;9:115.
268. Marton S, Garcia MR, Robello C, et al. Small RNAs analysis in CLL reveals a deregulation of miRNA expression and novel miRNA candidates of putative relevance in CLL pathogenesis. *Leukemia*. 2008;22(2):330-338.
269. Li S, Moffett HF, Lu J, et al. MicroRNA expression profiling identifies activated B cell status in chronic lymphocytic leukemia cells. *PLoS One*. 2011;6(3):e16956.
270. Rosenwald A, Alizadeh AA, Widhopf G, et al. Relation of gene expression phenotype to immunoglobulin mutation genotype in B cell chronic lymphocytic leukemia. *J Exp Med*. 2001;194(11):1639-1647.
271. Woyach JA, Johnson AJ, Byrd JC. The B-cell receptor signaling pathway as a therapeutic target in CLL. *Blood*. 2012;120(6):1175-1184.
272. Chen P, Price C, Li Z, et al. miR-9 is an essential oncogenic microRNA specifically overexpressed in mixed lineage leukemia-rearranged leukemia. *Proc Natl Acad Sci U S A*. 2013;110(28):11511-11516.
273. Yao Y, Xue Y, Ma J, et al. MiR-330-mediated regulation of SH3GL2 expression enhances malignant behaviors of glioblastoma stem cells by activating ERK and PI3K/AKT signaling pathways. *PLoS One*. 2014;9(4):e95060.
274. Wu Z, He B, He J, Mao X. Upregulation of miR-153 promotes cell proliferation via downregulation of the PTEN tumor suppressor gene in human prostate cancer. *Prostate*. 2013;73(6):596-604.
275. Wong TS, Liu XB, Wong BY, Ng RW, Yuen AP, Wei WI. Mature miR-184 as Potential Oncogenic microRNA of Squamous Cell Carcinoma of Tongue. *Clin Cancer Res*. 2008;14(9):2588-2592.
276. Emmrich S, Katsman-Kuipers JE, Henke K, et al. miR-9 is a tumor suppressor in pediatric AML with t(8;21). *Leukemia*. 2014;28(5):1022-1032.
277. Foley NH, Bray IM, Tivnan A, et al. MicroRNA-184 inhibits neuroblastoma cell survival through targeting the serine/threonine kinase AKT2. *Mol Cancer*. 2010;9:83.
278. Li Y, Zhu X, Xu W, Wang D, Yan J. miR-330 regulates the proliferation of colorectal cancer cells by targeting Cdc42. *Biochem Biophys Res Commun*. 2013;431(3):560-565.

279. Davids MS, Brown JR. Ibrutinib: a first in class covalent inhibitor of Bruton's tyrosine kinase. *Future Oncol*. 2014;10(6):957-967.
280. Cui B, Chen L, Zhang S, et al. MicroRNA-155 influences B-cell receptor signaling and associates with aggressive disease in chronic lymphocytic leukemia. *Blood*. 2014.
281. Decker S, Finter J, Forde AJ, et al. PIM kinases are essential for chronic lymphocytic leukemia cell survival (PIM2/3) and CXCR4-mediated microenvironmental interactions (PIM1). *Mol Cancer Ther*. 2014;13(5):1231-1245.
282. Mraz M, Kipps TJ. MicroRNAs And B Cell Receptor Signaling in Chronic Lymphocytic Leukemia. *Leuk Lymphoma*. 2013.
283. Sandhu SK, Fassan M, Volinia S, et al. B-cell malignancies in microRNA Emu-miR-17~92 transgenic mice. *Proc Natl Acad Sci U S A*. 2013;110(45):18208-18213.
284. Psathas JN, Doonan PJ, Raman P, Freedman BD, Minn AJ, Thomas-Tikhonenko A. The Myc-miR-17-92 axis amplifies B-cell receptor signaling via inhibition of ITIM proteins: a novel lymphomagenic feed-forward loop. *Blood*. 2013.
285. Kluiver J, Poppema S, de Jong D, et al. BIC and miR-155 are highly expressed in Hodgkin, primary mediastinal and diffuse large B cell lymphomas. *J Pathol*. 2005;207(2):243-249.
286. Yin Q, Wang X, McBride J, Fewell C, Flemington E. B-cell receptor activation induces BIC/miR-155 expression through a conserved AP-1 element. *J Biol Chem*. 2008;283(5):2654-2662.
287. Hermeking H. MicroRNAs in the p53 network: micromanagement of tumour suppression. *Nat Rev Cancer*. 2012;12(9):613-626.
288. Allen MA, Andrysik Z, Dengler VL, et al. Global analysis of p53-regulated transcription identifies its direct targets and unexpected regulatory mechanisms. *Elife (Cambridge)*. 2014;3:e02200.
289. Calin GA. MiR-sensing chemotherapy resistance in CLL. *Blood*. 2009;113(16):3652-3653.
290. Tarasov VJ, P.; Verdoodt, B.; Lodygin, D.; Epanchintsev, A.; Menssen, A.; Meister, G.; Hermeking, H.;. Differential Regulation of microRNAs by p53 Revealed by Massively Parallel Sequencing. *Cell Cycle*. 2007;6(13).
291. Xu X, Wu J, Li S, et al. Downregulation of microRNA-182-5p contributes to renal cell carcinoma proliferation via activating the AKT/FOXO3a signaling pathway. *Mol Cancer*. 2014;13(1):109.
292. Zhang N, Li X, Wu CW, et al. microRNA-7 is a novel inhibitor of YY1 contributing to colorectal tumorigenesis. *Oncogene*. 2013;32(42):5078-5088.
293. Sanchez N, Gallagher M, Lao N, et al. MiR-7 triggers cell cycle arrest at the G1/S transition by targeting multiple genes including Skp2 and Psme3. *PLoS One*. 2013;8(6):e65671.
294. Kefas B, Godlewski J, Comeau L, et al. microRNA-7 inhibits the epidermal growth factor receptor and the Akt pathway and is down-regulated in glioblastoma. *Cancer Res*. 2008;68(10):3566-3572.
295. Zhang L, Huang J, Yang N, et al. microRNAs exhibit high frequency genomic alterations in human cancer. *Proc Natl Acad Sci U S A*. 2006;103(24):9136-9141.
296. Schepeler T, Reinert JT, Ostenfeld MS, et al. Diagnostic and prognostic microRNAs in stage II colon cancer. *Cancer Res*. 2008;68(15):6416-6424.
297. Liu J, Chen G, Feng L, et al. Loss of p53 and altered miR15-a/16-1 -> MCL-1 pathway in CLL: insights from TCL1-Tg:p53(-/-) mouse model and primary human leukemia cells. *Leukemia*. 2014;28(1):118-128.
298. Yan HL, Xue G, Mei Q, et al. Repression of the miR-17-92 cluster by p53 has an important function in hypoxia-induced apoptosis. *EMBO J*. 2009;28(18):2719-2732.
299. Dimitrova N, Zamudio JR, Jong RM, et al. LincRNA-p21 activates p21 in cis to promote Polycomb target gene expression and to enforce the G1/S checkpoint. *Mol Cell*. 2014;54(5):777-790.

300. Zhai H, Fesler A, Schee K, Fodstad O, Flatmark K, Ju J. Clinical Significance of Long Intergenic Noncoding RNA-p21 in Colorectal Cancer. *Clin Colorectal Cancer*. 2013.
301. Ozgur E, Mert U, Isin M, Okutan M, Dalay N, Gezer U. Differential expression of long non-coding RNAs during genotoxic stress-induced apoptosis in HeLa and MCF-7 cells. *Clin Exp Med*. 2012.
302. Isin M, Ozgur E, Cetin G, et al. Investigation of circulating lncRNAs in B-cell neoplasms. *Clin Chim Acta*. 2014;431:255-259.
303. Gibb EA, Vucic EA, Enfield KS, et al. Human cancer long non-coding RNA transcriptomes. *PLoS One*. 2011;6(10):e25915.
304. Chen LL, Carmichael GG. Altered nuclear retention of mRNAs containing inverted repeats in human embryonic stem cells: functional role of a nuclear noncoding RNA. *Mol Cell*. 2009;35(4):467-478.
305. Sunwoo H, Dinger ME, Wilusz JE, Amaral PP, Mattick JS, Spector DL. MEN epsilon/beta nuclear-retained non-coding RNAs are up-regulated upon muscle differentiation and are essential components of paraspeckles. *Genome Res*. 2009;19(3):347-359.
306. Hutchinson JN, Ensminger AW, Clemson CM, Lynch CR, Lawrence JB, Chess A. A screen for nuclear transcripts identifies two linked noncoding RNAs associated with SC35 splicing domains. *BMC Genomics*. 2007;8:39.
307. Naganuma T, Nakagawa S, Tanigawa A, Sasaki YF, Goshima N, Hirose T. Alternative 3'-end processing of long noncoding RNA initiates construction of nuclear paraspeckles. *EMBO J*. 2012;31(20):4020-4034.
308. Nakagawa S, Naganuma T, Shioi G, Hirose T. Paraspeckles are subpopulation-specific nuclear bodies that are not essential in mice. *J Cell Biol*. 2011;193(1):31-39.
309. Ruohan L, Stuart H, Alan H, Tetsuro H, Gerard P, Archa F. The long non-coding RNA NEAT1 is transcribed under stress conditions and influences gene expression via transcription factor sequestration. *ACT2014 Conference Abstract*. 2014.
310. Kenzelmann Broz D, Spano Mello S, Bieging KT, et al. Global genomic profiling reveals an extensive p53-regulated autophagy program contributing to key p53 responses. *Genes Dev*. 2013;27(9):1016-1031.
311. Imamura K, Imamachi N, Akizuki G, et al. Long noncoding RNA NEAT1-dependent SFPQ relocation from promoter region to paraspeckle mediates IL8 expression upon immune stimuli. *Mol Cell*. 2014;53(3):393-406.
312. Hirose T, Virnicchi G, Tanigawa A, et al. NEAT1 long noncoding RNA regulates transcription via protein sequestration within subnuclear bodies. *Mol Biol Cell*. 2014;25(1):169-183.
313. West JA, Davis CP, Sunwoo H, et al. The Long Noncoding RNAs NEAT1 and MALAT1 Bind Active Chromatin Sites. *Mol Cell*. 2014;55(5):791-802.
314. Ho J, Benchimol S. Transcriptional repression mediated by the p53 tumour suppressor. *Cell Death Differ*. 2003;10(4):404-408.
315. Brady CAA, L.D. p53 at a glance. *J Cell Sci*. 2010(123):2527-2532.
316. Heyd F, Lynch KW. Phosphorylation-dependent regulation of PSF by GSK3 controls CD45 alternative splicing. *Mol Cell*. 2010;40(1):126-137.
317. Salton M, Lerenthal Y, Wang SY, Chen DJ, Shiloh Y. Involvement of Matrin 3 and SFPQ/NONO in the DNA damage response. *Cell Cycle*. 2010;9(8):1568-1576.
318. Rajesh C, Baker DK, Pierce AJ, Pittman DL. The splicing-factor related protein SFPQ/PSF interacts with RAD51D and is necessary for homology-directed repair and sister chromatid cohesion. *Nucleic Acids Res*. 2011;39(1):132-145.
319. Yuan M, Eberhart CG, Kai M. RNA binding protein RBM14 promotes radio-resistance in glioblastoma by regulating DNA repair and cell differentiation. *Oncotarget*. 2014;5(9):2820-2826.
320. Christoffersen NR, Shalgi R, Frankel LB, et al. p53-independent upregulation of miR-34a during oncogene-induced senescence represses MYC. *Cell Death Differ*. 2010;17(2):236-245.

321. Navarro F, Gutman D, Meire E, et al. miR-34a contributes to megakaryocytic differentiation of K562 cells independently of p53. *Blood*. 2009;114(10):2181-2192.
322. Rossi D. Disruption of BIRC3 associates with fludarabine chemorefractoriness in TP53 wt CLL. *Blood*. 2012.
323. Messina M, Del Giudice I, Khiabanian H, et al. Genetic lesions associated with chronic lymphocytic leukemia chemo-refractoriness. *Blood*. 2014;123(15):2378-2388.

Appendix

Table S1. Detailed sample genetics and grouping for comparison of ncRNA expression.

Group 1 = *TP53*^{wt} patients without del11q, no prior treatment; group 2 = *TP53*^{wt} 'high-risk' patients, previously treated; group 3 = *TP53*$^{del/mut}$ patients. Y = yes, N = no. *A sample containing 6% *TP53* mutation was considered *TP53*^{wt}.

group	Sample Nr.	del17p, %	*TP53*^{mut}, %	del11q, %	other, %	*IGHV*	Prior treatment
1	1	0	0	0	MYD88, 65	M	N
	2	0	0	0	tris12, 78	UM	N
	3	0	0	0	0	UM	N
	4	0	0	0	0	UM	N
	5	0	0	0	0	M	N
	6	0	0	0	0	M	N
	7	0	0	0	0	UM	N
	8	0	0	0	0	M	N
	9	0	0	0	0	M	N
	10	0	0	0	0	M	N
	11	0	0	0	0	M	N
	12	0	0	0	0	UM	N
	13	0	0	0	0	M	N
	14	0	0	0	0	M	N
	15	0	0	0	tris 12, 57	M	N
2	16	0	0	95	BRAF, 12	UM	Y
	17	0	0	88	NOTCH1, 45	UM	Y
	18	0	0	81	SF3B1, 48	UM	Y
	19	0	0	79	ATM, 37	UM	Y
	20	0	0	0	SF3B1, 34	UM	Y
	21	0	0	0	8q24+, 78; SF3B1, 45	M	Y
	22	0	6	11	SF3B1, 34	M	Y
	23	0	0	0	8q24+, 78	M	Y
	24	0	7	0	ATM, 33	UM	Y
3	25	13	71	0	0	M	Y
	26	23	26	0	0	UM	Y
	27	Y	30	0	NOTCH1, 50	UM	Y
	28	91	0	0	MYD88, 50	M	N
	29	Y	54	0	SF3B1, 52; BRAF, 49	UM	Y
	30	58	44	0	0	M	Y
	31	11	35	0	BRAF, 17; SF3B1, 44	UM	Y
	32	52	80	0	0	UM	N
	33	?	44	0	SF3B1, 48	UM	Y
	34	47	92	0	0	UM	Y

Table S2. *TP53* mutation status of the BL cell lines used.

Cell line	*TP53* status	Amino acid change
BL-2	wt	-
BL-7	wt	-
Cheptanges	wt	-
Ly-47	wt	-
Salina	wt	-
Seraphine	wt	-
BJAB	c.578A>G	p.H193R
BL-60	c.742C>T; c.844C>T	p.R248W; p.R282W
CA-46	c.743G>A	p.R248Q
Namalwa	c.743G>A	p.R248Q
Ramos	c.760_761AT>GA	p.I254D

Table S3. Comparison of the 30 highest expressed miRNAs in CLL baseline samples to previously reported CLL sequencing screens. Normalized read counts are provided.

	This work		Jima *et al.*[232]		Landgraf et al.[227]	
rank	**name**	**average read count NT**	**name**	**average read count NT**	**name**	**average read count NT**
1	miR-21-5p	531914	let-7f-1	1166618	miR-142-3p	247
2	miR-26a-5p	234464	let-7g	841349	miR-142-5p	165
3	let-7g-5p	206540	let-7a-2	358095	miR-29b-3p	112
4	miR-101-3p	160967	miR-21	215094	miR-16-5p	85
5	miR-150-5p	136475	let-7i	174294	miR-150-3p	70
6	miR-148a-3p	112555	miR-140-3p	170300	miR-26a-5p	61
7	let-7f-5p	93963	miR-29a	116065	miR-21-5p	55
8	miR-29a-3p	84091	miR-101-1	93093	miR-30e-5p	37
9	let-7i-5p	74492	miR-142	54372	miR-15a-5p	35
10	miR-155-5p	63073	miR-378	43937	miR-29a-3p	33
11	miR-142-3p	34047	miR-103-1	43831	miR-26b-5p	24
12	miR-142-5p	31798	miR-320c-1	32030	let-7f-5p	22
13	let-7a-5p	31678	miR-320a	30631	let-7a-5p	19
14	miR-26b-5p	31105	miR-101-2	29796	miR-101-3p	18
15	miR-27a-3p	29320	miR-103-2	27408	miR-30d-5p	17
16	miR-30d-5p	23499	miR-107	25865	miR-155-5p	15
17	miR-92a-3p	20473	miR-423	24503	mir-29c-3p	13
18	miR-16-5p	20436	miR-25	20142	miR-140-5p	12
19	miR-103a-3p	19451	miR-26b	19647	let-7g-5p	8
20	miR-191-5p	18884	miR-26a-1	18373	miR-28-5p	7
21	miR-20a-5p	18854	miR-92a-1	14005	let-7i-5p	6
22	miR-361-3p	17263	miR-30e*	11068	miR-32-5p	5
23	miR-1246	16815	miR-221	10882	miR-191-5p	5
24	miR-30e-5p	14928	miR-30e	8944	miR-27a-3p	5
25	miR-29b-3p	12868	miR-191	7248	miR-19b-3p	4
26	miR-140-3p	11523	miR-16-1	7239	miR-186-5p	3
27	miR-25-3p	10692	miR-192	6898	miR-146a-5p	3
28	miR-186-5p	9726	miR-29c	5770	miR-24-3p	3
29	miR-30b-5p	9225	miR-30d	5456	miR-92a-3p	3
30	miR-146a-5p	9197	miR-151-3p	4801	miR-30c-5p	3

Table S4. mRNAs inversely correlating to miR-574-5p expression, and predicted to be targeted by miR-574-5p. Target prediction was performed by miRWalk, miRanda and TargetScan algorithms. Pearson's correlation coefficient (R) is provided and p-values corrected for multiple testing are provided.

Gene / protein name	R	p-value
SLC16A14 / solute carrier family 16, member 4	-0.67	0.009
IMPACT / impact RWD domain protein	-0.65	0.010
MLLT3 / myeloid/lymphoid or mixed-lineage leukemia translocated to, 3	-0.64	0.012
PIM3 / PIM3	-0.64	0.013
CLDN6 / claudin-6	-0.62	0.016
DCDC2 / doublecortin domain-containing protein 2	-0.61	0.017
PHOSPHO1 / phosphatase, orphan 1	-0.61	0.017
LECT1 / chondromodulin-1	-0.59	0.023
SLIT2 / slit homolog 2	-0.58	0.028
STXBP5L / syntaxin-binding protein 5	-0.57	0.030
MAOB / monoamine oxidase B	-0.56	0.031
MYO5B / myosin V B	-0.56	0.035
TRMT5 / tRNA methyltransferase 5	-0.55	0.036
GPR83 / orphan receptor Gpr83	-0.55	0.037
TLN2 / talin 2	-0.55	0.039
NSL1 / kinetochore-associated protein NSL1 homolog	-0.55	0.040
FOXO4 / forkhead box O4	-0.54	0.040
HOXC8 / homeobox C8	-0.54	0.041
XPO-7 / exportin-7	-0.54	0.042
INSIG1 / insulin induced gene 1	-0.54	0.043

Table S5. ncRNAs differentially expressed between previously untreated *TP53*^{wt} and high-risk *TP53*^{wt} samples at baseline. Previously untreated *TP53*^{wt} samples (UT, n = 15) were compared to high-risk *TP53*^{wt} samples that had all received prior treatment (PT, n = 9). Mean normalized read counts and Benjamini-Hochberg corrected p-values are provided.

RNA identifier	RNA type	UT *TP53*^{wt}	PT *TP53*^{wt}	Fold difference	p-value
ENSG00000201570	snRNA	2407	32	0.01	1.3E-4
ENSG00000245526	lincRNA	225	1718	7.56	0.009
ENSG00000261786	lincRNA	117	6	0.05	0.009
ENSG00000230590	lincRNA	314	23	0.06	0.009
miR-1285-3p	miRNA	21	36	1.86	0.014
let-7b-5p	miRNA	3343	7523	2.17	0.026
ENSG00000201198	snRNA	65	21	0.33	0.019
ENSG00000239075	snRNA	51	14	0.25	0.019
ENSG00000207227	snRNA	50	14	0.26	0.032
ENSG00000206595	snRNA	51	14	0.26	0.034
ENSG00000207099	snRNA	85	31	0.36	0.042

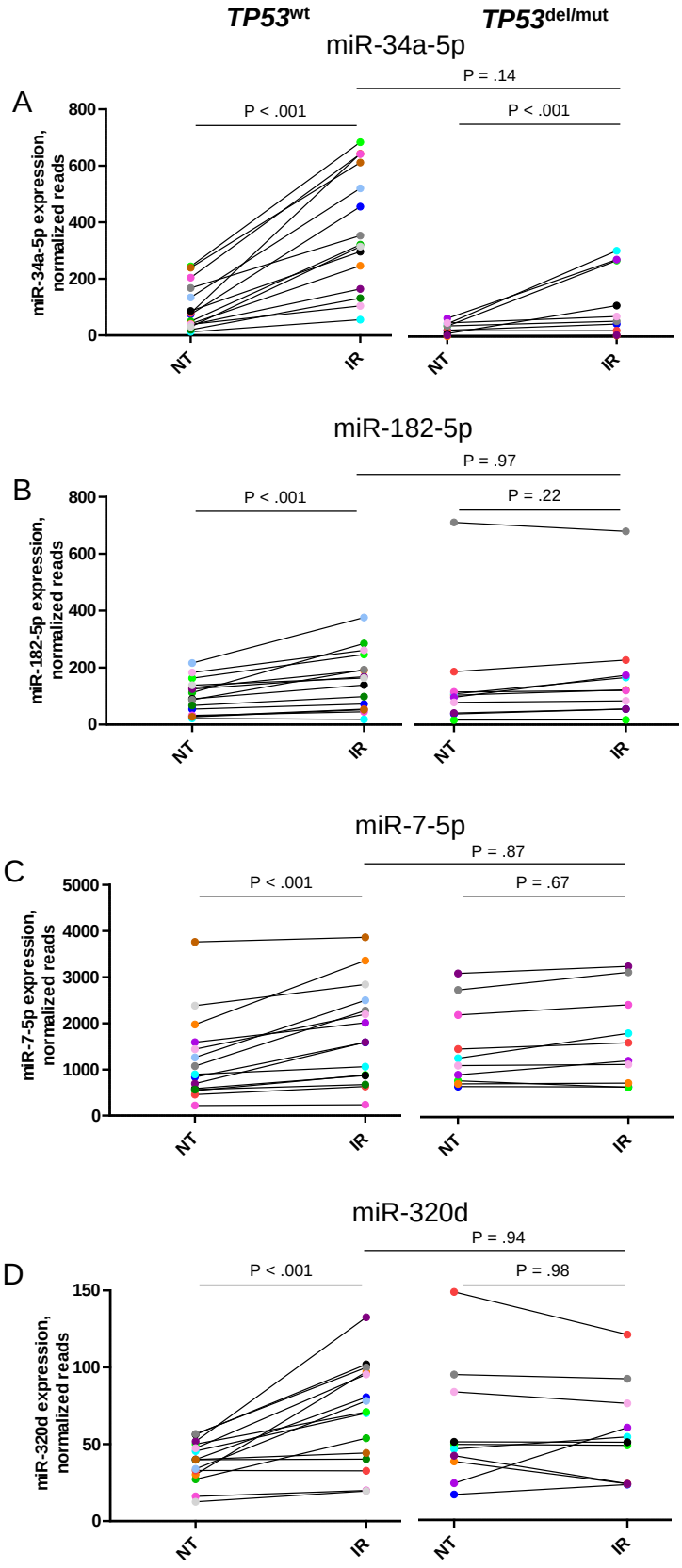

Figure S1. Induction of the top four p53-dependently regulated miRNAs upon irradiation. NT = non-treated, IR = irradiated. Normalized read counts and Benjamini-Hochberg corrected p-values are provided. One colour encodes one specific *TP53*^{wt} or *TP53*$^{del/mut}$ sample.

Publications and Conferences

Publications

Targeted resequencing for analysis of clonal composition of recurrent gene mutations in chronic lymphocytic leukaemia.
*Jethwa A, Hüllein J, Stolz T, **Blume C**, Sellner L, Jauch A, Sill M, Kater AP, te Raa GD, Geisler C, van Oers M, Dietrich S, Dreger P, Ho AD, Paruzynski A, Schmidt M, von Kalle C, Glimm H, Zenz T. Br J Haematol. 2013 Nov; 163(4):496-500.*

Next-generation sequencing of cancer consensus genes in lymphoma.
*Hüllein J, Jethwa A, Stolz T, **Blume C**, Sellner L, Sill M, Langer C, Jauch A, Paruzynski A, von Kalle C, Schmidt M, Glimm H, Zenz T. Leuk Lymphoma. 2013 Aug; 54(8): 1831-5.*

Continued response off treatment after BRAF inhibition in refractory hairy cell leukemia.
*Dietrich S, Hüllein J, Hundemer M, Lehners N, Jethwa A, Capper D, Acker T, Garvalov BK, Andrulis M, **Blume C**, Schulte C, Mandel T, Meissner J, Fröhling S, von Kalle C, Glimm H, Ho AD, Zenz T. J Clin Oncol. 2013 Jul 1;31(19):e300-3.*

p53-dependent non-coding RNA networks in Chronic Lymphocytic Leukemia.
***Blume C**, Hotz-Wagenblatt A, Hüllein J, Sellner L, Stolz T, Slabicki M, Lee KS, Benner A, Dietrich S, Oakes CC, Dreger P, Te Raa D, Kater AP, Jauch A, Merkel O, Hielscher T, Zenz T.*
Manuscript in preparation.

Selected oral presentations at scientific meetings

Novel p53-dependent non-coding RNAs in Chronic Lymphocytic Leukemia.
***Blume CJ**, Hielscher T, Hotz-Wagenblatt A, Hüllein J, Jethwa A, Sellner L, Stolz T, Merkel O and Zenz T.*
DKFZ PhD Retreat, July 2014, Weil der Stadt

Poster presentations at scientific meetings

Identifying microRNAs involved in DNA damage response in Chronic Lymphocytic Leukemia.

***Blume C**, Hotz-Wagenblatt A, Hielscher T, Sellner L, Stolz T, Hüllein J, Merkel O and Zenz T.*

DKFZ PhD Student Poster Presentation July 2014, Heidelberg

Small RNA sequencing identifies microRNAs involved in B-cell receptor signaling in chronic lymphocytic leukemia

***Blume C**, Hielscher T, Hotz-Wagenblatt A, Sellner L, Hüllein J, Stolz T, Oakes CC, Merkel O and Zenz T.*

23rd Biennial Contress of the European Association for Cancer Research, July 2014, Munich

microRNAs involved in chronic lymphocytic leukemia B-cell receptor signaling revealed by small RNA sequencing.

***Blume CJ**, Hielscher T, Hotz-Wagenblatt A, Sellner L, Hüllein J, Stolz T, Oakes CC, Merkel O and Zenz T.*

International Conference on Non-coding RNA – From Basic Mechanisms to Cancer, June 2014, Heidelberg

Declaration

Hiermit erkläre ich, dass ich die vorliegende Arbeit selbständig angefertigt habe. Es wurden nur die in der Arbeit ausdrücklich benannten Quellen und Hilfsmittel benutzt. Wörtlich oder sinngemäß übernommenes Gedankengut habe ich als solches kenntlich gemacht.
Ich erkläre außerdem, dass diese Arbeit weder in dieser noch in einer anderen Form anderweitig als Dissertation oder Prüfungsarbeit verwendet oder einer anderen Fakultät als Dissertation vorgelegt wurde.

Heidelberg, _____ _____

Ort, Datum Unterschrift

Acknowledgements

I herewith would like to thank all the people who supported me in any way during the course of this work.

First and foremost I would like to thank Prof. Dr. Thorsten Zenz for giving me the opportunity to work on this interesting and motivating topic, and to present and discuss my results at international conferences. Many thanks for your enthusiasm, supervision and the critical review of my work including this thesis.

I would like to thank Prof. Dr. Christof von Kalle, PD Dr. Suat Özbek, PD Dr. Stefan Wiemann and Dr. Anne Hamacher-Brady for participating in my examination committee.

Further, I am very grateful for the discussions with Prof. Dr. Christof von Kalle, PD Dr. Daniel Mertens, Dr. Sven Diederichs and PD Dr. Jan Dürig during our thesis advisory committee meetings.

Thomas Hielscher I would like to thank for providing statistical analyses I was not able to perform on my own, and Dr. Agnes Hotz-Wagenblatt for her great support with read processing and mapping.

I would especially like to thank all CLL patients who were willing to donate their blood for this research. Without their support this work would have been impossible.

I would like to thank Jennifer Hüllein and Tatjana Stolz for determining the p53 mutation status of the patient samples, Dr. Anna Jauch and Dr. Chris Oakes for providing FISH and *IGHV* mutation data, respectively, and Kwang S. Lee for help with ChIP.

For their support concerning RNA sequencing I would like to thank Nicolle Diessl and Sabine Schmidt.

Alexander Knurr I thank for first aid in IT-related matters.

Dr. Mikolaj Slabicki and Dr. Leopold Sellner I thank for lively discussions of results, valuable comments and general support, as well as for proofreading parts of my thesis.

Many thanks also to the whole ‘G100 family’ for helpful comments and the positive working atmosphere, particularly to Jennifer Hüllein, Tatjana Stolz, Kwang S. Lee, Alexander Jethwa, Elias Eckert, Dr. Eva-Maria Hartinger, Dr. Felix Oppel, Dr. Roland Ehrenberg, Sanne Kwakmann, Kasia Tomska, Marina Lukas, Dr. Friederike Herbst, Dr. Oksana Zavidij and Taronish Dubash with whom I shared the lab or office.

A big thank you goes to my friends, who have supported me through the ups and downs of the past years, particularly Dr. Susanne Mükusch – also for proofreading parts of this thesis – and Janina Schmid as well as Judith Grigo and Andrea Kunz, who reminded me there is a life beyond the lab in Heidelberg.

In this regard, I also want to thank Dr. Tobias Bellmann for his constant support in many ways during the course of this work and beyond.

I am deeply grateful for the support by my parents, who have not only taught me the value of knowledge and of staying open-minded and curious, but also persistence and endurance, which can be just as important in research. I would like to dedicate this work to my mother Dr. Izabella, a source of power and inspiration.